ANALYSIS AND DESIGN OF STATIC POWER CONVERTERS WITH RESONANT HIGH FREQUENCY LINKS

V. T. Ranganathan

A Thesis

in

The Department

of

Electrical Engineering

Presented in Partial Fulfillment of the Requirements
for the degree of Doctor of Philosophy
Concordia University
Montreal, Quebec, Canada

March 1983

ABSTRACT

ANALYSIS AND DESIGN OF STATIC POWER CONVERTERS WITH RESONANT HIGH FREQUENCY LINKS

V.T. Ranganathan, Ph.D.
Concordia University, 1983

High frequency link schemes for dc-dc and dc-ac power conversion, employing a resonant inverter as the link, are investigated in this thesis. The inverter configuration consists of a series resonant LC circuit with the load connected across the resonating capacitor. A technique is developed for steady-state analysis of the inverter when feeding converter loads. Simple closed form solutions are obtained for the operating point of the inverter under both forward and regenerative power flow conditions.

The following power conversion schemes incorporating the resonant inverter are considered in particular.

A dc-dc converter consisting of the inverter feeding an uncontrolled rectifier load is investigated. It is shown that the output voltage can be regulated by varying the inverter frequency. Converter performance is obtained using the results of the analysis and a design procedure is given.

A four quadrant converter, in which the two functions of inversion and cycloconversion are performed in a single stage, is developed using the inverter. The load current is made to follow an external reference signal by controlling the on/off times of the inverter.

A dc-ac power conversion technique which utilises two resonant inverters as twin high frequency links is developed. The two inverters operate at frequencies which differ by twice the required low output frequency. The difference between their voltages is then a high frequency wave enveloped within a sinusoid at the low output frequency. Low frequency output is obtained by a process of cycloconversion in which the modulation is incorporated in the input voltage instead of the switching.

To facilitate understanding and applicability of the analytical results, several design examples are presented. Also selected predicted results are verified experimentally.

ACKNOWLEDGEMENTS

I am grateful to Professors P.D. Ziogas and V.R. Stefanovic for their guidance and help during the course of my studies.

I would like to express my appreciation to Prof. J.F. Lindsay for the many instructive hours that I spent with him.

I am grateful to the Electrical Engineering Department for help in the form of teaching assistantships.

Help given by Danny Juras in the laboratory is very much appreciated.

Special thanks to Mrs. Monica Etwaroo for her excellent typing of the thesis.

TABLE OF CONTENTS

LIST OF FIGURES

PAGE

PAGE

PAGE

PAGE

PAGE

NOMENCLATURE

a,b,c	-	coefficients in trigonometric equation defining inverter operating point.
C	-	resonating capacitor in the inverter.
C_b	-	DC blcoking capacitor
D_i	-	Diodes
E	-	DC supply voltage from centre-tap to either pole.
f	-	Resonant frequency of the L,C components of the inverter.
f_1, f_2	-	Frequencies of the two sinusoidal sources in the twin link scheme.
f_o	-	Output frequency in twin link scheme.
f_c	-	Frequency of the high frequency carrier component in twin link scheme.
f_s	-	Inverter operating frequency
g_1, g_2, g_3, g_4	-	Thyristor gating signals.
i	-	Resonant current in the inverter.
i_C	-	Current in resonating capacitor.
i_{Crms}	-	RMS current in resonating capacitor.

i_{Dav} - Average diode current.

i_{DP} - Peak diode current.

i_{Drms} - RMS diode current.

i_i - Initial current in resonating inductor at the beginning of a circuit mode.

i_{in} - Input current of cycloconverter in twin link scheme.

i_o - Load current in twin link scheme.

i_{rms} - RMS current in resonating inductor.

i_{TP} - Peak thyristor current.

i_{Trms} - RMS thyristor current.

i_0 - Initial current in the resonating inductor at the beginning of a half-cycle.

i_1 - Current in resonating inductor at the end of the first mode in half-cycle.

I_L - Load current reflected onto the link

I	-	Instantaneous magnitude of load current; hence amplitude of I_L .
I_R	-	External reference signal for load current in the current regulated converter.
I_1, I_2	-	Currents drawn from the two sources in the twin link scheme.
ΔI	-	Allowed deviation between reference and load current in the current regulated converter.
L	-	Resonating inductor in the inverter.
P_o	-	Instantaneous power at the output of twin link scheme.
P_0	-	Maximum specified load power for the current regulated converter.
P_1, P_2	-	Average powers supplied over a cycle by the two sources in twin link scheme.
Q	-	Quality facotr.
R	-	Series resistance of resonant circuit in the current regulated converter.

R_L - Equivalent load resistance.

t - Time.

T - Resonant period of inverter L,C components.

T_s - Half-period of inverter operation; also period of switching in current regulated converter.

T' - Time for one current pulse in resonant circuit of current regulated converter.

t_q - Thyristor commutation time.

t_{AB}, t_{BC} - Time intervals.

t_1, t_2, t_3 - Specific instants during half-cycle in the twin link scheme.

Th_i - Thyristors.

v - Link voltage.

v_{av} - Average rectified link voltage.

v_i - Voltage across resonating capacitor at the beginning of a circuit mode.

v_L - Voltage across resonating inductor.

v_{Lrms} - RMS value of v_L.

v_p - Peak value of link voltage.

v_{rms} - RMS value of link voltage.

v_1 - Voltage across resonating capacitor at the end of the first mode in half-cycle.

V_m - Peak voltage of each sinusoidal source in the twin link scheme.

V_{out} - Output dc voltage of dc-dc converter.

V_{odc} - DC value of output voltage in the current regulated converter.

V_o - Low frequency output voltage of twin link scheme.

V_{ow} - Wanted component of V_o.

V_{ref} - Reference voltage in control circuit of dc-dc converter.

V_s - Square-wave voltage applied across LC circuit.

V_{sl} - Fundamental component of V_s.

V_{sw} - Switching function representing action of cycloconverter in twin link scheme.

z - Characteristic impedance of inverter L,C elements.

α	-	Firing angle in output converter (on w_s scale); also decrement factor for RLC circuit.
α_a	-	Firing angle, advance firing.
α_{ac}	-	Critical value of α_a.
α_d	-	Firing angle, delayed firing.
δ	-	Angle on w scale defined by a,b,c.
ζ	-	Damping factor of RLC circuit.
η	-	Efficiency.
θ	-	General symbol for angles on w sclae; also load phase angle in twin link scheme.
$\theta_B, \theta_C, \theta_D, \theta_{CD}$	-	Angles on w scale.
θ_{del}	-	Firing delay angle in output converter (on w scale).
θ_{adv}	-	Firing advance angle in output converter (on w scale).
θ_{advc}	-	Critical value of θ_{adv}.

θ_1, θ_2 - Phase angles at which the two sources see the reflected load current in twin link scheme.

$(*)_{base}$ - Base value for the quantity (*).

CHAPTER 1

INTRODUCTION

1.1 Introduction

The advent of semiconductor power switching devices and the consequent developments in power converter circuits has led to widespread use of static power conversion. Electromechanical means such as motor-generator sets, traditionally employed to convert electric power from one form to another, such as for example, from fixed frequency fixed voltage ac to variable voltage dc or variable frequency variable voltage ac, have been largely replaced by static equipment. Static power conversion offers several advantages, such as ease of installation and maintenance of equipment and longer life due to absence of moving parts. Various functional features such as output voltage control and regulation, and output frequency control can be easily incorporated in the static power conversion process.

Among the various conversion processes, conversion of power starting from a dc voltage source is of considerable practical importance. Variable frequency inverters operating from a constant voltage dc supply find widespread application in adjustable speed ac drives. The same approach is used in constant frequency general power supplies.

This is especially true of uninterruptible power supplies for critical equipment. The standby power source in such applications is usually a battery and the use of a constant voltage dc intermediate circuit becomes essential. Fig. 1.1 shows in schematic form a static power conversion arrangement that is widely employed for ac-ac conversion. The input ac is passed through a 60 Hz transformer, which provides isolation and voltage matching. The ac is then rectified to create a constant voltage dc stage. The dc is then converted into the output ac using a static inverter employing forced commutation. This is termed dc link power conversion.

The inclusion of a high frequency stage in such a power conversion scheme can yield several attractive features. Fig. 1.2 shows in schematic form an ac-ac conversion arrangement with a high frequency link. The dc voltage, instead of being directly inverted into the low output frequency, is first inverted into high frequency ac. The low output frequency is then obtained using an ac-ac converter. This converter uses the high frequency ac voltage for commutation and does not require forced commutation.

The high frequency in the present context is of the order of a few KHz. With such an arrangement, isolation and voltage matching can be performed at the high frequency,

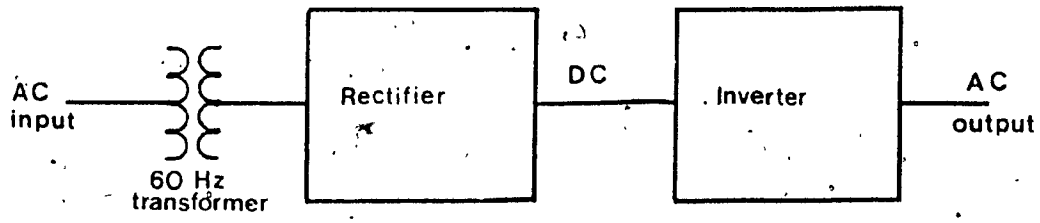

Fig. 1.1 Static ac-ac conversion scheme with dc link.

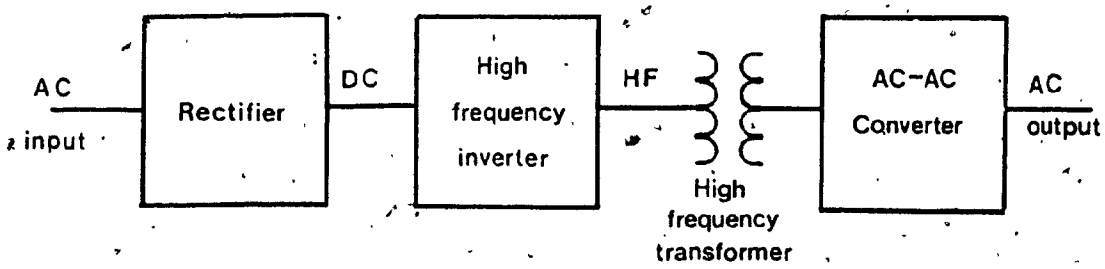

Fig. 1.2 Static ac-ac conversion scheme with high frequency link.

leading to considerable reduction in size and weight of equipment. The high frequency also results in reduced size of other magnetic and reactive components such as filters. A further significant advantage of a high internal frequency is that the converter has an increased speed of response. Consequently the use of high frequency links in power conversion is of considerable interest. Recent advances in device technology have resulted in the availability of switching devices with very low recovery times and this has led to renewed interest in the utilisation of such high frequency capabilities.

In order to realise the high frequency link, resonant inverters are the natural choice. Such inverters produce a sinusoidal output, which is necessary for feeding the output converters employing line commutation and phase control. They have a simple circuit implementation and the commutation results naturally from the circuit operation. They are especially well-suited for high frequency operation. Due to the smooth voltage and current waveforms inherent in resonant circuit operation, such inverters cause reduced electromagnetic interference, a factor which is assuming increasing importance due to the widespread use of switching converters.

Fig. 1.3 shows single-phase half-bridge versions of two possible resonant inverter configurations operating from a dc voltage source. Both inverters have series resonant inverter circuits connected at their output. They both rely on the resonant reversal of current for commutation. The difference between the two configurations arises from the manner in which the load is connected to the resonant circuit. In the inverter shown in Fig. 1.3a, the load is connected in series with the resonant LC circuit. In this case the load sees the inverter as a current source. In the inverter in Fig. 1.3b, the load is connected in parallel to the resonating capacitor. The inverter therefore appears to the load as a voltage source. For general power conditioning applications requiring a regulated output voltage, the voltage source configuration of Fig. 1.3b is the more compatible of the two. The use of this configuration to obtain a variable high frequency link leads to different techniques and circuit configurations in dc-dc and dc-ac power conversion. This thesis is concerned with the investigation of such conversion methods.

1.2 Review of Previous Work

The use of a high frequency link in power conversion has been suggested in the past in connection with various applications. The concept was considered in the Soviet

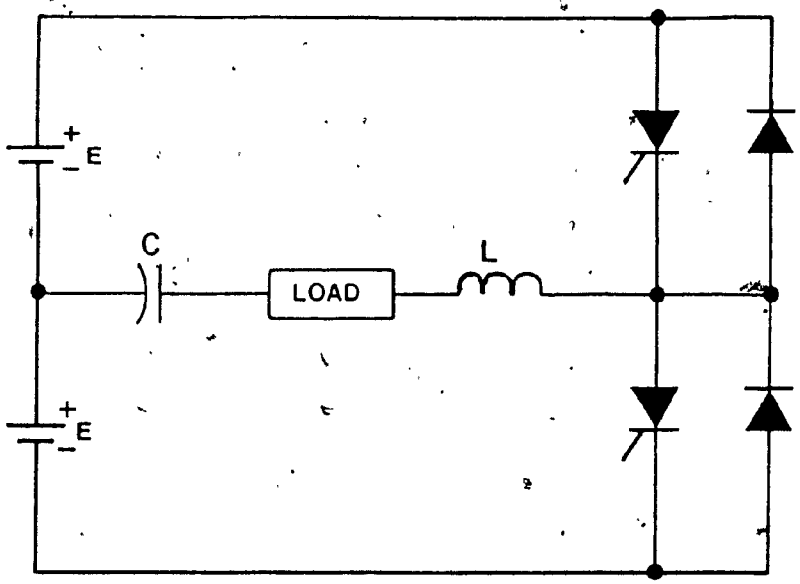

Fig. 1.3a Half-bridge resonant inverter with the load in series.

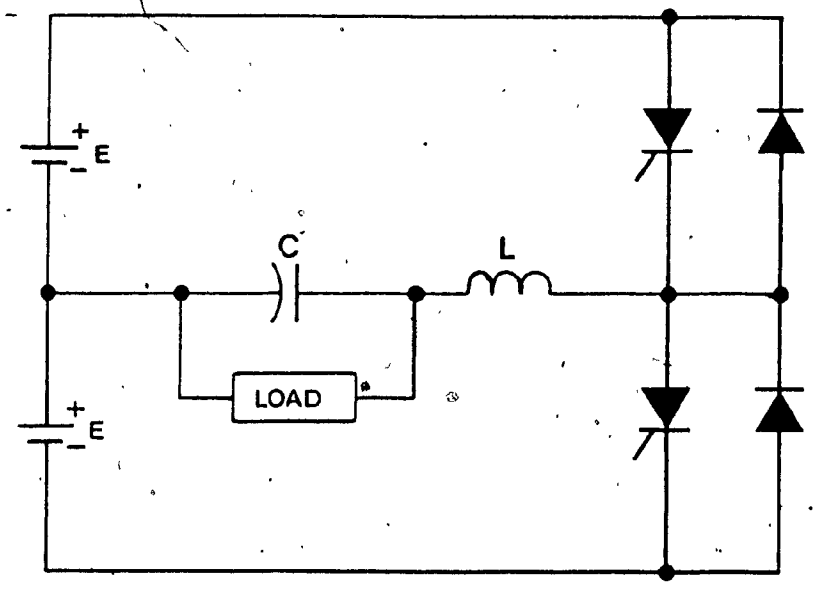

Fig. 1.3b Half-bridge resonant inverter with the load across the resonating capacitor.

literature for traction applications [1], [2], for driving high power ac locomotives supplied from a high voltage dc line. A high frequency link system can be used in such a situation to achieve voltage transformation and obtain manageable transformer sizes. In the absence of a high frequency link, very large transformer sizes would be necessary to accommodate the low frequencies required for starting.

The power converter cascade consisting of a dc-high frequency ac inverter followed by a cycloconverter is referred to as a cycloinverter [3]. The use of cycloinverters for power conversion from fuel cells for aerospace applications was proposed by Lawson [4]. Size and weight of equipment are of critical importance in such applications and so the use of high frequency power conversion is attractive.

Nishimura et. al. investigated a pulse-width controlled cycloinverter and used it to control the exciting current of an induction generator [5]. The cycloinverter in this case consisted of a parallel capacitor commutated square-wave high frequency inverter; the inverter voltage pulses are selectively allowed to appear on the output lines by the cycloconverter switches. Output voltage control is

achieved by dropping or including pulses. Sinusoidal output is obtained by filtering the discrete pulses at the output.

An inverter-cycloconverter system was proposed by Bourbeau for synchronous motor railcar propulsion [6]. In this scheme, a three-phase resonant inverter is coupled to a three-phase three pulse cycloconverter by means of series coupling capacitors. The system is used to supply a controlled current to the synchronous motor; the current is controlled by varying the frequency of operation of the resonant inverter. The high frequency currents are also used to provide excitation for the field of the synchronous machine through a current transformer, the field current thus being made proportional to the armature current.

A dc-dc conversion scheme utilising a series resonant inverter as a high frequency link was proposed by Schwarz [7],[8],[9]. The rectifier load is connected in series with the LC resonant circuit. The converter therefore possesses the characteristics of a current source. Current is regulated by controlling the frequency of operation of the inverter. Although ac output can be obtained using anti-parallel output converters [10],[11], such arrangements do not employ straightforward cycloconversion

techniques. The reason is that, the output converters, being connected in series with the resonant circuit, see a high frequency current rather than voltage.

McMurray investigated an electronic transformer utilising a high frequency link [12]. 60 Hz ac input is chopped at a high frequency of about 10 kHz using a thyristor series inverter. The high chopping frequency results in a reduction in the transformer size. The 60 Hz waveform is reconstructed on the secondary side of the transformer by further thyristor switches which are operated in synchronism with the switches on the primary side. Thus the input and output are at the same frequency and the system is primarily envisaged as a transformer. The link again acts as a high frequency current source.

Bedford proposed a family of power converters employing a high-frequency link, for supplying power to loads such as ac motors [13]. The link is constituted by a parallel resonant LC tank circuit. Typically, with a dc input, the tank is excited by an inverter. The inverter is operated at a frequency slightly above the resonant frequency of the tank, so that the tank impedance is effectively capacitive. The tank therefore draws leading current and provides commutation for the inverter. The output converter is a cycloconverter or phase-controlled

rectifier which uses the tank voltage as its input. By increasing the inverter operating frequency, additional leading kVA is obtained for commutating the inverter under conditions of increased loading. The inverter operating frequency is thus mainly used to adjust the commutation margin [14], and regulation of the output voltage is achieved through phase control in the output converter. For ac input, the inverter is replaced by a cycloconverter. The control and potential performance of this type of system were investigated by Bose and Espelage [15].

The use of high frequency links has also been considered for high power utility applications. Gyugyi et. al. investigated a high frequency link scheme for applications such as interconnection of power systems [16],[17]. In this case, the link consists of a three phase parallel LC tank circuit, excited by a separate current-fed inverter. The tank voltage is then used to provide commutation means for cycloconverters which handle the main power flow between the two systems being interconnected. Since the cycloconverters depend on the link voltage for commutation, their operation is not affected by fluctuations or transients in the line voltages. The scheme allows control of the power factor at the interface to the power systems. In terms of anticipated cost, it appears to compare well with more conventional systems [16].

It promises to be a potential alternative in such utility applications.

High-frequency link conversion schemes have been proposed for interfacing solar cell arrays to the ac power line. The small transformer size resulting from high frequency operation makes this arrangement attractive [18], [19]. Considerations of weight and size are of major importance in on-board power supplies for vehicles. This is another area where the potential offered by high frequency links has attracted investigation [20].

Thus high frequency link power conversion has been considered for a number of applications. Such schemes generally involve an additional stage of power conversion. Therefore, for very high power utility applications, extensive investigation will be required before their credentials are established. For power levels up to a few tens of kilo-watts, however, and especially in applications requiring light weight and small size of conversion equipment, such as auxiliary vehicle power supplies, high frequency links are attractive. Their acceptance has also been accelerated by recent improvements in power semiconductor technology, which have resulted increased switching speeds for power thyristors and also in continuing improvement in the power handling capability of

transistors. The technique of high frequency conversion should therefore find increasingly widespread application.

1.3 Scope of the thesis:

In the context of power conversion starting from a dc voltage source, high frequency inverters are necessary to realise a high frequency link stage. The circuit of Fig. 1.3b is a very simple inverter realisation and satisfies many of the requirements in such an application. This thesis investigates the performance of the inverter of Fig. 1.3b when it is used as the link inverter in high frequency link schemes and presents techniques of dc-dc and dc-ac power conversion using the inverter as a high frequency link.

A comprehensive steady-state analysis of the inverter is developed in Chapter 2, with the load on the inverter being a phase-controlled converter, as is the case in high frequency link schemes. The analysis leads to a closed form solution for the operating point of the inverter, under conditions of lagging as well as leading control angle in the phase-controlled converter and for both forward and reverse power flow. Losses are not considered in the analysis.

In Chapter 3, the performance of the inverter with an uncontrolled (diode) rectifier load is obtained using the

analysis developed in Chapter 2. The results are used to characterise a dc-dc conversion scheme using the resonant inverter as a variable high frequency link. Regulation of the output voltage by control of the inverter frequency is explained.

In Chapter 4, the use of the inverter circuit as a current-regulated four-quadrant conversion arrangement is described. This arrangement includes the composite functions of inversion and cycloconversion in a single stage.

In Chapter 5, a dc-ac power conversion scheme, using two high frequency links is developed and the phenomena associated with power flow are analysed.

The different conversion techniques are confirmed experimentally using laboratory breadboards. Design guidelines are provided for selecting components.

CHAPTER 2

STEADY-STATE ANALYSIS OF THE HIGH FREQUENCY INVERTER

2.1 Introduction:

The high frequency inverter configuration of Fig. 1.3b is redrawn in Fig. 2.1 and shown feeding a converter load. The inverter was originally developed to supply high frequency sine-wave power to ac loads [21]. Analysis of the circuit then has to take into account the fact that the time constants of the load across the resonating capacitor are of the same order as the period of inverter operation. Consequently, a closed form solution for the steady-state operating point of the inverter is difficult to obtain. The technique conventionally employed is to represent the behaviour of the circuit by the governing simultaneous differential equations. These equations are then numerically solved using the digital computer. The solution is allowed to proceed through a number of transient cycles until the steady-state is detected by noting matching end conditions [21]. The results of such an analysis are tabulated for different parameter combinations in the inverter and used in designing the inverter.

When the inverter is used as a high frequency link stage in dc-dc or dc-ac power conversion, however, the

loading on the inverter is different from the situation considered in the above analysis in several respects. For example, the link inverter can encounter regenerative loads. Typically, this situation occurs in a dc-ac conversion process, because the reactive portions of the low frequency output cycle are reflected onto the inverter as a regenerative load for several cycles of inverter operation. This condition cannot be conveniently handled by the conventional analysis. There is a further motivation for adopting a different technique of analysis. In link applications, the load current, whether dc or ac, varies at a rate very much slower than the operating frequency of the inverter. Therefore the load current reflected onto the link inverter by the output converter of the link scheme is essentially a square wave. This fact can be utilised to provide considerable simplification in analysis and leads to an analytical solution for the steady-state operating point of the inverter.

A steady-state analysis of the inverter is therefore developed, in order to obtain the operating point of the inverter. The parameters which give rise to a particular operating point are the circuit component values, operating frequency, magnitude of the load current reflected onto the inverter and the phase angle of this reflected load current with respect to the link voltage. The steady-state is characterised in terms of the capacitor voltage

and inductor current at the beginning of an operating cycle of the inverter. Various other quantities of interest, such as the commutation margin, the current carried by the semiconductor devices, the link voltage etc. can then be derived in a straightforward manner.

2.2. Basic Inverter Circuit:

The basic circuit that is considered in the analysis is shown in Fig. 2.1. The inverter has a half-bridge configuration, with a centre-tapped dc source. Other versions such as a full-bridge or centre-tapped load are also possible. The analysis can be easily adapted to such alternative configurations. Therefore the half-bridge configuration is considered throughout. Thyristors are shown as the power switches. Other switching devices such as power transistors can equally well be employed, although in that case the commutating ability of the resonant circuit is no longer a critical factor. Thyristors, because of their many attractive characteristics such as ruggedness and ease of gating, enjoy a dominant role in power conversion. Since the resonant circuit configuration considered here results in the thyristors being commutated naturally, it is particularly well-suited for thyristor inverters. Therefore thyristors with low recovery times are used as the switching elements in the inverter throughout this thesis.

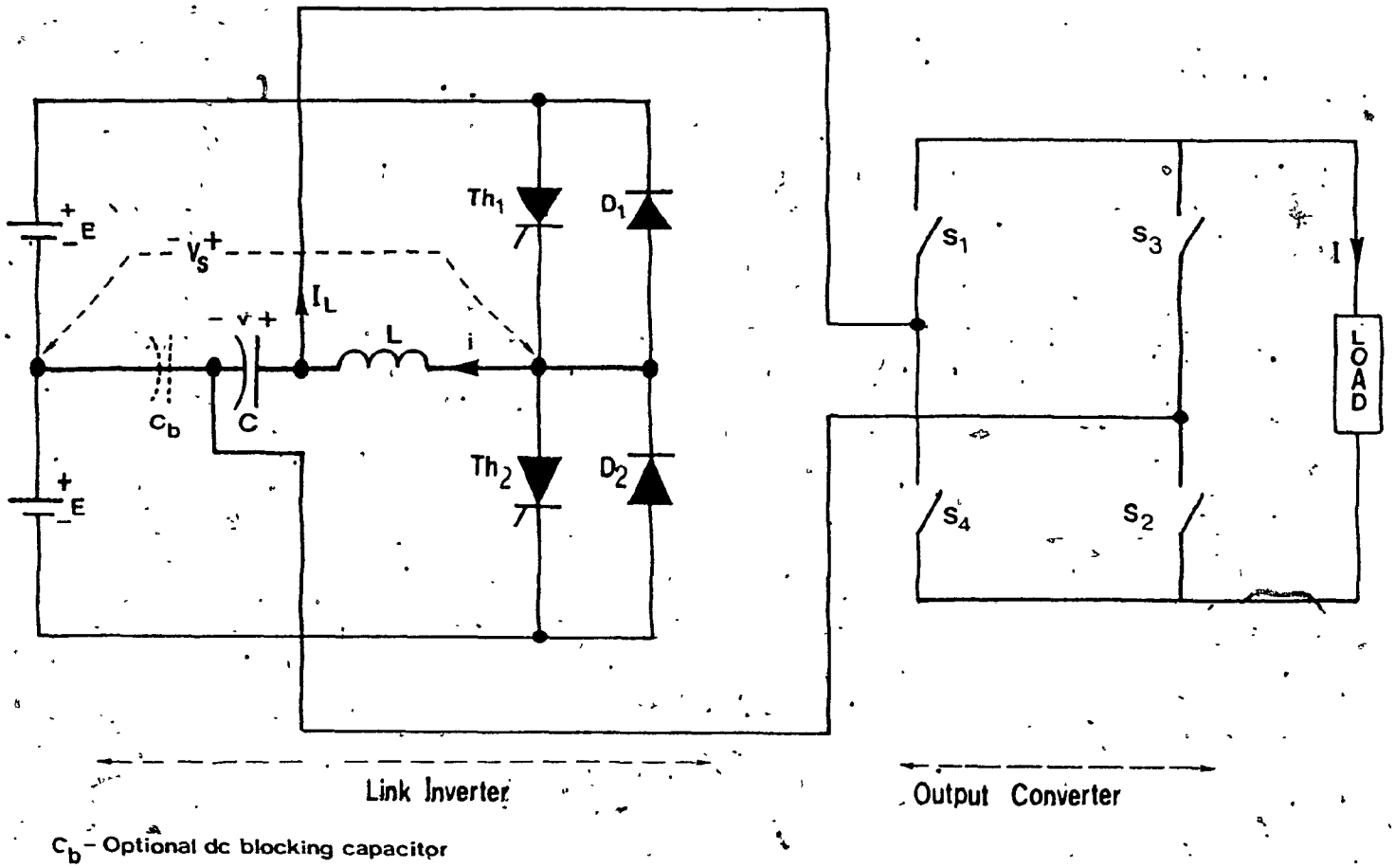

Fig. 2.1 Basic circuit of high frequency link converter

The semiconductor elements in the inverter consist of the two thyristors Th1 and Th2, accompanied by their respective feed-back diodes D1 and D2. The inverter feeds a series LC circuit. Typically, for inverter frequencies of the order of a few kilo-hertz, the inductor is of the order of a few tens of microhenries and the capacitor of the order of a few microfarads. The voltage across the capacitor is used as the output of the inverter, i.e. the capacitor voltage is the link voltage. The load on the inverter is the output converter consisting of the four switches S1 to S4, the typical situation in a link application. In a dc-dc conversion scheme, for example, the output converter will be a rectifier (controlled or uncontrolled), whereas for dc-ac conversion, it will be a cycloconverter. The polarity conventions for different circuit quantities such as capacitor voltage, resonant current in the inductor and the load current reflected onto the inverter by the output converter are established in Fig. ?.1.

Auxiliary circuit elements, such as di/dt limiting reactors, snubbers and possible dc blocking capacitors are not shown in the diagram. Their effects are not considered in the analysis, which concentrates on investigating the effect of various power flow conditions on the steady-state operating point of the inverter. Losses are also not considered.

2.3 Operation Under No-load:

In order to follow the operation of the inverter, it is helpful as a first step to consider the operation under no-load i.e. with the output converter disconnected in Fig. 2.1. Assuming that there is no initial voltage across the capacitor and no initial current in the inductor, a resonant pulse of current flows in the LC circuit on firing Th1. The waveforms of the current and the capacitor voltage are shown in Fig. 2.2a. When the current reverses, it flows through the diode D1 and thyristor Th1 is reverse biased by the voltage drop across the diode. Similar phenomena occur in the lower half of the circuit when Th2 is fired.

In Fig. 2.2a it is assumed that the time T_s between the instants at which Th1 and Th2 are fired is greater than the period of oscillation $T=2\pi\sqrt{LC}$ of the LC circuit. In this case, the current pulses in the upper and lower halves of the circuit are separated from each other. If now the interval T_s is reduced and made equal to T, the two current pulses join to produce a continuous wave. The capacitor voltage pulses also join to produce an ac voltage waveform. This waveform is of course not purely sinusoidal, the positive and negative halves being described by the function $1-\cos wt$, where $w=1/\sqrt{LC}$. This mode of operation

is depicted in Fig. 2.2b. The turn-off time available to the thyristors is the time for which the corresponding feed-back diodes conduct. In Fig. 2.2b the recovery time available is T/2.

It is possible to reduce the firing interval T_s still further so that $T_{s_1} < T$. Fig. 2.2c shows the first two cycles of this mode of operation. It can be seen from the figure that the current in the feed-back diode is not allowed to proceed to zero. Instead, current is transferred from D1 to Th2, when Th2 is fired. When the second oscillation starts through Th2, the capacitor has an initial voltage and the inductor an initial current. During the second oscillation, the amplitude of the voltage swing exceeds 2E. The circuit obtains its steady-state after a few oscillations and the waveforms repeat themselves during successive oscillations. Fig. 2.2d shows typical steady-state waveforms. It can be seen that the capacitor voltage waveform is an alternating one whose frequency is $1/2T_s$ and whose amplitude and shape are determined by the interval T_s between the firing of alternate thyristors. Therefore the frequency of firing provides a means of controlling the amplitude of the ac waveform. It must however be noted that the turn-off time available to the thyristors is the duration for which the feed-back diodes conduct and this duration decreases as the inverter half-period T_s is reduced.

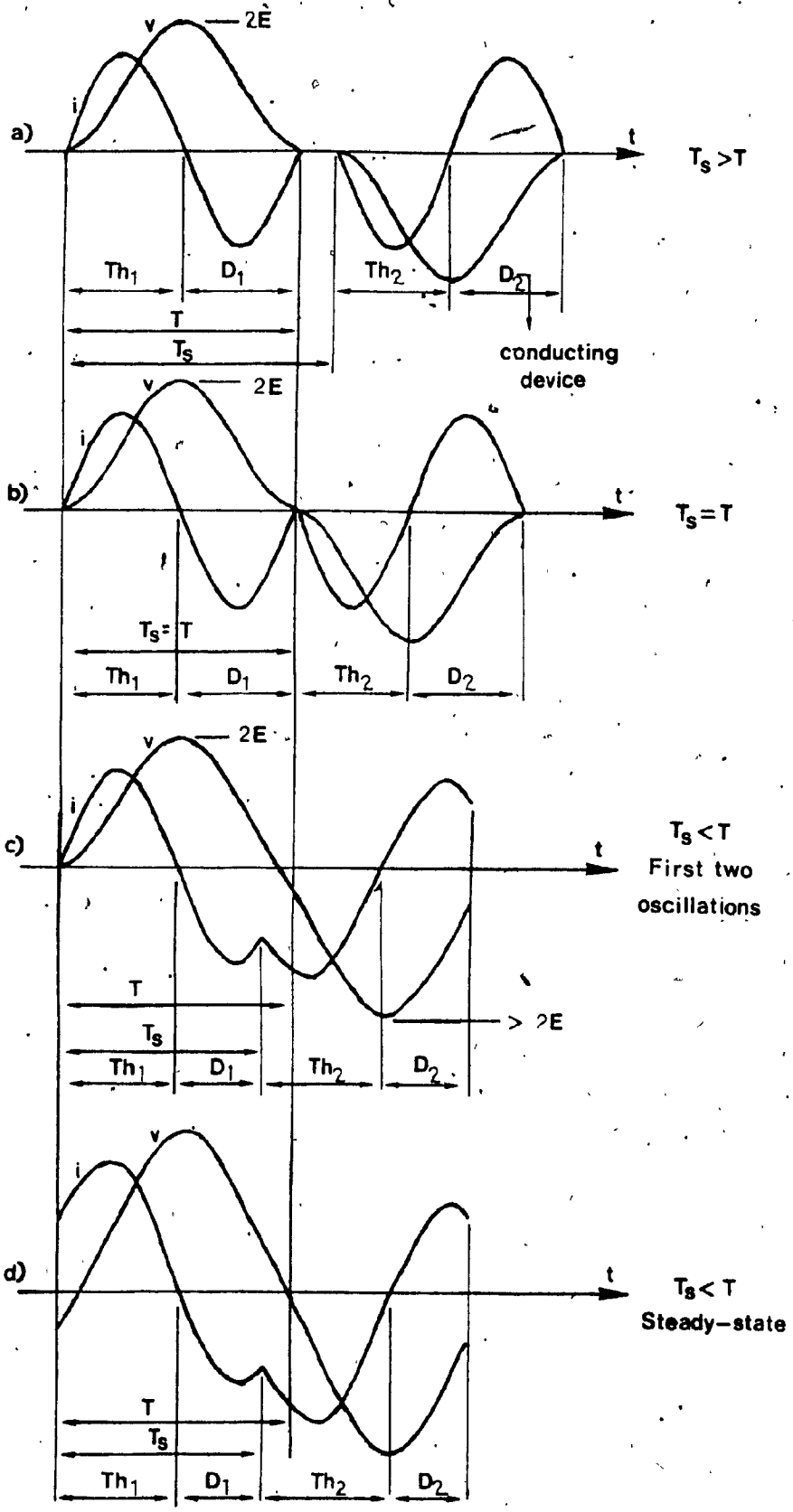

Fig. 2.2 Circuit waveforms without converter load.

2.4 Characteristics of Converter Load:

In link applications, the load on the high frequency inverter is a converter, as shown in Fig. 2.1. The load current I is either dc or low frequency ac (typically 60 Hz). Any ripple in the load current is caused by the high frequency components in the output voltage of the converter and occur at frequencies of the order of twice the inverter frequency. Since the inverter frequency is of the order of kilo-hertz and thus very much greater than the load frequency, it is reasonable to assume that there is sufficient inductance present in the load to suppress all ripple currents and consequently load current I consists only of the wanted frequency component. Therefore the magnitude of I can be assumed to be constant over a cycle of the high frequency inverter. The load current I is therefore reflected as a square current wave I_L of amplitude I across the link capacitor over one cycle of the link voltage. Fig. 2.3 shows typical waveforms of the link voltage v and the reflected load current. The phase displacement between the two waves is equal to the firing angle in the output converter.

In the case of dc output, the firing angle and the magnitude of the load current are constant. Therefore Fig.2.3 represents the actual loading conditions.

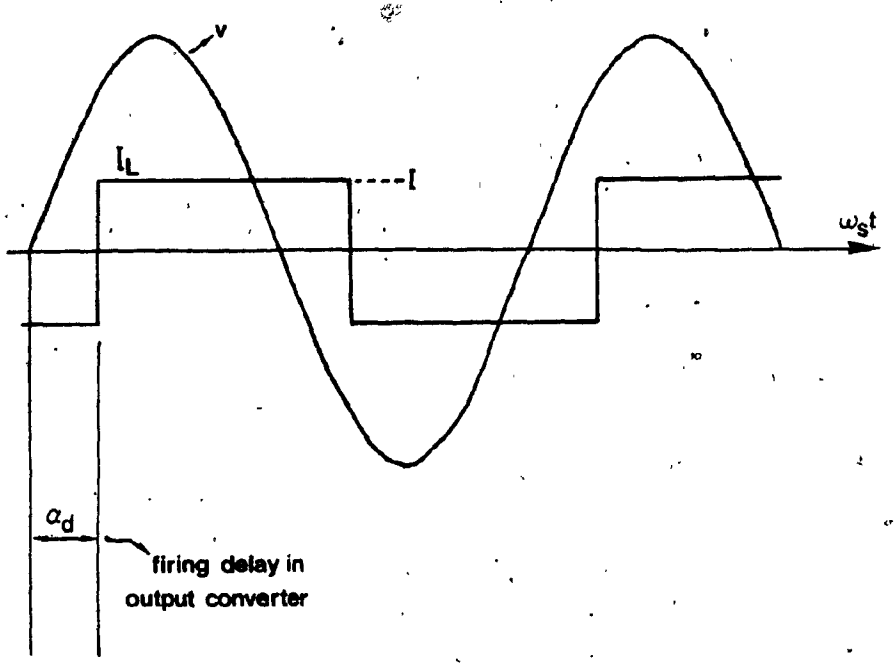

Fig. 2.3 Waveforms of link voltage and reflected load current.

In the case of ac output, the output converter is a cycloconverter and the firing angle is modulated. The magnitude of the load current also varies at the load frequency. Therefore the phase and amplitude of the square current wave in Fig.2.3 vary continuously from one inverter cycle to the next. The cycloconverter can be represented to a first approximation by a phase-controlled rectifier and the effect of loading can be studied at various firing angles and loading current magnitudes. This approach provides adequate indication of the effect of the loading on the link voltage, the current ratings for the components etc. and is more amenable to analysis.

The output converter shown in Fig.2.1 consists of ideal bidirectional switches, which can be turned on or off as desired. If thyristors are used as the switches in the output converter, they have to depend on the alternating link voltage for turning off. In that case only lagging control angles can be implemented in the output converter. But if switches capable of turning off are assumed, it is also possible to have leading or advanced firing angles in the output converter. Analogous loading conditions also arise in the new configuration described in Chapter 5. Closely related to the firing angle is the direction of power flow in the overall power conversion arrangement.

The forward direction for power flow is considered to be from the dc supply to the link and consequently from the link to the load through the output converter. The reverse direction for power flow is then from the load to the link and thus from the link to the dc supply. Thus, the link can encounter the following four classes of loading.

1) lagging (delayed) firing in the output converter, forward power flow ($0<\alpha_d<90$).

2) lagging (delayed) firing in the output converter, reverse power flow ($90<\alpha_d<180$).

3) leading (advanced) firing angle in the output converter, forward power flow ($0<\alpha_a<90$).

4) leading (advanced) firing angle in the output converter, reverse power flow ($90<\alpha_a<180$).

The link voltage and reflected load current corresponding to these four classes of loading are shown in Fig. 2.4.

2.5 Basis of Analysis:

The steady-state operating point of the inverter corresponding to a given loading condition can be characterised by two variables: the initial capacitor

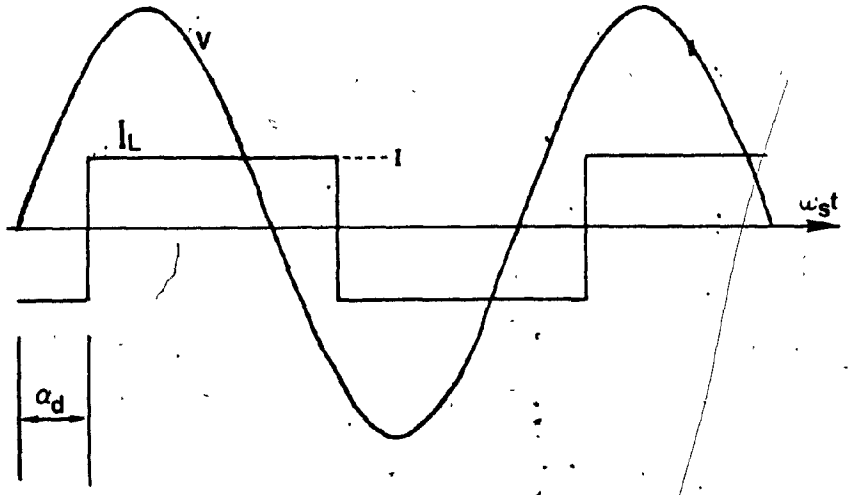

Fig. 2.4a Delayed firing in output converter; forward power flow ($0<\alpha_d<90^\circ$)

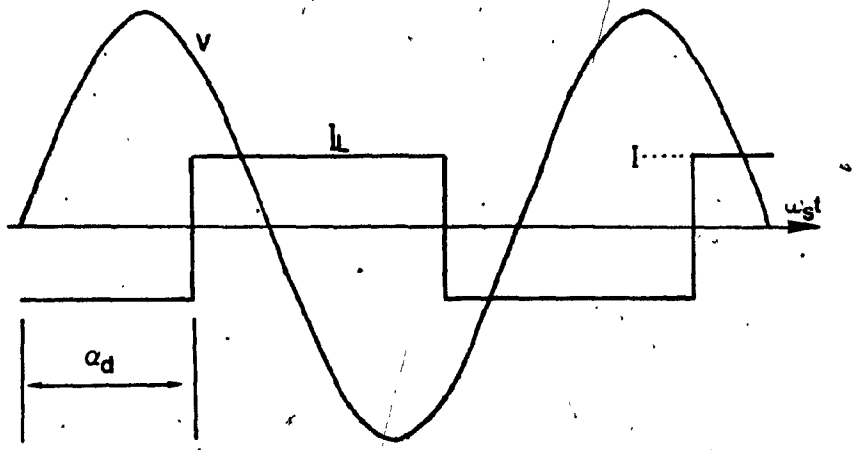

Fig. 2.4b Delayed firing in output converter; reverse power flow ($90<\alpha_d<180$)

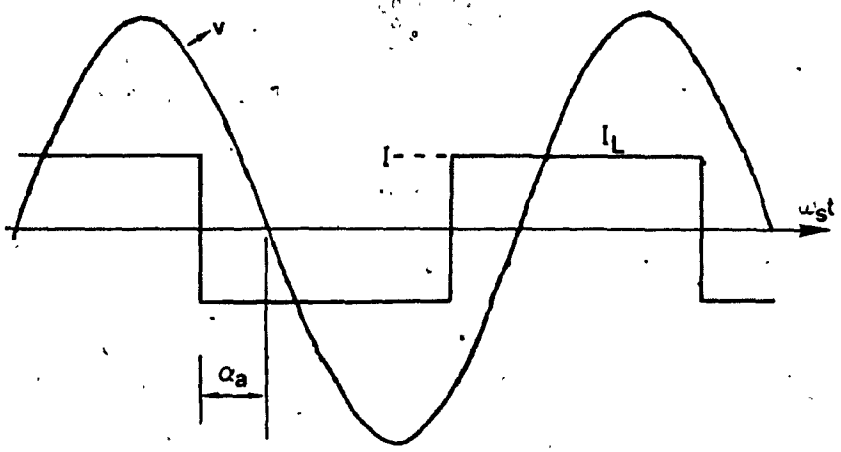

Fig. 2.4c Advance firing in output converter; forward power flow ($0<\alpha_a<90$)

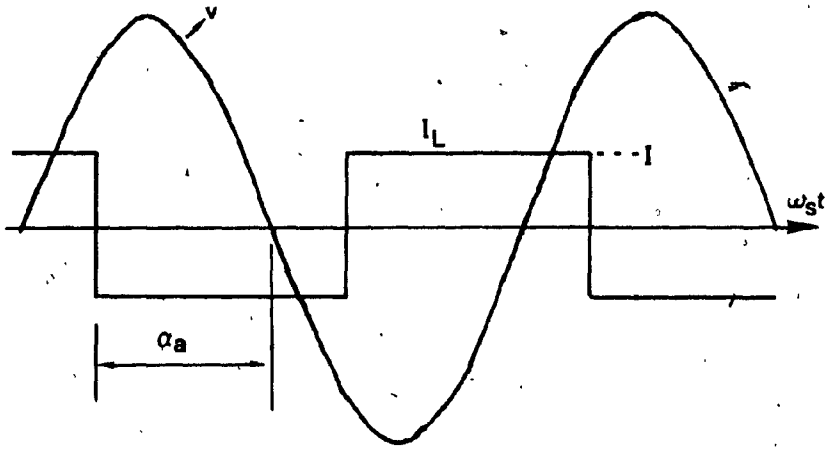

Fig. 2.4d Advance firing in output converter; reverse power flow ($90<\alpha_a<180$)

Fig. 2.4 Waveform of link voltage and reflected load current for the four classes of loading.

voltage v_0 and the initial inductor current i_0. Further, since the top and bottom halves of the inverter are identical, the capacitor voltage and inductor current have the same magnitudes and opposite signs at the beginning and end of a half-cycle of the inverter. This fact is used as the basis of the analysis. The response of the inverter is traced over a half-cycle. The steady-state operating point is obtained by constraining the capacitor voltage and the inductor current to be equal and opposite at the beginning and the end of the half-cycle. To this end it is first necessary to obtain expressions for the circuit response over a half-cycle, corresponding to different loading conditions.

2.6 Two Basic Circuit Modes:

Examination of the circuit in Fig.2.1 reveals that, during a half-cycle of inverter operation when one of the two halves (upper/lower) is active, there are basically two possible modes of circuit operation. The modes arise because the load current I can be reflected onto the link in two possible directions. In the first mode, labelled Mode I, the dc source attempts to charge the capacitor while the load current drains it. In the second mode, labelled Mode II, the load current aids the dc source in charging the capacitor. The equivalent circuits for the two modes are shown in Fig.2.5. Following the assumption

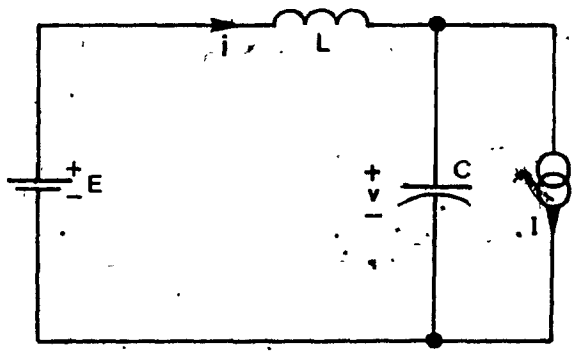

Fig. 2.5a Equivalent circuit for mode I.

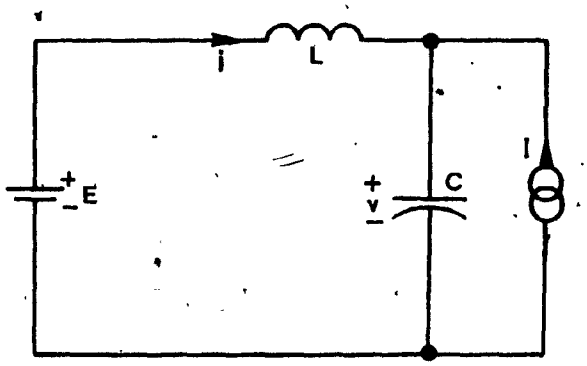

Fig. 2.5b Equivalent circuit for mode II

Fig. 2.5 Equivalent circuits for the two circuit modes.

that the magnitude of the load current does not change appreciably over a cycle of the inverter, the load is represented in the equivalent circuits as a constant current source I. Circuit operation changes from one mode to the other when one pair of switches along a diagonal in the output converter is turned off and the complimentary pair is turned on. The occurance of the two modes is brought out in Fig.2.6 for each half of the inverter. It can be seen, by comparing Figures 2.6b and 2.6c, and similarly Figures 2.6a and 2.6d, that when operation is transferred in the inverter from one half to the other, the prevailing circuit mode changes.

The response of the circuit for the two modes can be obtained from the respective equivalent circuits.

Response For Mode I:

From Fig. 2.5a, the resonant current i and the capacitor voltage v are governed by the following differential equations:

$$L(di/dt)+(1/C)\int_{t_1}^{t} (i-I)dt = E \qquad (2.1)$$

$$v = E-L(di/dt) \qquad (2.2)$$

Solving (2.1) for i and subsequently (2.2) for v, the solutions can be written as follows:

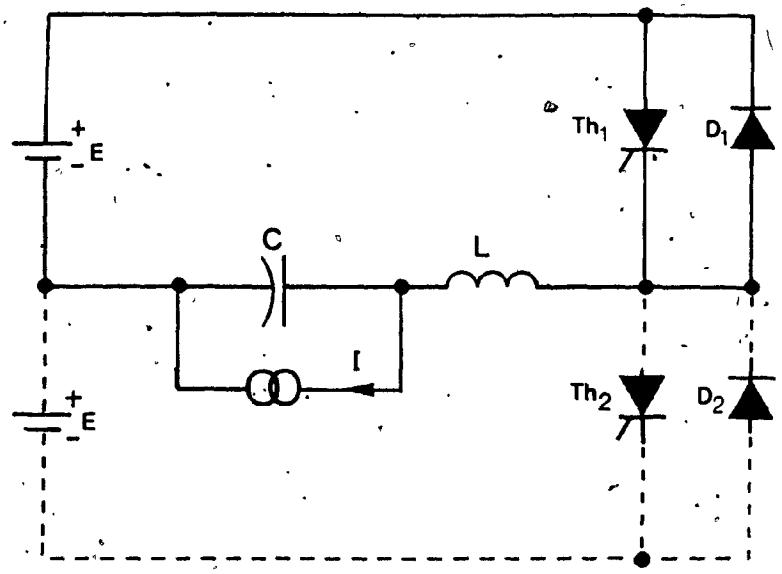

Fig. 2.6a Mode I with upper half of inverter active.

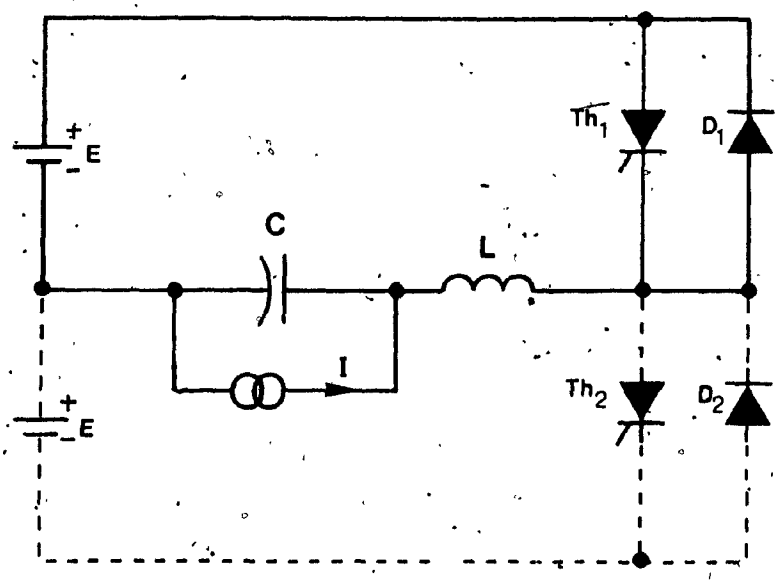

Fig. 2.6b Mode II with upper half of inverter active.

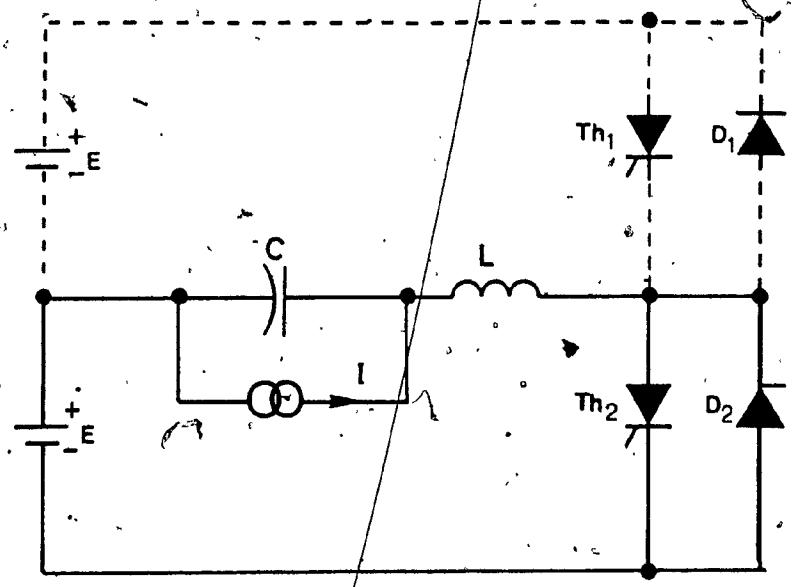

Fig. 2.6c Mode I with lower half of inverter active.

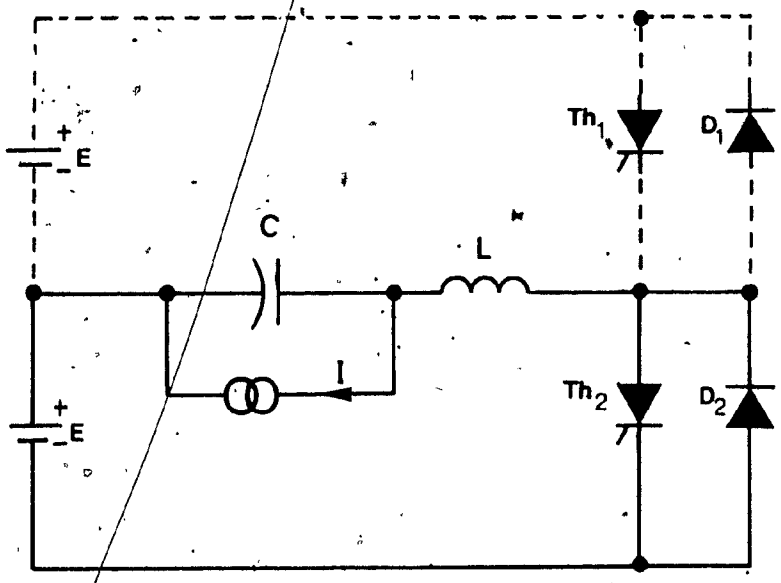

Fig. 2.6d Mode II with lower half of inverter active.

Fig. 2.6 Occurance of the two modes in each half of the inverter.

$$i = (1/z)(E-v_i)\sin wt + (i_i-I)\cos wt + I \qquad (2.3)$$

$$v = E-(E-v_i)\cos wt + z(i_i-I)\sin wt \qquad (2.4)$$

where,

$$z = \sqrt{L/C} \qquad (2.5)$$

$$w = 1/\sqrt{LC} \qquad (2.6)$$

v_i -initial value of v at the beginning of the mode;

i_i -initial value of i at the beginning of the mode.

Response For Mode II:

The solutions for the resonant current i and the capacitor voltage v corresponding to Mode II can be similarly written as:

$$i = (1/z)(E-v_i)\sin wt + (i_i+I)\cos wt - I \qquad (2.7)$$

$$v = E-(E-v_i)\cos wt + z(i_i+I)\sin wt \qquad (2.8)$$

Therefore, over a half-cycle of inverter operation, corresponding to the interval over which one half of the inverter is active, the response of the circuit can be analytically defined, provided the order in which the

modes occur and the duration of each mode is known.

2.7 Mode Sequences Corresponding to Different Load Conditions:

The mechanism of power flow in the inverter of Fig. 2.1 can be appreciated by examining the phase relationship between the two voltages V_s and v. V_s is the square-wave that is applied across the entire LC circuit in the inverter. Its amplitude is E, the dc supply voltage from centre-tap to either pole. v is the link voltage i.e. the voltage across the resonating capacitor alone and it closely approximates a sinusoid. The two voltages V_s and v can be regarded as ac voltages separated by a reactor, namely the resonating inductor L. As is known from the theory of power systems the phase relationship between V_s and v is decided by the direction of power flow between the two voltages. For forward power flow i.e. power flow from the dc supply to the link, the fundamental component V_{s1} of V_s leads v. For reverse power flow, V_{s1} lags v. V_s being a square wave, its zero-crossings coincide with those of its fundamental V_{s1} and so the above conclusions regarding phase relationships apply for the square wave V_s as a whole. Thus V_s leads v for forward power flow whereas V_s lags v for reverse power flow.

In terms of the phase relationship between the link voltage v and the reflected load current I_L seen by the link, the above observations can be restated as follows:

If the reflected load current lags or leads the link voltage v by an angle less than 90 degrees in magnitude, then V_s leads v.

If the reflected load current lags or leads the link voltage by an angle greater than 90 degrees in magnitude, then V_s lags v.

Based on these observations, the circuit waveforms can be drawn corresponding to various loading conditions and from these the corresponding mode sequences within a half-cycle of inverter operation can be deduced. This is illustrated in Fig.2.7 and Fig.2.8 for lagging and leading phase relationship, respectively, between the link voltage and reflected load current. One detail to be noticed in the latter case of leading phase relationship is that the order in which the modes occur changes as the lead angle α_a becomes equal to a particular value α_{ac} and again as it becomes equal to $180-\alpha_{ac}$. It can be seen that for $\alpha=\alpha_{ac}$ and again for $\alpha=180-\alpha_{ac}$, a single circuit mode prevails for the entire half-cycle of the inverter. For all other values of α, both modes occur during a half-cycle. The value of α_{ac} is decided by the circuit parameters and the operating frequency

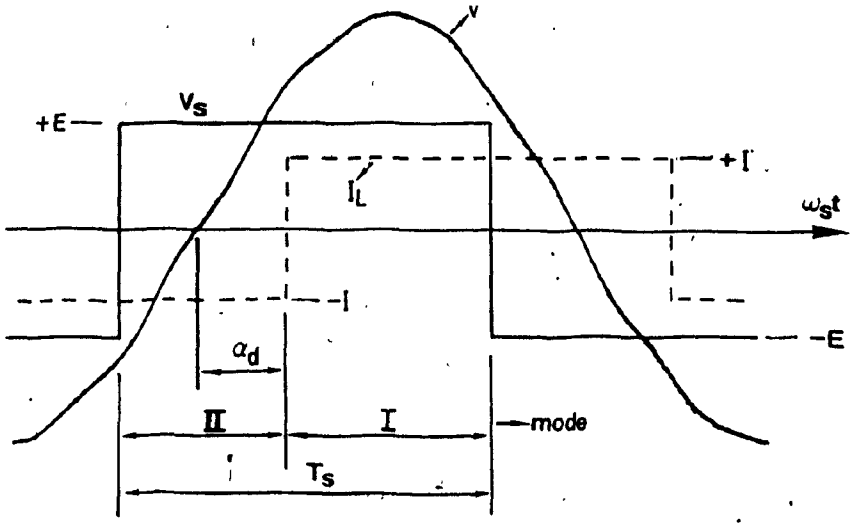

Fig. 2.7a Forward power flow; $0<\alpha_d<90$; V_s leads v.

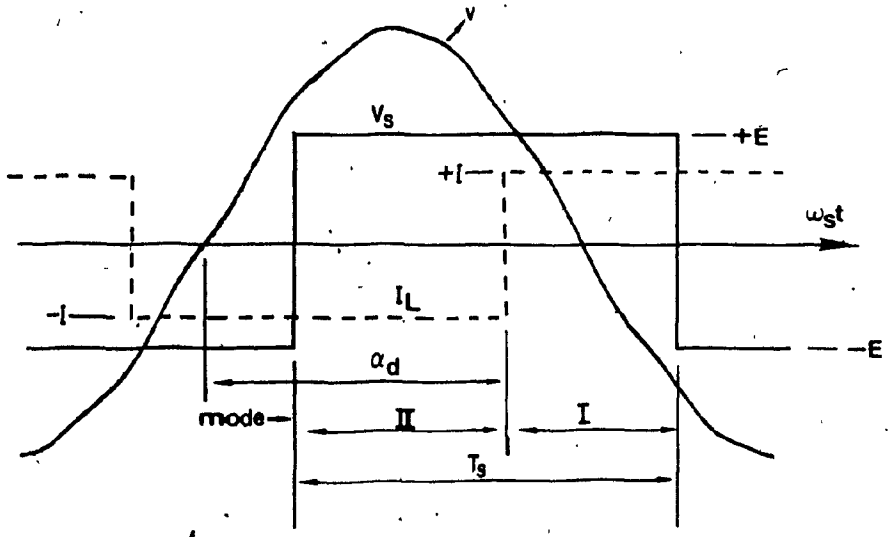

Fig. 2.7b Reverse power flow; $90<\alpha_d<180$; V_s lags v

Fig. 2.7 Mode sequences for lagging phase relationship between link voltage and reflected load current.

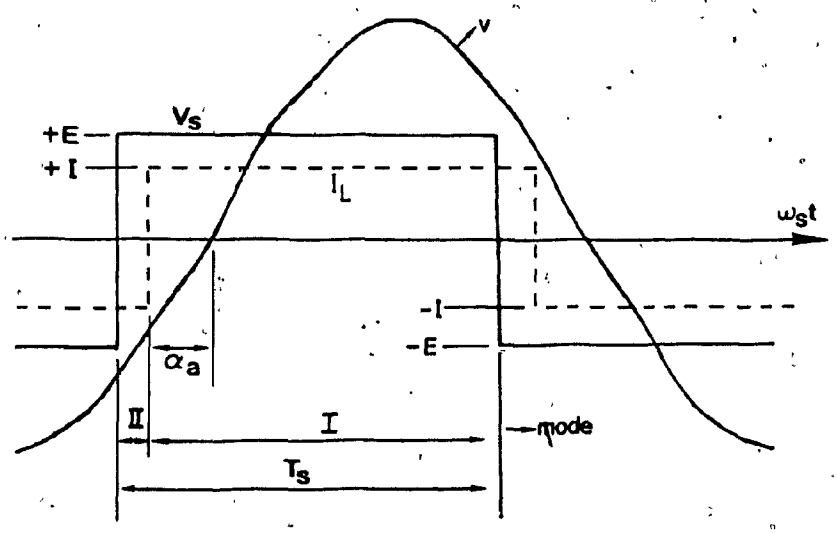

Fig. 2.8a Forward power flow; $0<\alpha_a<\alpha_{ac}$; V_s leads V

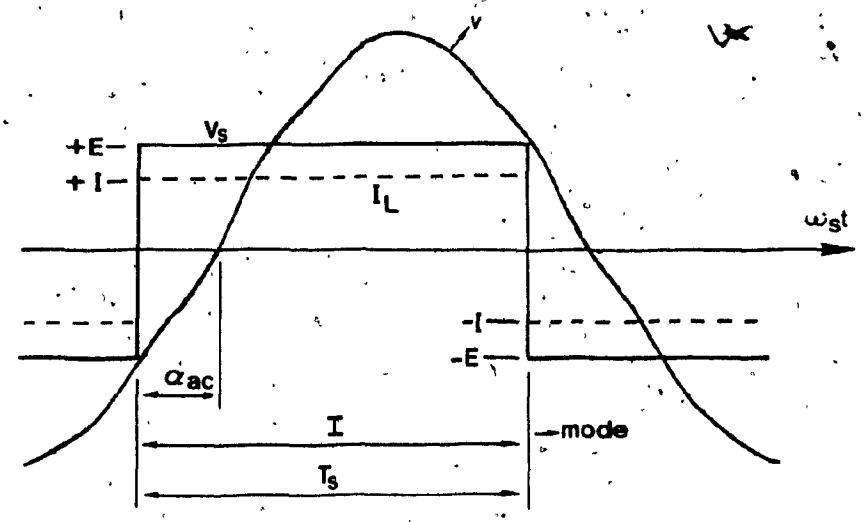

Fig. 2.8b Forward power flow; $\alpha_a=\alpha_{ac}$; V_s leads v.

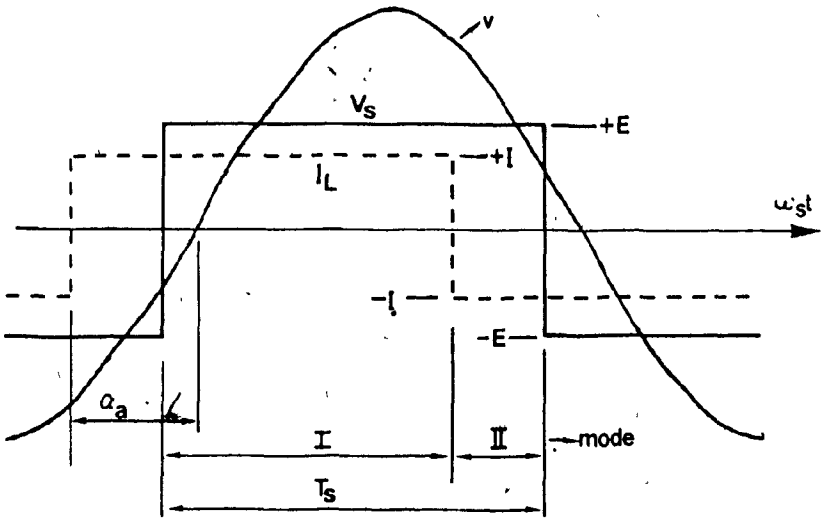

Fig. 2.8c Forward power flow; $\alpha_{ac} < \alpha_a < 90$; V_s leads v.

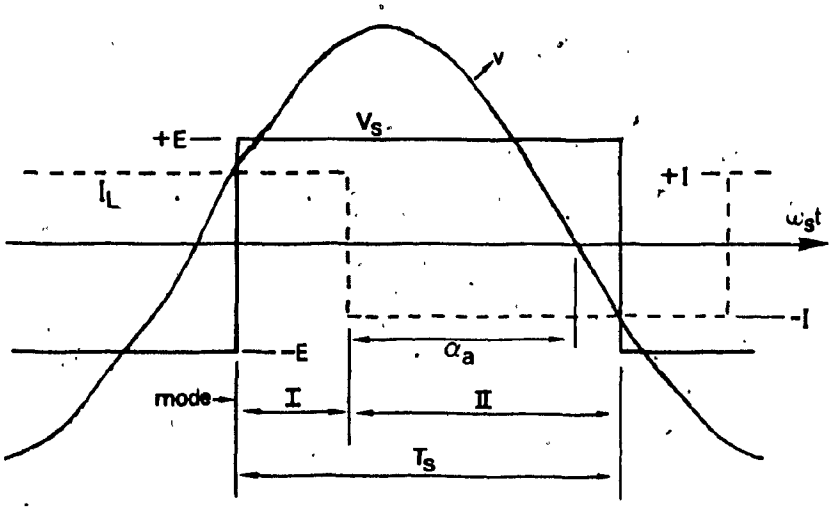

Fig. 2.8d Reverse power flow; $90 < \alpha_a < 180 - \alpha_{ac}$; V_s lags v.

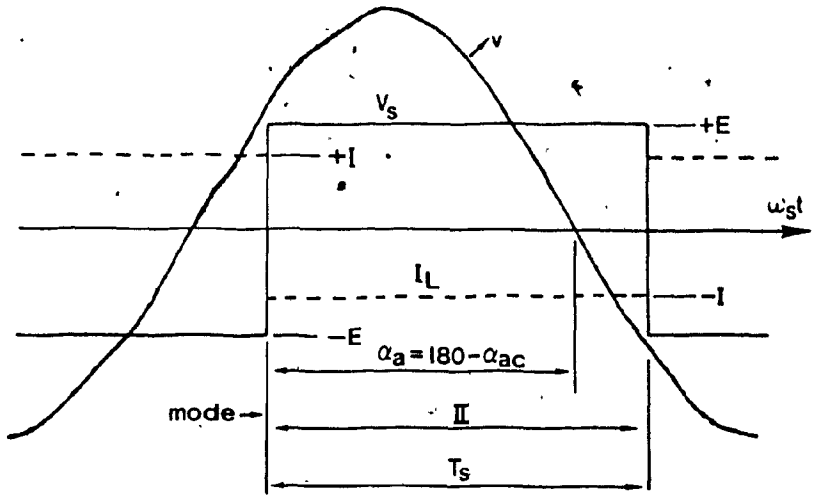

Fig. 2.8e Reverse power flow; $\alpha_a = 180 - \alpha_{ac}$; V_s lags v.

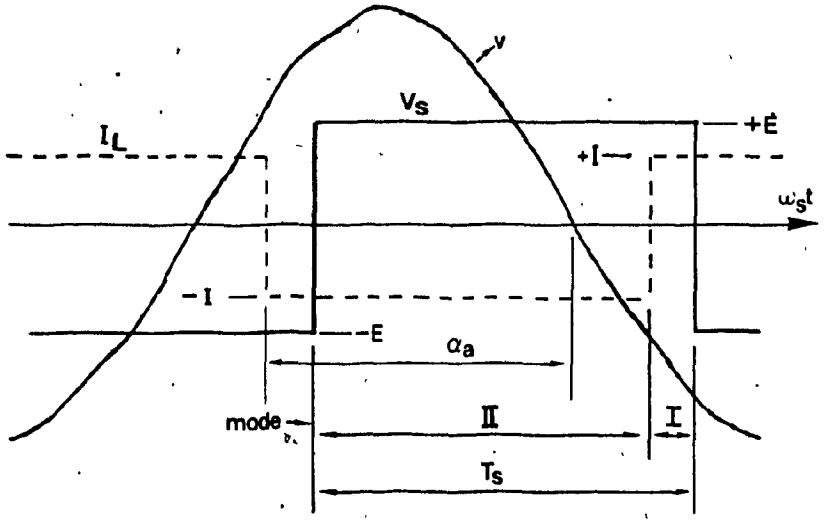

Fig. 2.8f Reverse power flow; $180 - \alpha_{ac} < \alpha_a < 180$; V_s lags v.

Fig. 2.8 Mode sequences for leading phase relationships between link voltage and reflected load current.

of the inverter. Relevant expressions are given in Appendix A.

2.8 Analysis Corresponding To Two Loading Conditions:

Once having deduced the order of occurrence of the modes corresponding to various operating conditions as above, the steady-state operating point can be obtained. The analysis is carried out in detail for the two situations described in Fig.2.7a and 2.7b. The results for the loading conditions of Fig.2.8a to 2.8f are summarised in Appendix A, as their derivation is essentially similar to the procedure described here.

A) Reflected load current lags v, forward power flow ($0<\alpha_d<90$):

This condition is described in Fig.2.7a. Typical circuit waveforms, including resonant current i, for such a loading condition are drawn in Fig.2.9. The horizontal scale in Fig.2.9 is in terms of the natural resonant frequency w of the LC circuit. i_0, v_0 are the instantaneous values of the resonant current i and the link voltage v at the point A, which is considered as the beginning of a half-cycle for the inverter; i_1, v_1 are the respective values at point C. The values i_0 and v_0 are the unknowns which characterise the operating point of the inverter.

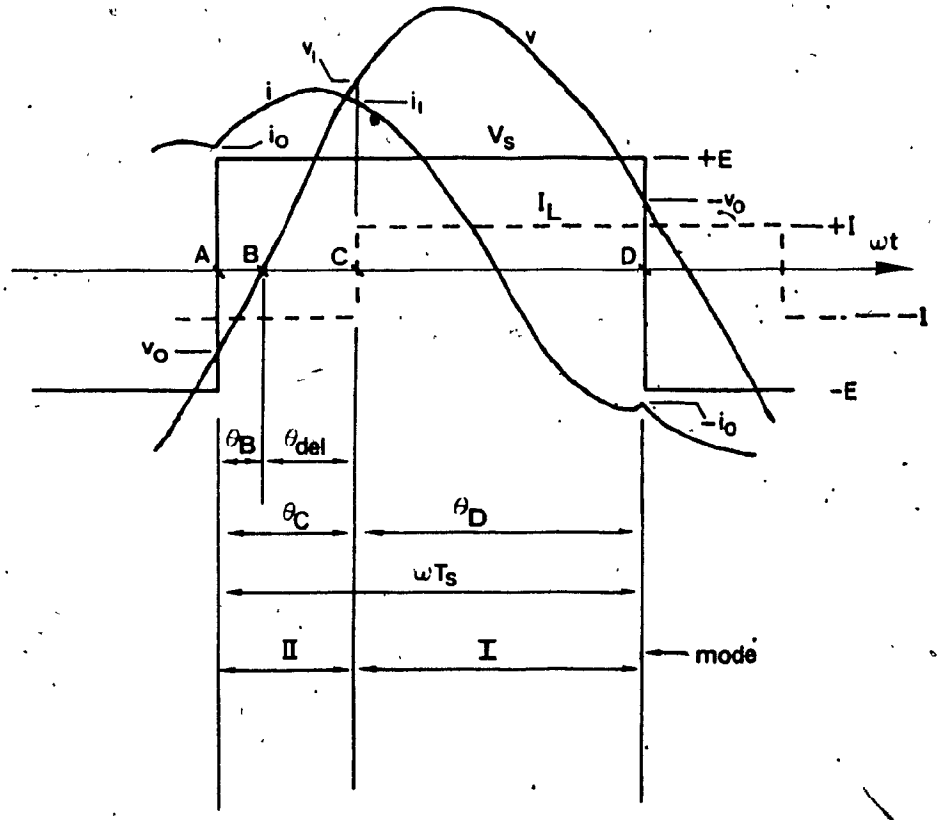

Fig. 2.9 Circuit waveforms for forward power flow with the reflected load current lagging the link voltage.

From A to C, the circuit operates in Mode II (Fig.2.5b) The response is governed by equations (2.7) and (2.8) Therefore,

$$i_1 = (1/z)(E-v_0)\sin\theta_C + (i_0+I)\cos\theta_C - I \qquad (2.9)$$

$$v_1 = E-(E-v_0)\cos\theta_C + z(i_0+I)\sin\theta_C \qquad (2.10)$$

At point B, v=0. Therefore,

$$E-(E-v_0)\cos\theta_B + z(i_0+I)\sin\theta_B = 0 \qquad (2.11)$$

The interval BC corresponds to the phase delay angle α_d on the w_s scale. So,

$$\theta_{del} = (\alpha_d/\pi)\ wT_s \qquad (2.12)$$

From C to D the circuit operates in Mode I (Fig.2.5a) and the response is governed by equations (2.3) and (2.4). Point D represents the end of the inverter half-cycle under consideration. In the steady-state, therefore, the values of i,v at D are equal and opposite to those at A. Thus, using (2.3) and (2.4) with i_1 and v_1 as initial conditions.

$$-i_0 = (1/z)(E-v_1)\sin\theta_D + (i_1-I)\cos\theta_D + I \qquad (2.13)$$

$$-v_0 = E-(E-v_1)\cos\theta_D + z(i_1-I)\sin\theta_D \qquad (2.14)$$

Substituting for i_1 and v_1 from (2.9) and (2.10) in (2.13) and (2.14),

$$-i_0 = (1/z)(E-v_0)\sin(\theta_C+\theta_D)+(i_o+I)\cos(\theta_C+\theta_D) -2I\cos\theta_D+I \qquad (2.15)$$

$$-v_0 = E-(E-v_0)\cos(\theta_C+\theta_D)+z(i_0+I)\sin(\theta_C+\theta_D) -2zI\sin\theta_D \qquad (2.16)$$

Now $\theta_C+\theta_D = wT_s$. Substituting in (2.15) and (2.16) and rearranging,

$$-v_0\sin wT_s + zi_0(1+\cos wT_s) = 2zI\cos\theta_D -E\sin wT_s-zI(1+\cos wT_s) \qquad (2.17)$$

$$v_0(1+\cos wT_s)+zi_0\sin wT_s = 2zI\sin\theta_D -E(1-\cos wT_s)-zI\sin wT_s \qquad (2.18)$$

(2.17) and (2.18) can be solved for i_0, v_0 in terms of θ_D and wT_s, giving:

$$i_0 = I\,\frac{\cos(wT_s-\theta_D)+\cos\theta_D}{1+\cos wT_s} - \frac{E\sin wT_s}{z(1+\cos wT_s)} - I \qquad (2.19)$$

$$v_0 = zI\,\frac{\sin\theta_D-\sin(wT_s-\theta_D)}{1+\cos wT_s} \qquad (2.20)$$

In terms of the angles θ_B and θ_{del}, (2.19) and (2.20) can be expressed as:

$$i_0 = I\,\frac{\cos(\theta_B+\theta_{del})+\cos(wT_s-\theta_B-\theta_{del})}{1+\cos wT_s} - \frac{E\sin wT_s}{z(1+\cos wT_s)} - I \qquad (2.21)$$

$$v_0 = zI\,\frac{\sin(wT_s-\theta_B-\theta_{del})-\sin(\theta_B+\theta_{del})}{1+\cos wT_s} \qquad (2.22)$$

(2.21), (2.22) can be substituted in (2.11) to obtain an equation in the unknown θ_B. This resulting equation can be solved for θ_B and the solution then used in (2.21) and (2.22) to obtain the operating point for any given phase delay angle θ_{del}. Thus, substituting (2.21) and (2.22) in (2.11),

$$E(1+\cos wT_s)-E(1+\cos wT_s)\cos\theta_B-E\sin wT_s\sin\theta_B$$
$$+zI\sin(\theta_D+\theta_B)-zI\sin(wT_s-\theta_D-\theta_B) = 0 \qquad (2.23)$$

Since $\theta_D+\theta_B = wT_s-\theta_{del}$, (2.23) becomes,

$$E\sin wT_s\sin\theta_B+E(1+\cos wT_s)\cos\theta_B$$
$$= E(1+\cos wT_s)+zI\sin(wT_s-\theta_{del})-zI\sin\theta_{del} \qquad (2.24).$$

(2.24) is of the form:

$$a\sin\theta_B+b\cos\theta_B = c, \qquad (2.25)$$

where,

$$a = E\sin wT_s \tag{2.26}$$

$$b = E(1+\cos wT_s) \tag{2.27}$$

$$c = E(1+\cos wT_s)+zI\sin(wT_s-\theta_{del}) - zI\sin\theta_{del} \tag{2.28}$$

In these equations a, b and c are constants defined by the circuit parameters, the operating frequency, the load current and the delay angle θ_{del}. (2.25) can be rewritten as:

$$\sqrt{a^2+b^2}\sin(\theta_B+\delta) = c \tag{2.29}$$

where

$$\cos\delta = a/\sqrt{(a^2+b^2)} \text{ and } \sin\delta = b/\sqrt{a^2+b^2} \tag{2.30}$$

$$\text{Now the angle } wT_s = w\pi/w_s = \pi(w/w_s) \tag{2.31}$$

For proper operation of the inverter circuit, it is necessary that the ratio w/w_s of the resonant frequency of the LC circuit to the inverter operating frequency be between 1 and 2, i.e.

$$1 < w/w_s < 2 \tag{2.32}$$

Therefore,

$$\pi < wT_s < 2\pi \tag{2.33}$$

Consequently, from (2.26) and (2.27), a is always negative and b is always positive. The angle δ therefore lies in the second quadrant. Therefore the solution of (2.25) for θ_B can be written as:

$$\theta_B = (\pi - \sin^{-1}(c/\sqrt{(a^2+b^2)}) - (\pi + \tan^{-1}(b/a)) \qquad (2.34)$$

Equations (2.34), (2.21) and (2.22) determine the initial conditions i_0, v_0 and thus the steady-state operating point of the circuit.

Example: The following numerical example illustrates the procedure for determining the operating point:

Let E = 100V, I = 10A, C = 5μF, L = 60 μH

and f_s = 6500Hz.

Then $z = \sqrt{L/C} = 3.464$ ohms.

$w = 1/\sqrt{LC} = .0577 \times 10^6$ rad/sec

$T_s = 1/(2f_s) = 153.8$ μsec

$WT_s = 4.44$ rad = 254.46 deg.

From (2.26) and (2.27),

$a = E \sin wT_s = -96.34$

$b = E(1+\cos wT_s) = 73.208$

Let the delay angle α_d (on w_s scale) be 0, corresponding to an uncontrolled (diode) rectifier load. Then, from (2.12), $\theta_{del} = 0$ deg.

From (2.28) $c = 39.83$

From (2.34) $\theta_B = 18.10$ deg. (on w scale)

From (2.21) $i_0 = 33.43$ A

From (2.22) $v_0 = -54.06$ V

B. Reflected load current lags v, reverse power flow ($90<\alpha_d<180$):

This situation is described in Fig. 2.7b. Typical circuit waveforms including the resonant current i are shown in Fig. 2.10. Since the direction of power flow is reversed, V_s lags v. i_0 and v_0 are again the initial values of the resonant current and the link voltage at the beginning of the inverter half-cycle, viz. the instant A; i_1, v_1 are the values at the instant B.

From A to B, Fig. 2.10, the circuit operates in Mode II. The response is given by equations (2.7) and (2.8). Therefore,

$$i_1 = (1/z)(E-v_0)\sin\theta_B+(i_0+I)\cos\theta_B-I \qquad (2.35)$$

$$v_1 = E-(E-v_0)\cos\theta_B+z(i_0+I)\sin\theta_B \qquad (2.36)$$

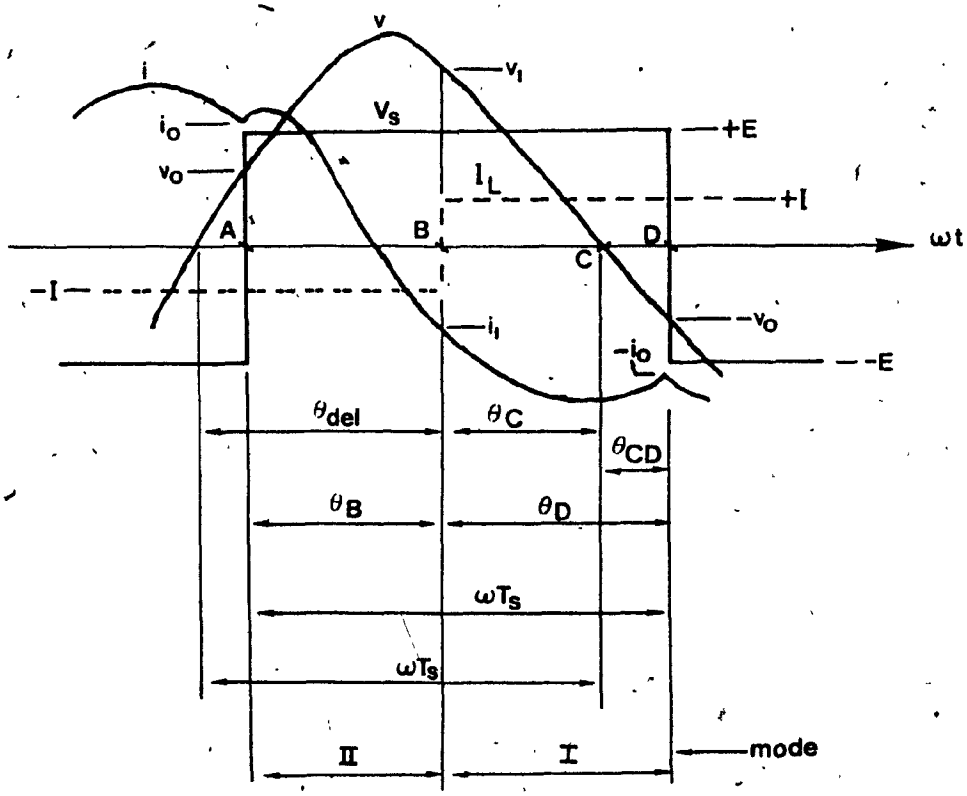

Fig. 2.10 Circuit waveforms for reverse power flow, with the reflected load current lagging the link voltage.

Over the interval BD the circuit operates in Mode I. Response is governed by equations (2.3) and (2.4) with i_1 and v_1 as initial conditions. Also D being the end of the half-cycle, in the steady-state the values of i,v at D are $-i_0, -v_0$ respectively. Therefore,

$$-i_0 = (1/z)(E-v_1)\sin\theta_D+(I_1-I)\cos\theta_D+I \qquad (2.37)$$

$$-v_0 = E-(E-v_1)\cos\theta_D+z(i_1-I)\sin\theta_D \qquad (2.38)$$

If the values i_1, v_1 are substituted from (2.35) and (2.36) in (2.37) and (2.38) and it is recognised that $\theta_B+\theta_D = wT_s$, the following solutions are obtained for i_0 and v_0 in terms of θ_D:

$$i_0 = I\frac{\cos(wT_s-\theta_D)+\cos\theta_D}{1+\cos wT_s} - \frac{E\sin wT_s}{z(1+\cos wT_s)} - I \qquad (2.39)$$

$$v_0 = zI\,\frac{\sin\theta_D-\sin(wT_s-\theta_D)}{1+\cos wT_s} \qquad (2.40)$$

From Fig. 2.10 $\qquad \theta_D = wT_s-\theta_{del}+\theta_{CD} \qquad (2.41)$

Using this relationship in (2.39) and (2.40), i_0 and v_0 can be expressed as follows:

$$i_0 = I\,\frac{\cos(\theta_{del}-\theta_{CD})+\cos(wT_s-\theta_{del}+\theta_{CD})}{1+\cos wT_s} - \frac{E\sin wT_s}{z(1+\cos wT_s)} - I \qquad (2.42)$$

$$v_0 = zI\,\frac{\sin(wT_s-\theta_{del}+\theta_{CD})-\sin(\theta_{del}-\theta_{CD})}{1+\cos wT_s} \qquad (2.43)$$

These are analogous to (2.21) and (2.22) with $-\theta_{CD}$ replacing θ_B. An equation in θ_{CD}, similar to equation (2.11) in θ_B, can be obtained by recognising that (2.4) is satisfied over the interval CD with the value:

$$v = 0,\ wt = -\theta_{CD},\quad v_i = v_0,\quad i_i = -i_0 .$$

This gives:

$$E-(E+v_0)\cos(-\theta_{CD})+z(-i_0-I)\sin(-\theta_{CD}) = 0$$

i.e.
$$E-(E+v_0)\cos\theta_{CD}+z(i_0+I)\sin\theta_{CD} = 0 \qquad (2.44)$$

Substituting for i_0, v_0 from (2.42) and (2.43) in (2.44),

$$E\sin wT_s\sin\theta_{CD}+E(1+\cos wT_s)\cos\theta_{CD}$$
$$= E(1+\cos wT_s)-zI\sin(wT_s-\theta_{del})+zI\sin\theta_{del} \qquad (2.45)$$

This is of the form:

$$a\sin\theta_{CD}+b\cos\theta_{CD} = c \qquad (2.46)$$

The values of a and b are once again given by (2.26) and (2.27), whereas:

$$c = E(1+\cos wT_s)-zI\sin(wT_s-\theta_{del}) + zI\sin\theta_{del} \qquad (2.47)$$

The solution for θ_{CD} is giving by:

$$\theta_{CD} = (\pi - \sin^{-1}(c/\sqrt{a^2+b^2})) - (\pi + \tan^{-1}(b/a) \qquad (2.48)$$

(2.48) together with (2.42) and (2.43) determines the steady-state operating point of the inverter.

Example: With the same parameter values as in the previous example, let

α_d = 141 deg.

From (2.12) θ_{del} = 199.3 deg.

From (2.47) c = 33.15

Using (2.48) θ_{CD} = 21.33 deg.

From (2.42) i_0 = 17.53 A

From (2.43) v_0 = 44.3 V

The initial conditions, together with the circuit waveforms, serve to fully define circuit operation corresponding to each loading condition. Various circuit quantities of interest, such as inverter output voltage, amplitude, device currents, commutation time etc., can then be easily determined from the waveforms. An illustration of this procedure is presented in Chapter 3, in which the load on the inverter is an uncontrolled rectifier.

CHAPTER 3

DC-DC CONVERTER WITH THE RESONANT INVERTER AS A HIGH FREQUENCY LINK

3.1 Introduction:

Power conversion from dc to dc is required in various applications, such as regulated power supplies and front-end power stages for inverters. Conventionally, choppers have been employed to perform dc-dc conversion. However, if the use of transformers to provide isolation and voltage transformation is mandatory, it is necessary to employ an intermediate ac link stage. High link frequencies of the order of several kHz can be used to advantage, leading to reduced transformer sizes. The resonant inverter of Fig. 1.3b can be used to realise the high frequency ac link stage in a dc-dc conversion process. The load on the inverter in this case is an uncontrolled rectifier. The characteristics of such a dc-dc conversion arrangement are considered in this chapter. The dc-dc converter is first described and its operation is explained. It is shown that the output voltage can be regulated by controlling the inverter frequency, while the inverter is operating in the normal continuous current mode (Fig.2.2d). The steady-state analysis described in Chapter 2 is then utilised to

characterise the performance of the circuit and generate design curves which can be used to select the circuit components. Results from a laboratory breadboard are also presented to verify the power conversion concept.

3.2 DC-DC Converter Operation:

The basic circuit of the dc-dc converter with the resonant inverter as the high frequency link is shown in Fig.3.1. The conversion proceeds in two stages. In the first stage, the input dc is inverted into the high link frequency using the resonant inverter. A high frequency transformer is then used to provide isolation and voltage transformation if needed. The high frequency ac is then rectified and filtered to obtain the output dc. Typical circuit waveforms under steady-state are shown in Fig.3,2. Since the load on the inverter is an uncontrolled rectifier, the waveform of the reflected load current I_L is in phase with link voltage v. The direction of power flow is from the link to the load i.e. in the forward direction. Therefore, with an uncontrolled rectifier load, the operation of the inverter corresponds to the situation considered in Section 2.8-A, with the delay angle $\theta_{del} = 0$. From equations (2.21), (2.25)-(2.28) and (2.34), the solution for the initial conditions v_0, i_0 can be obtained as follows:

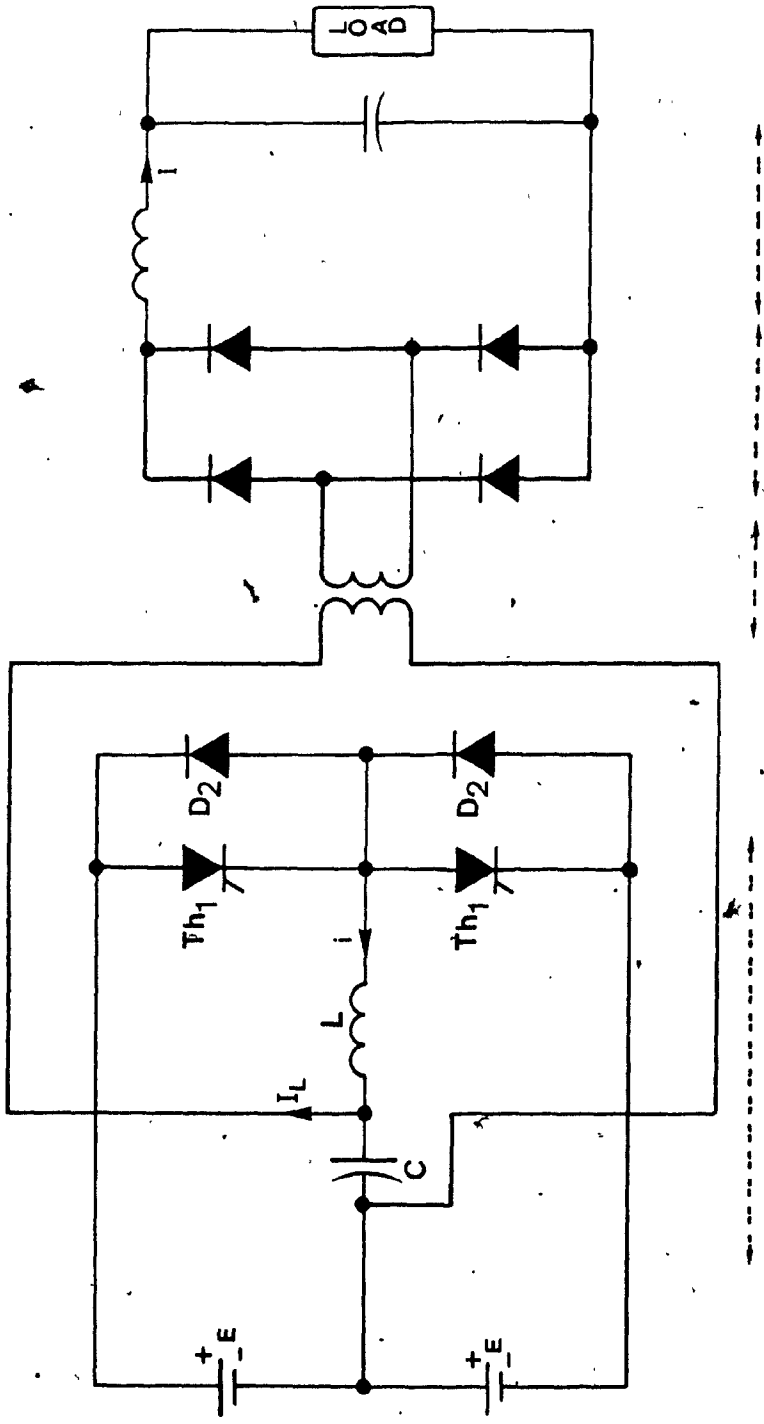

Fig. 3.1 Basic circuit of dc-dc converter.

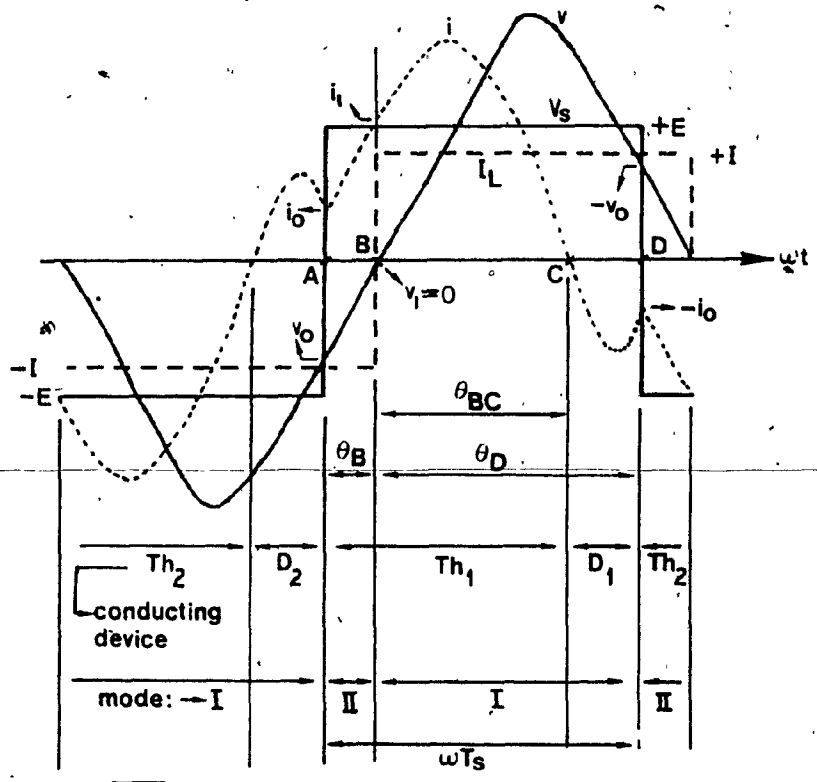

Fig. 3.2 Steady-state waveforms.

$$i_0 = I\,\frac{\cos\theta_B+\cos(wT_s-\theta_B)}{1+\cos wT_s} - \frac{E\sin wT_s}{Z(1+\cos wt_s)} - I \qquad (3.1)$$

$$v_0 = zI\,\frac{\sin(wT_s-\theta_B)-\sin\theta_B}{1+\cos wT_s} \qquad (3.2)$$

$$a\sin\theta_B+b\cos\theta_B = c \qquad (3.3)$$

and

$$a = E\sin wT_s \qquad (3.4)$$

$$b = E(1+\cos wT_s) \qquad (3.5)$$

$$c = E(1+\cos wT_s)+zI\sin wT_s \qquad (3.6)$$

Therefore,

$$B = (\pi-\sin^{-1}(c/\sqrt{a^2+b^2}))-(\pi+\tan^{-1}(b/a)) \qquad (3.7)$$

Since the rectifier is uncontrolled, regulation of the output voltage has to be performed in the inverter stage. The inverter has the characteristic feature that the amplitude of its output voltage can be varied by varying the operating frequency f_s. In the present instance, the variation of the inverter voltage with frequency can be intuitively explained as follows. From Fig.3.2, it can be seen that at the beginning of a half-cycle, when operation is transferred from one half of the inverter to the other, the initial voltage v_0 on the capacitor is negative. On increasing the frequency of operation of the inverter, this initial voltage increases

in magnitude, resulting in an increased swing of the capacitor voltage and thus an increased amplitude for the output voltage. Therefore, the operating frequency of the inverter can be used as the means for achieving regulation of the output dc voltage.

The effect of frequency on the voltage can be placed on a quantitative basis by calculating the average rectified link voltage v_{av} i.e. the average voltage at the output of the bridge rectifier in Fig. 3.1. This can be written as follows:

$$v_{av} = (1/T_s)\left[\int_A^B -v\,dt + \int_B^D v\,dt\right] \qquad (3.8)$$

During the interval AB, the circuit is operating in Mode II (Fig. 2.5b) and v is given by (2.8). Similarly, over the interval BD, the inverter is operating in Mode I (Fig. 2.5a) and the expression for v is given by (2.4). Therefore,

$$v_{av} = (1/wT_s)\left[\int_0^{\theta_B} -\{E-(E-v_o)\cos\theta+z(i_0+I)\sin\theta\}d\theta + \int_0^{\theta_D} \{E-(E-v_1)\cos\theta+z(i_1-I)\sin\theta\}d\theta\right] \qquad (3.9)$$

where $\theta = wt$. Therefore,

$$v_{av} = (1/wT_s)[-E\theta_B+(E-v_0)\sin\theta_B-z(i_0+I)(1-\cos\theta_B)$$

$$+E\theta_D-(E-v_1)\sin\theta_D+z(i_1-I)(1-\cos\theta_D)] \qquad (3.10)$$

Note that $v_1=0$ with a rectifier load. A typical plot of v_{av} as a function of the inverter frequency $f_s=1/2T_s$ is shown in Fig. 3.3. The plot is given in terms of per-unit values. The basis of the per-unit system is explained in Appendix B.

It can be seen from the curve of Fig. 3.3 that the output voltage can be regulated by varying the inverter frequency. For small variations of the inverter frequency from a quiescent value, the average voltage v_{av} is nearly a linear function of the frequency. Fig. 3.4 shows in block diagram form a simple control scheme for achieving a regulated dc output voltage.

3.3 Expressions for Other Circuit Quantities:

The operating point corresponding to a given set of parameters, such as dc input voltage, operating frequency, load current and circuit component values, can be determined using (3.1) to (3.7). It is then possible to obtain expressions for various other quantities of interest in a straightforward manner, using the waveforms of Fig. 3.2.

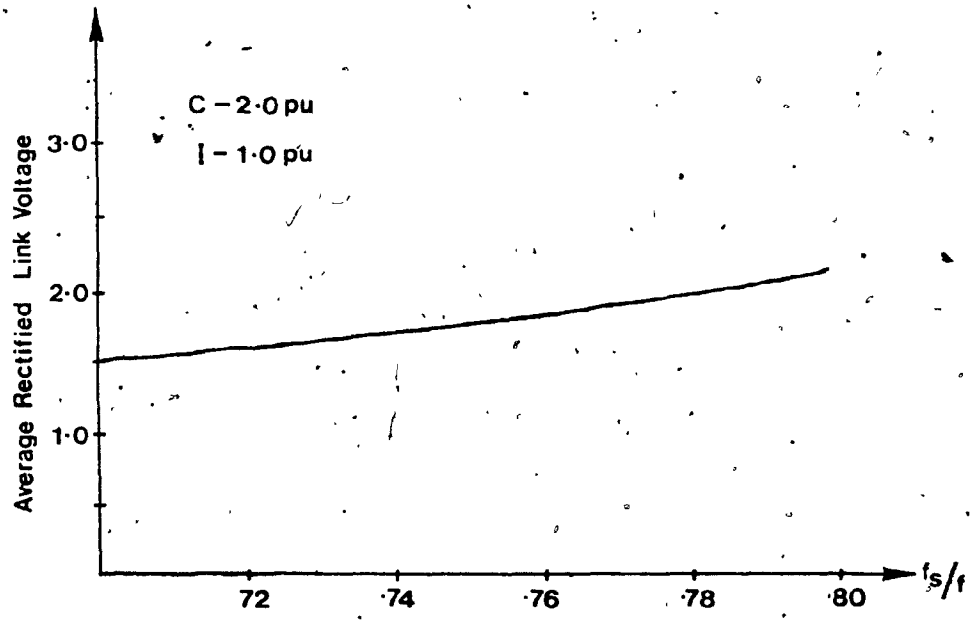

Fig. 3.3 Variation of average rectified link voltage with inverter frequency.

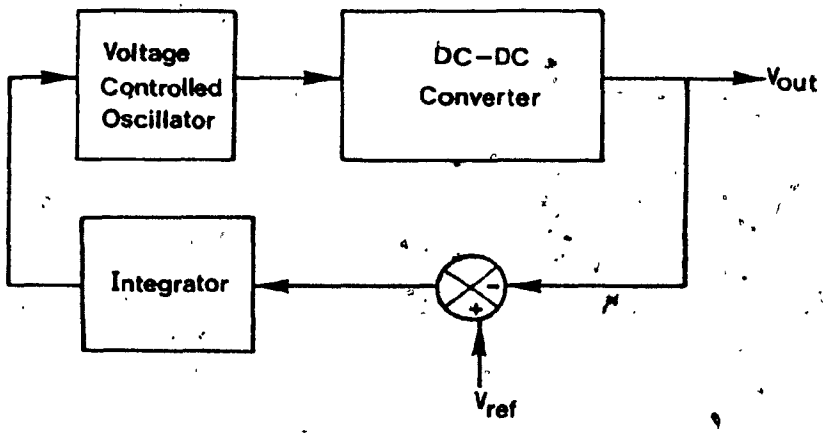

Fig. 3.4 Simplified block diagram of control scheme for regulating output voltage.

3.3.1 Expression for v_1, i_1:

v_1, i_1 are the values of the link voltage and the resonant current at the end of the first mode in the inverter half-cycle. In the present instance, as can be seen from Fig. 3.1, the first mode in Mode II and it ends at the instant B. Consequently,

$$v_1 = 0 \tag{3.11}$$

Using (2.7)

$$i_1 = \frac{E-v_o}{z}\sin\theta_B + (i_0+I)\cos\theta_B - I \tag{3.12}$$

3.3.2 Peak Link Voltage v_p:

Over the interval BD, the inverter operates in Mode I. From (2.4), with $i_i = i_1$, $v_i = 0$,

$$v = E - E\cos wt + z(i_1 - I)\sin wt \tag{3.13}$$

Therefore

$$v_p = E + \sqrt{E^2 + z^2(i_1 - I)^2} \tag{3.14}$$

3.3.3 Peak Thyristor and Diode Currents:

The peak thyristor current occurs during the interval BD. The circuit operates in Mode I and the resonant current is given by (2.3) with $i_1 = i_1$, $v_i = 0$. Thus,

$$i = (E/z)\sin wt + (i_1 - I)\cos wt + I \qquad (3.15)$$

The peak thyristor current is thus given by

$$i_{TP} = I + \sqrt{(E/z)^2 + (i_1 - I)^2} \qquad (3.16)$$

The peak diode current is given by

$$i_{DP} = i_0 \qquad \text{if } |v_0| > E \qquad (3.17)$$

$$i_{DP} = I - \sqrt{(E/z)^2 + (i_1 - I)^2} \qquad \text{if } |v_0| < E$$

3.3.4 Commutation Time t_q:

The commutation time t_q available to the thyristors in the inverter is the time for which the feedback diodes conduct. It is represented by the interval CD in Fig. 3.2.

$$\text{Commutation time } t_q = T_s - (t_{AB} + t_{BC}) \qquad (3.18)$$

Now, using (3.15),

$$wt_{BC} = \theta_{BC} = (\pi - \sin^{-1}(-1/A)) - \tan^{-1}(z(i_1 - I)/E) \qquad (3.19)$$

where $A = \sqrt{(E/z)^2 + (i_1 - I)^2}$

Therefore, $t_q = T_s - (1/w)(\theta_B + \theta_{BC}) \qquad (3.20)$

θ_B is given by (3.7).

3.3.5 RMS Capacitor Voltage:

Consider the half-cycle AD in Fig. 3.1; the rms capacitor voltage can be expressed as follows:

$$v_{rms} = [(1/wT_s)\{\int_0^{\theta_B} \{E-(E-v_0)\cos\theta+z(i_0+I)\sin\theta\}^2 d\theta + \int_0^{\theta_D} \{E-E\cos\theta+z(i_1-I)\sin\theta\}^2 d\theta\}]^{1/2} \quad (3.12)$$

3.3.6 RMS Inductor Current:

Again considering the interval AD, the rms inductor current can be expressed as follows:

$$i_{rms} = [(1/wT_s)\{\int_0^{\theta_B} \{((E-v_0)/z)\sin\theta+(i_0+I)\cos\theta-I\}^2 d\theta + \int_0^{\theta_D} (E/z)\sin\theta+(i_1-I)\cos\theta+I]^2 d\theta\}]^{1/2} \quad (3.22)$$

In an analogous manner, the rms capacitor current and the rms reactor voltage can be obtained.

3.3.7 RMS Capacitor Current:

$$i_{Crms} = [(1/wT_s)\{\int_0^{\theta_B}(i+I)^2 d\theta + \int_0^{\theta_D}(i-I)^2 d\theta\}]^{1/2}$$

$$= [(1/wT_s)\{\int_0^{\theta_B}\{((E-v_0)/z)\sin\theta+(i_0+I)\cos\theta\}^2 d\theta$$

$$+ \int_0^{\theta_D}\{(E/z)\sin\theta+(i_1-I)\cos\theta\}^2 d\theta\}]^{1/2} \qquad (3.23)$$

3.3.8 RMS Inductor Voltage

$$v_{Lrms} = [(1/wT_S)\{\int_0^{\theta_B}(E-v)^2 d\theta + \int_0^{\theta_D}(E-v)^2 d\theta\}]^{1/2}$$

$$= [(1/wT_S)\{\int_0^{\theta_B}\{((E-v_0)\cos\theta - z(i_0+I)\sin\theta\}^2 d\theta$$

$$+ \int_0^{\theta_D}\{E\cos\theta - z(i_1-I)\sin\theta\}^2 d\theta\}]^{1/2}$$

(3.24)

3.3.9 RMS Thyristor and Diode Currents:

The rms thyristor current is

$$i_{Trms} = [(1/2wT_s)\{\int_0^{\theta_B}\{\frac{E-v_o}{z}\sin\theta+(i_0+I)\cos\theta-I\}^2d\theta + \int_0^{\theta_{BC}}\{(E/z)\sin\theta+(i_1-I)\cos\theta+I\}^2d\theta\}]^{1/2} \quad (3.25)$$

The rms diode current is:

$$i_{Drms} = [(1/2wT_s)\int_{\theta_{BC}}^{\theta_D}\{(E/z)\sin\theta+(i_1-1)\cos\theta+I\}^2d\theta\}]^{1/2} \quad (3.26)$$

3.3.10 Average Thyristor and Diode Currents:

The average thyristor current is

$$i_{Tav} = (1/2wT_s)\{\int_0^{\theta_B}[((E-v_0)/z)\sin\theta+(i_0+I)\cos\theta-I]d\theta + \int_0^{\theta_{BC}}\{(E/z)\sin\theta+(i_1-I)\cos\theta+I\}d\theta\} \quad (3.27)$$

The average diode current is

$$i_{Dav} = (1/2wT_s)\int_{\theta_{BC}}^{\theta_D} -id\theta \quad (3.28)$$

$$= (1/2wT_s) \int_{\theta_{BC}}^{\theta_D} \{-(E/z)\sin\theta-(i_1-I)\cos\theta-I)d\theta\} \qquad (3.29)$$

All the integrals ocurring above are simple in nature and have been evaluated to yield expressions for the circuit quantities.

3.4 Design of The DC-DC Converter:

The various relationships derived in the previous section are used next to generate performance curves for different parameter combinations. Using such curves, circuit components can be selected to meet a particular set of requirements. Typically, the required output dc voltage has to be maintained over a specified range of operating conditions. The worst case conditions viz. the minimum supply voltage and the maximum load current are specified. The first step in the design is to select the values of the inductor L and the capacitor C.

Two major considerations influence the selection of these resonant circuit components. These are reliable commutation of the thyristors in the inverter and good efficiency for the overall circuit. To ensure commutation, the component values must be selected to provide adequate turn-off time to the thyristors under all conditions. To improve the efficiency, it is necessary to select the components so as to have a minimum of ringing current in

the inverter, while meeting the load requirements. Reducing the ringing current reduces the losses in the circuit and also the kVA ratings of the components. Therefore the values of L,C have to be chosen to achieve the two objectives of commutation margin and minimum ringing current. The amplitude of current oscillations in the circuit is dependent on the quality $\sqrt{C/L} = 1/z$. Therefore, the relation between the amplitude of the resonant current in the inverter and the L-C component values should be known in order to select L and C. Usually the resonant frequency w of the circuit is decided by considerations of transformer size and ease of supressing interference with other equipment. Therefore the L-C product can be assumed known. Once C is chosen, L is also determined.

The peak thyristor current i_{TP} can be regarded as a measure of the ringing current in the inverter. Fig. 3.5 shows the variation of i_{TP} with the capacitor value, with the average rectified link voltage v_{av} as a parameter. It can be seen that the ringing current decreases as the capacitor value is reduced. It is therefore desirable to use as low a value of capacitance as possible. But the recovery time available to the thyristors also decreases as the value of C is reduced. Fig. 3.6 shows the variation of recovery time t_q with the capacitor value,

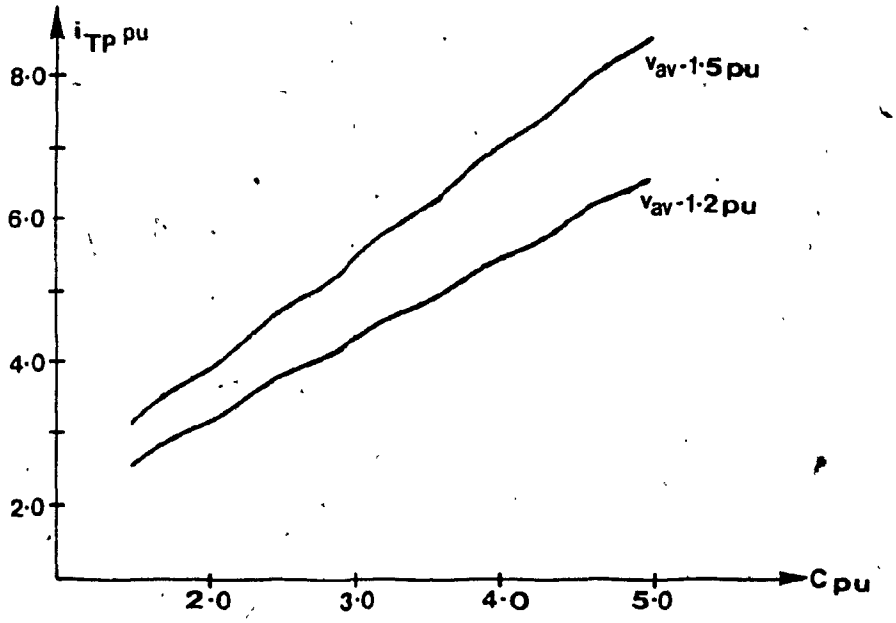

Fig. 3.5 Variation of peak thyristor current with capacitor value.

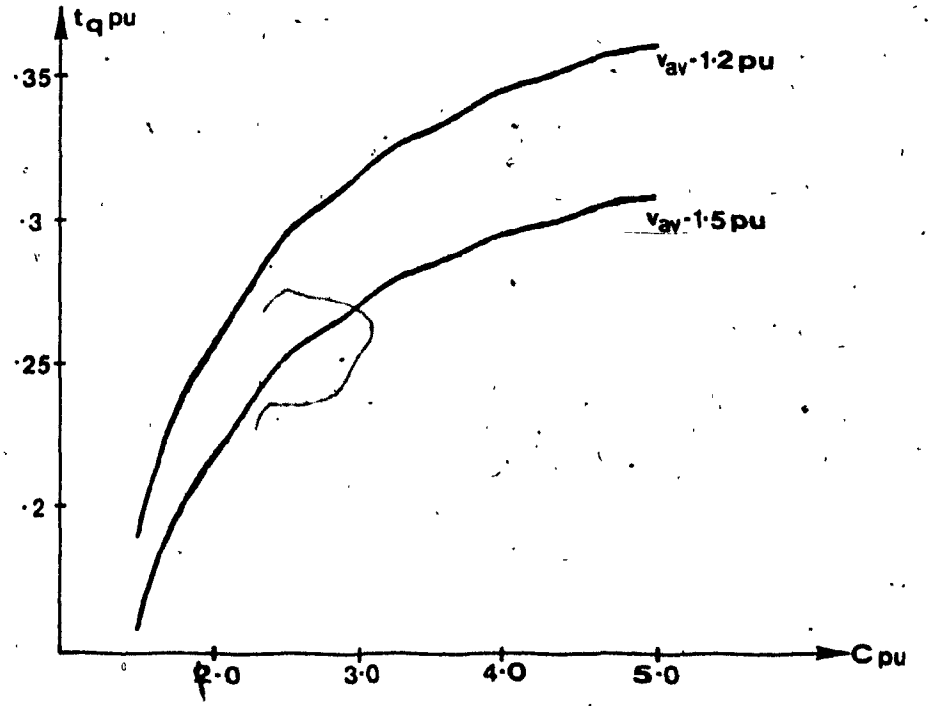

Fig. 3.6 Variation of recovery time with capacitor value.

again with v_{av} as a parameter. The commutation time falls sharply with the capacitor value. Thus the appropriate value for C is the lowest value that will provide sufficient recovery time to the thyristors employed in the inverter circuit.

Once the values of the resonant circuit components have been selected, their ratings and the ratings of the thyristors and diodes can be decided using performance curves such as those shown in Fig. 3.7 and 3.8. Fig. 3.7 shows the rms current carried by the reactor and the capacitor as a function of the capacitor value, for a particular v_{av}. Fig. 3.8 shows the rms and average current carried by the thyristors. The design process is illustrated by the following example. In order to enhance the utility of the results, the design is performed in terms of per-unit values.

Example:

Assume that a 2kW unit is to be designed; the minimum dc supply voltage is 100V. The output voltage is to be regulated at 120V. The resonant frequency of the LC circuit is taken to be 8.33 kHz, corresponding to a resonant period of 125μsec. The turn-off time requirement for the thyristors is 25μsec. The design proceeds as follows:

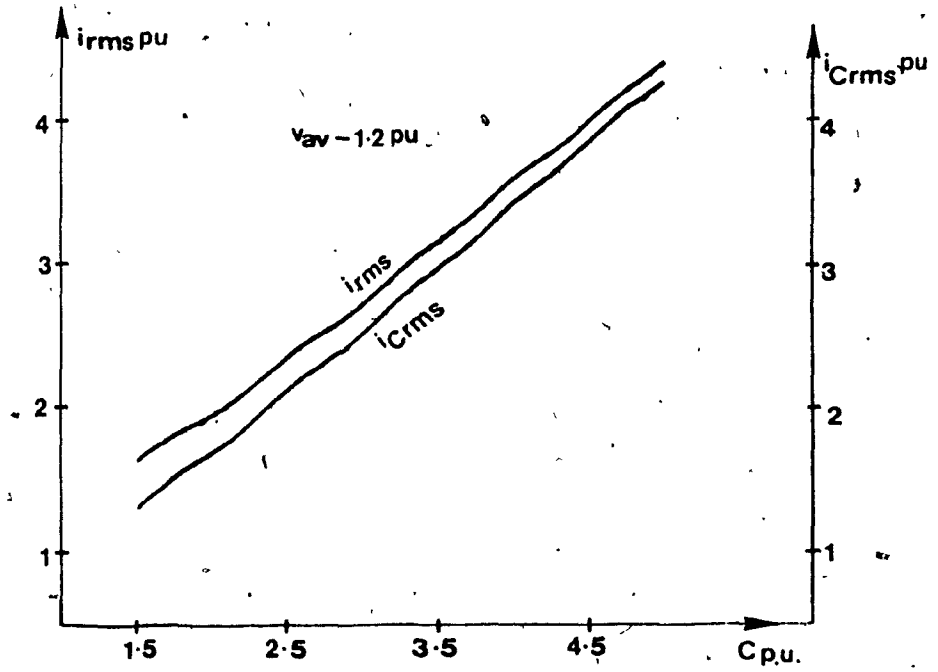

Fig. 3.7 Variation of rms current in the capacitor and the reactor as a function of capacitor value.

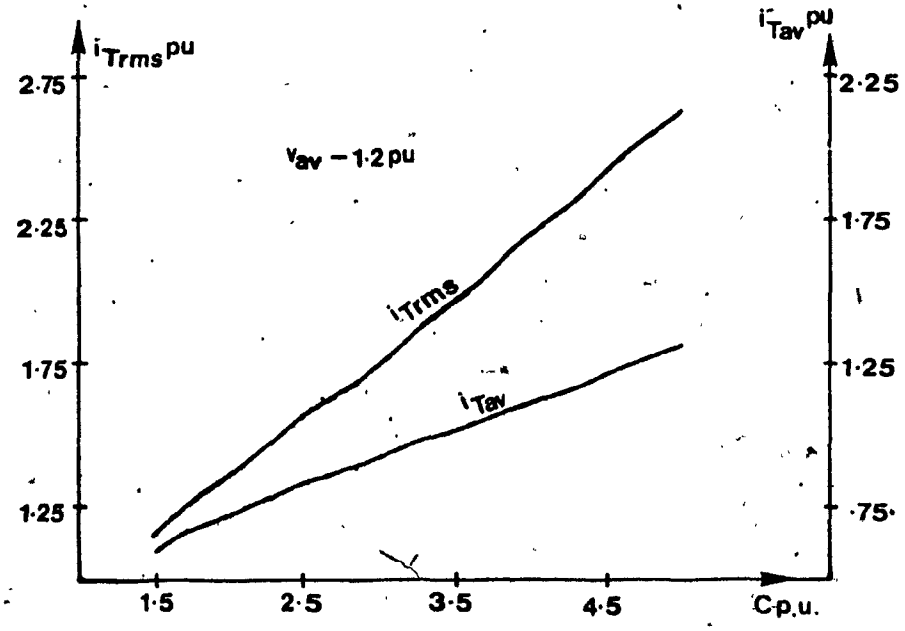

Fig. 3.8 Variation of rms and average thyristor current as a function of capacitor value.

Minimum dc supply voltage = 100 V

Specified dc output voltage = 120V

Maximum load current = 2kW/120V = 16.67A

The transformer is assumed to have a 1:1 turns ratio. The base value for various quantities are computed as follows:

Base voltage v_{base} = 100 V

Base current i_{base} = 16.67 A

Base angular frequency $w_{base} = 2x8.33x10^3$

$=52.3x10^3$rad/sec

Base time $t_{base} = 2\pi/w_{base}$ = 125μsec

Base inductance $L_{base} = v_{base}/(i_{base} x w_{base})$

= 114.7μH

Base capacitance $C_{base} = i_{base}/(v_{base} x w_{base})$

= 3.18μF

The output dc voltage in per-unit = 120/100 = 1.2 p.u.

Turn-off time required in per-unit = 25/125 = .2 p.u.

From Fig 3.6, the minimum capacitor value that will provide a turn-off time of 0.2 p.u. for an output dc voltage of 1.2 p.u is found to be 1.55 p.u.

Therefore the capacitor value = 1.55x3.18 = 4.98 or 5μF

The inductor value = 114.7/1.55 = 74μH

From Fig. 3.7, for an output dc voltage of 1.2 p.u., the rms currents in the reactor and the capacitor for C = 1.55 p.u. are found to be:

$$i_{rms} = 1.675 \text{ p.u.} \qquad i_{Crms} = 1.35 \text{ p.u.}$$

In terms of actual values,

The rms reactor current = 1.675x16.67 = 27.9 A

The rms capacitor current = 1.35x16.67 = 22.5 A

For a particular output voltage, the rms voltage ratings of the capacitor and the reactor are fairly independent of the capacitor value. For a dc output of 1.2 p.u., these are found to be,

$$v_{rms} = 1.38 \text{ p.u.} \qquad v_{Lrms} = .79 \text{ p.u.}$$

In terms of actual values,

$$v_{rms} = 1.38x100 = 138 \text{ V}$$

$$v_{Lrms} = .79x100 = 79 \text{ V}$$

In terms of p.u. values,

VA rating of the capacitor = 1.38x1.35 = 1.863 p.u.

VA ratings of the reactor = .79x1.675 = 1.323 p.u.

In terms of actual units,

VA rating of the capacitor = 1.863x100x16.67 = 3106 VA

VA rating of the reactor = 1.323x100x16.67 = 2206 VA

From Fig. 3.8, for C = 1.55 p.u.,

Thyristor rms current rating = 1.175 p.u.

Thyristor average current rating = .6125 p.u.

In actual units,

Thyristor current rating = 1.175x16.67 = 19.6 A

Thyristor average rating = .6125x16.67 = 10.2 A

These ratings can also be utilised for the feed-back diodes, although the stress on them is somewhat lower. In the case of many actual devices such as reverse-conducting thyristors, the capacity of the in-built feed-back diode is the same as that of the main thyristor.

3.5 Results from Laboratory Breadboard:

An experimental version of the converter was tested in the laboratory. The experimental converter did not include the high frequency transformer shown in Fig. 3.1. The oscillating circuit consisted of a 5μF capacitor and a 74μH inductor, giving a resonant frequency of 8.33 kHz. The waveforms of link voltage v and reflected load current I_L are

shown in Fig. 3.9. Regulation of output voltage by the inverter frequency is illustrated by the waveforms in Fig. 3.10, showing the link voltage and the resonant current. Fig. 3.11 shows the measured losses and efficiency of the laboratory converter. The efficiency is of the order of 85% at an output power level of 2.15 KW, which agrees well with the order of efficiency to be expected from the circuit - generally 85 to 90%.

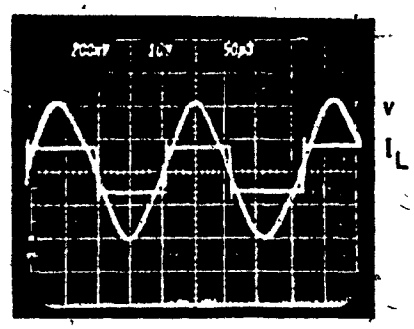

Fig. 3.9 Waveform of link voltage and load current reflected onto the link. E = 120 V, L = 74 μH; C = 5μF.

a) 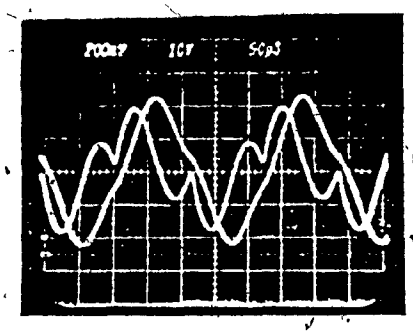

Load current = 7.2A
f_s = 4446 Hz.

b) 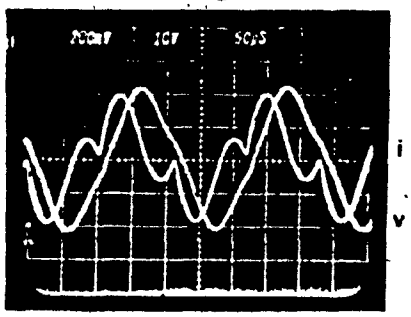

Load current = 10.3A;
f_s = 4509 Hz.

c) 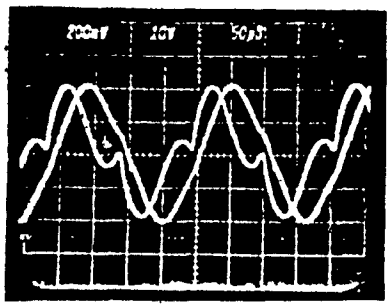

Load current = 13.4 A
f_s = 4603 Hz.

Fig. 3.10 Regulation of output voltage by varying inverter frequency; Output voltage = 125 V.

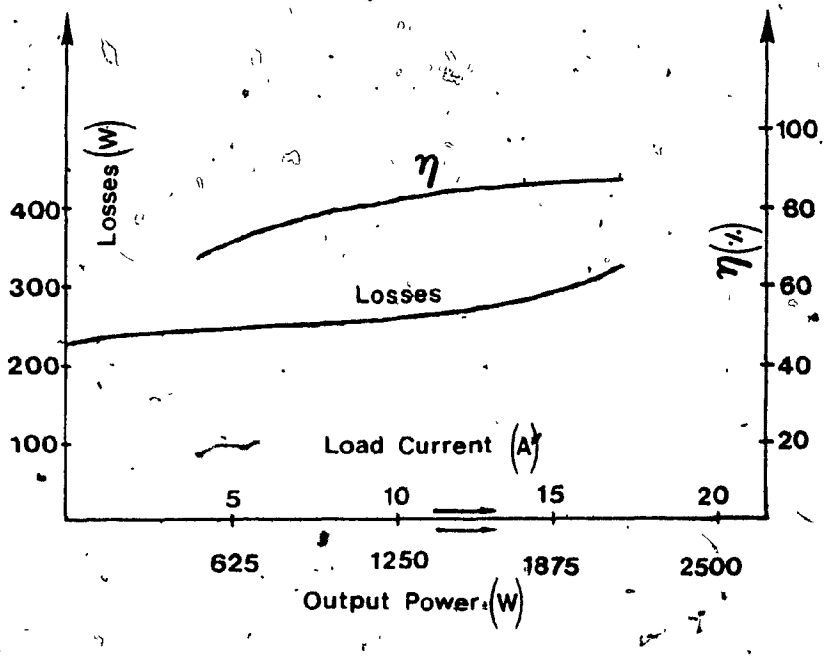

Fig. 3.11 Loss measurements on experimental converter. Output dc voltage = 125V.

CHAPTER 4

A CURRENT REGULATED FOUR QUADRANT CONVERTER USING THE RESONANT INVERTER

4.1 Introduction:

Power conversion schemes employing a high frequency link typically consist of two conversion stages. The first stage handles conversion from the input source to the high frequency link, while the second stage creates the required output from the link. The first stage is an inverter for systems with a dc input. The second stage is a rectifier if a dc output is required; while it is a four quadrant converter for ac and four quadrant dc outputs [13]. In the latter case it is possible to combine the inverter and four quadrant output converter stages into a single stage of power conversion. The high frequency link is not explicit but suppressed. A dc-ac converter based on this principle has been investigated by Robertson and Hebbar [22]. But in this case the firing of the inverter thyristors are not dynamically controlled with the output cycle and so control of the rms output voltage is difficult. Therefore in order to achieve voltage control at the output, the input dc voltage has to be controlled, thus requiring another conversion stage.

The resonant inverter circuit under consideration in this thesis can also be used to realise a dc-ac converter combining the functions of high frequency inversion and cycloconversion in one stage. Such a converter is considered in this chapter. In order to achieve control of the output, the ratio of the time intervals during which the firing signals to the inverter thyristors are applied/blocked is dynamically controlled so as to regulate the load current. This technique basically consists in forcing the current in an inductive load to be confined within a small band around a desired reference; the load current is sensed and compared with the reference and the load is appropriately energised and de-energised to make the load current stay within the specified band around the reference signal [23], [24], [25], [26]. Thus the load current can be made to follow the reference in amplitude and phase. The converter described here can therefore be looked upon as a current regulated voltage source inverter employing resonant commutation. The operation of the circuit is described and a design procedure for selecting components is outlined. Results from an experimental version of the converter, using an internal link resonant frequency of 30 kHz are presented.

4.2 Principle of Converter Operation:

A single phase full-bridge version of the converter is shown in Fig.4.1. It consists of the resonant inverter with the load connected across the resonating capacitor. The resonant frequency of the LC circuit is very high compared to the output frequency. The load current is sensed and compared with a reference in order to effect current regulation. There are two aspects involved in the operation of the converter. The macroscopic or low frequency operation, by which the load current is made to follow the reference and the microscopic or high frequency operation, which is decided by the inverter characteristics.

Macroscopically, the operation of the converter is controlled by the internal current regulating loop whose purpose is to maintain the load current I_L locked in amplitude and phase to the reference signal I_R. This is illustrated in Fig.4.2. During the positive half-cycle of the I_R and I_L signals, the positively sloped portions of the load current I_L are obtained by gating thyristors Th_1 and Th_4, while blocking the gating signals to Th_2 and Th_3. Energy is transferred from the dc supply to the load. When the load current increases beyond the reference signal I_R by a predetermined margin ΔI, the gating signals g_1 and g_4 are removed. The inductive load regenerates back to the

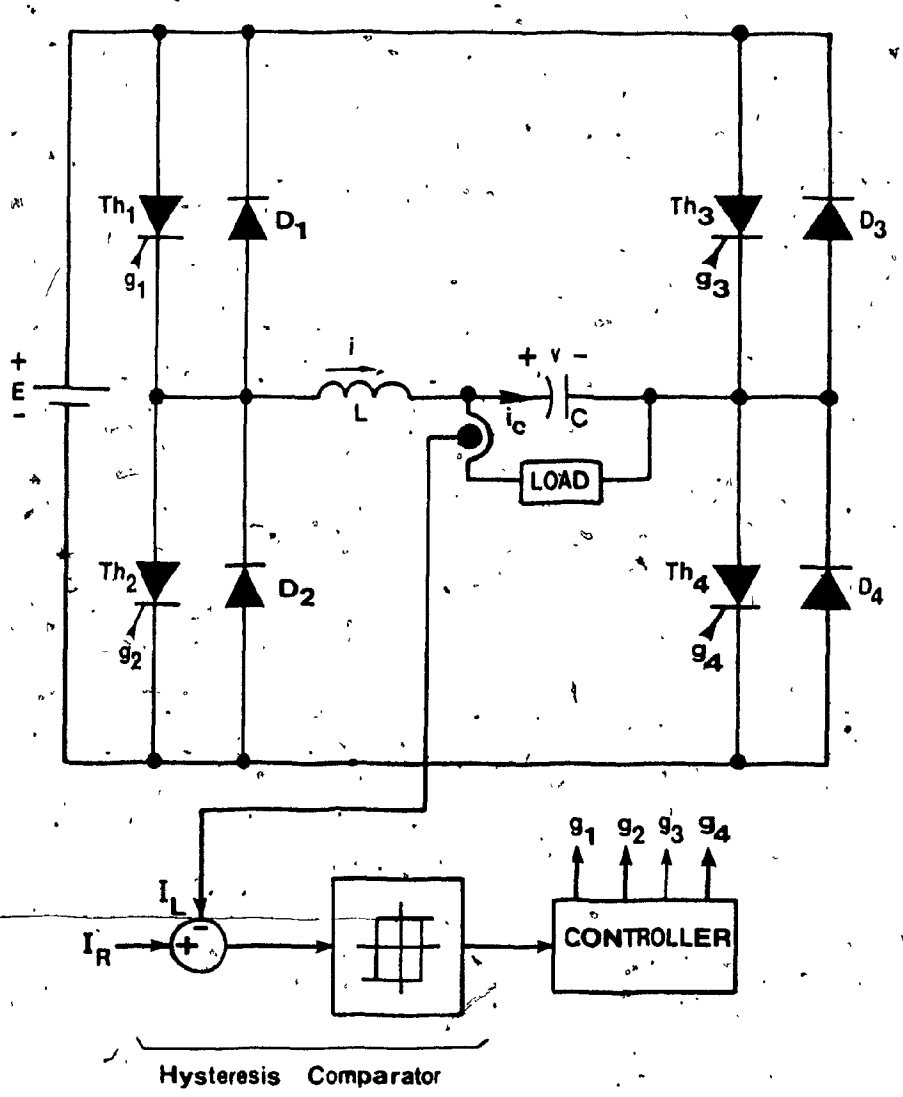

Fig. 4.1 Current regulated four quadrant converter using single phase full-bridge resonant inverter.

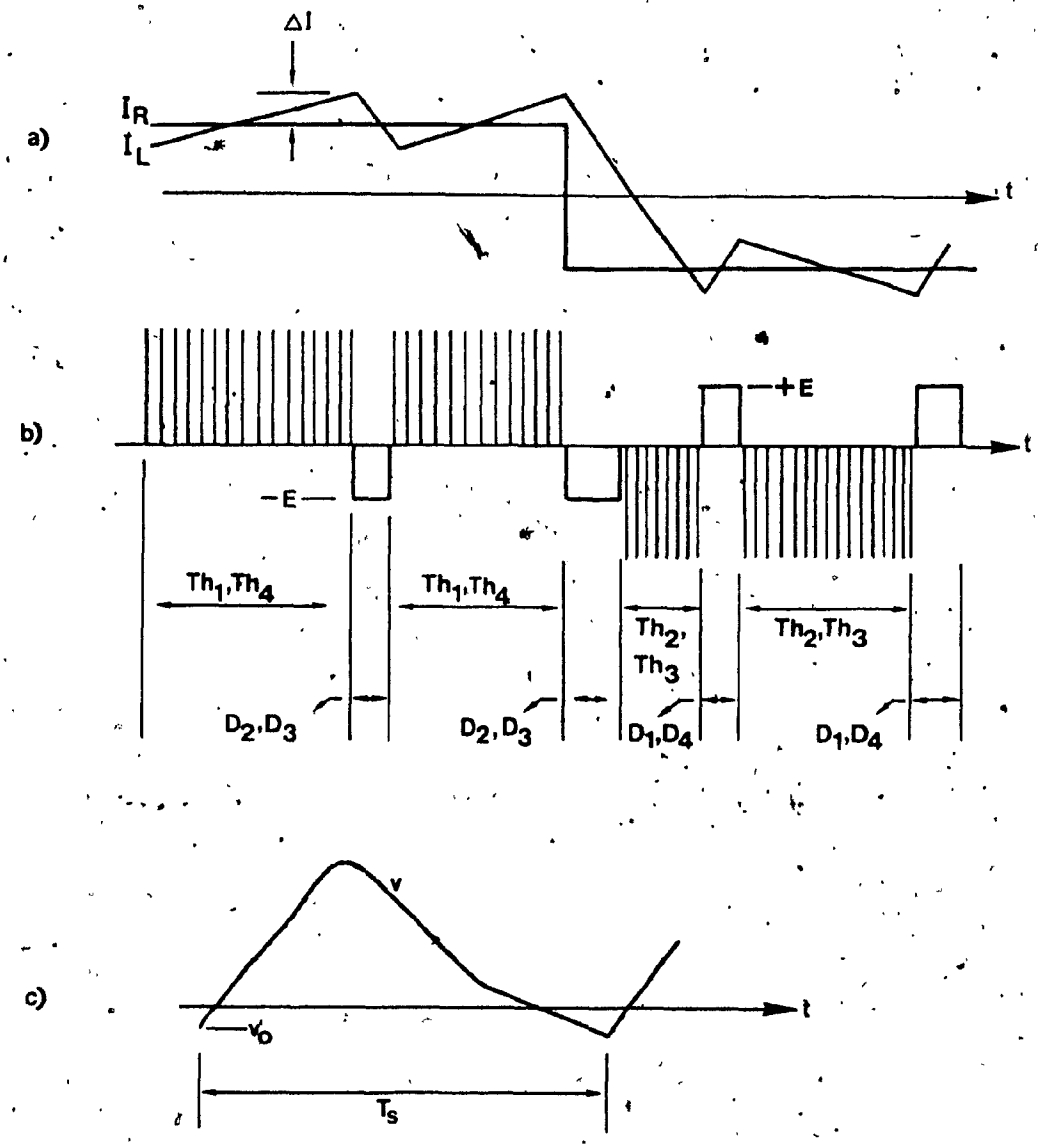

Fig. 4.2 Theoretical waveforms showing action of current regulator.

a) Load current I_L and reference signal I_R.

b) Load voltage.

c) Expanded view of each pulse of load voltage.

dc supply through the feedback diodes D_2 and D_3, giving rise to the negatively sloped portions of the load current waveform. During the negative half-cycle of the I_R signal, the complementary devices take part in similar phenomena i.e., Th_2 and Th_3 are gated on for transfer of energy from the supply to the load, while feedback diodes D_1 and D_4 conduct regenerative load current back to the dc supply. In this manner, the load current is confined to a narrow band around the reference signal I_R during both the positive and negative half-cycles of I_R. The margin ΔI, by which I_L is allowed to deviate from I_R, can be fixed, varied with amplitude and frequency or even modulated [27] to satisfy performance requirements.

Microscopically, the gating of a diagonally opposite pair of thyristors initiates the conduction of the oscillatory current i (Fig.4.3) through the dc source, the gated thyristors and the resonant circuit components L and C. The current i rises sinusoidally until it reaches its peak value i_m. At this point the reactor voltage $v_L = Ldi/dt$ is zero and the capacitor voltage v is equal to the dc source E. Past this point i begins to fall while v continues to rise beyond E. v becomes maximum the moment i falls below I_L. Eventually i becomes zero and changes polarity as it begins to flow against the dc source. Since thyristors cannot allow reverse conduction, i is transferred to the anti-parallel pair of diodes. During the diode conduction

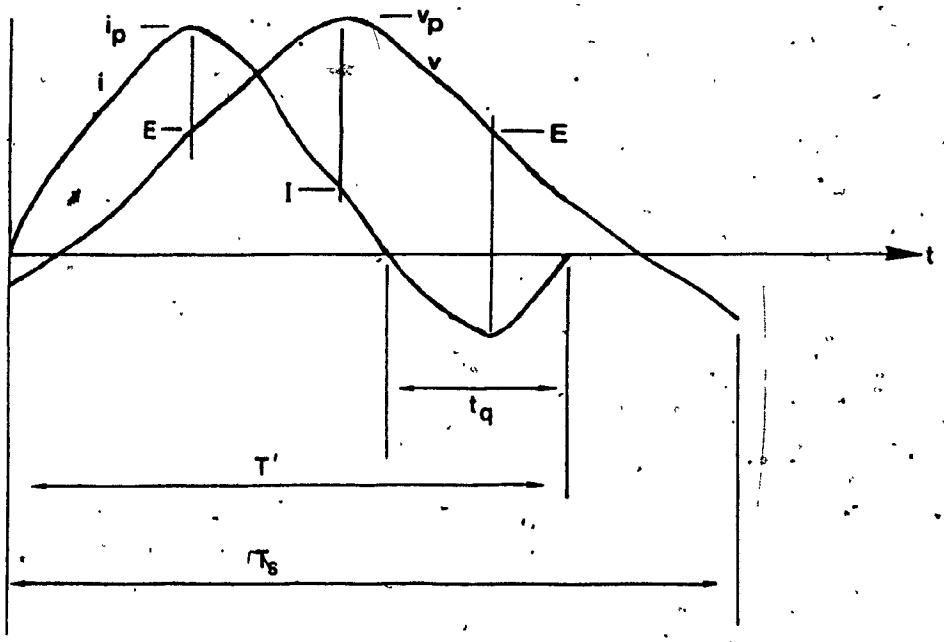

Fig. 4.3 Waveforms of resonant current and capacitor voltage.

interval, the previously conducting thyristors become reverse biased and recover their forward blocking capability. This interval lasts until i falls to zero again. For the next several microseconds the load current is supplied exclusively from the capacitor C. This mode lasts until either v becomes equal to -E, at which point I_L is transferred to the feed back diodes on the complementary diagonal, or the appropriate pair of thyristors is turned on again. The exact i and v waveforms depend on their respective initial conditions. These conditions in turn depend on factors such as the value of the load current I_L, the ratio of switching to resonant frequencies and the mode of operation of the converter.

4.3 Analysis of Circuit Operation:

For purposes of analysis, it is assumed that the load inductance is sufficient to make the load time constant large compared to the period of operation T_s of the converter. Since the thyristors in the converter are switched at the rate of several kHz, this is a reasonable assumption. Consequently, the load is considered to be represented by a constant current source I. The magnitude of I is taken to be V_{odc}/R_L, where R_L is an equivalent load resistance which accounts for the total power delivered to the load and V_{odc} is the dc value of the output voltage.

Considering the operation of the load in the first quadrant of the v-i plane, the polarity of the current source representing the load is as shown in Fig. 4.1 and the active thyristors are Th_1 and Th_4. The equivalent circuit for this mode of operation is shown in Fig. 4.4. The resistance R represents the losses in the circuit. The response of the circuit can be obtained in terms of the following quantities:

$w = 1/\sqrt{LC}$ natural resonant angular frequency

$\alpha = R/2L$ decrement factor

$\delta = \alpha/w$ damping factor

$w_d = w\sqrt{1-\delta^2}$ damped angular frequency

$z = \sqrt{L/C}$ characteristic impedance

$Q = z/R$ Quality factor

Initially, just before the thyrsitors are switched on, the oscillating current i is zero and the capacitor has an initial voltage $v(0) = v_0$. v_0 may be negative or positive depending on circuit parameters and operating conditions. When the thyristors are switched on a resonant pulse of current flows in the circuit. The circuit response is described by

$$Ri+L(di/dt)+(1/c)\int(i-I)dt + v_o = E \qquad (4.1)$$

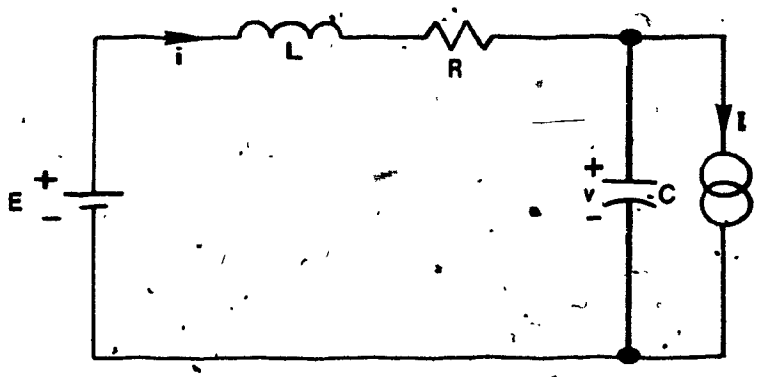

Fig. 4.4 Equivalent circuit of converter.

The solution of this equation yields the current i and consequently the capacitor voltage v as follows:

$$i(t)=[\frac{E-V_o}{z} - \frac{I}{2Q}]\, e^{-\alpha t}\sin w_d t - Ie^{-\alpha t}\cos w_d t + I \qquad (4.2)$$

$$v(t) = E-[E-v_0-RI]\, e^{-\alpha t}\cos w_d t - [\frac{E-v_o}{2Q} + Iz\,]e^{-\alpha t}\sin w_d t - RI \qquad (4.3)$$

In deriving these solutions, it has been assumed that the losses in the circuit are relatively small, so that $w>>\alpha$ and the following approximations hold:

$$w\simeq w_d, \quad z = \sqrt{L/C} \simeq wL \simeq 1/wC$$

$$\alpha/w_d \simeq \alpha/w = 1/2Q$$

Equations (4.2) and (4.3) are valid until the current i completes one full oscillation and reaches zero at time T' as shown in Fig. 4.3. In a lossless circuit with infinite Q, T' = T, the natural period of oscillation. The capacitor voltage at T' i.e. v(T') can be obtained from (4.3).

During the time interval from t=T' to $t=T_s$, where $1/T_s$ is the converter switching frequency, thyristors and diodes are not conducting. Consequently the current i remains at zero and the capacitor is forced to supply the load current.

The capacitor voltage during this time interval is given by:

$$v(t) = v(T') - \frac{I(t-T')}{C} \qquad (4.4)$$

For (4.4) the value of the capacitor voltage at $t=T_s$ is obtained as:

$$v(T_s) = v(T') - \frac{I(T_s-T')}{C} \qquad (4.5)$$

Under steady-state conditions, $v(T_s) = v_0$. Since (4.2)-(4.5) fully describe the operation of the HF link in terms of the load current, the switching period and the circuit component values, they can be employed to analyse the performance of the converter in terms of these parameters. The results of the analysis can be used to establish a design procedure for the converter circuit and provide guidelines for the selection of circuit components. For this purpose, variations of the output voltage, the turn-off time, the peak oscillating current etc. under varying load conditions and for different values of circuit components and switching frequencies are obtained and plotted. A computer program was written to perform the analysis. The program traces the circuit response over a few cycles, using (4.2)-(4.5) until the steady-state is reached.

The results of the analysis are presented in Figs. 4.5 to 4.7. A Q of ten has been assumed for the circuit. Under the assumption that the load inductance is sufficient to maintain the load current constant when the converter is being continuously operated as a chopper, turn-off time available to the thyristors is mainly determined by the ratio of the interval T_s between consecutive firings of the thyristors to the natural period of oscillation $T=2\pi\sqrt{LC}$ of the LC circuit. The variation of the turn-off time t_q as a function of the ratio T_s/T is shown in Fig. 4.6. Figs. 4.5a to 4.5c show the variation of the output capabilities of the converter with the capacitance value C. It is assumed that the LC product is determined from considerations of operating frequency. Therefore, as C is varied, L is varied correspondingly so that the LC product is constant. Using the curves of Fig. 4.5 it is possible to choose the capacitor value to meet given output power requirements. Given the load power and the load current requirements, the output dc voltage V_{odc} and the equivalent load resistance R_L can be determined. Therefore from the corresponding curve the value of the capacitor can be selected. It can also be noticed from Figs. 4.5a to 4.5c that for any given capacitor value, the output voltage increases and the regulation improves as the ratio T_s/T aproaches 1. However, the turn-off time available to the thyristors decreases as T_s/T tends to 1, as can be seen in

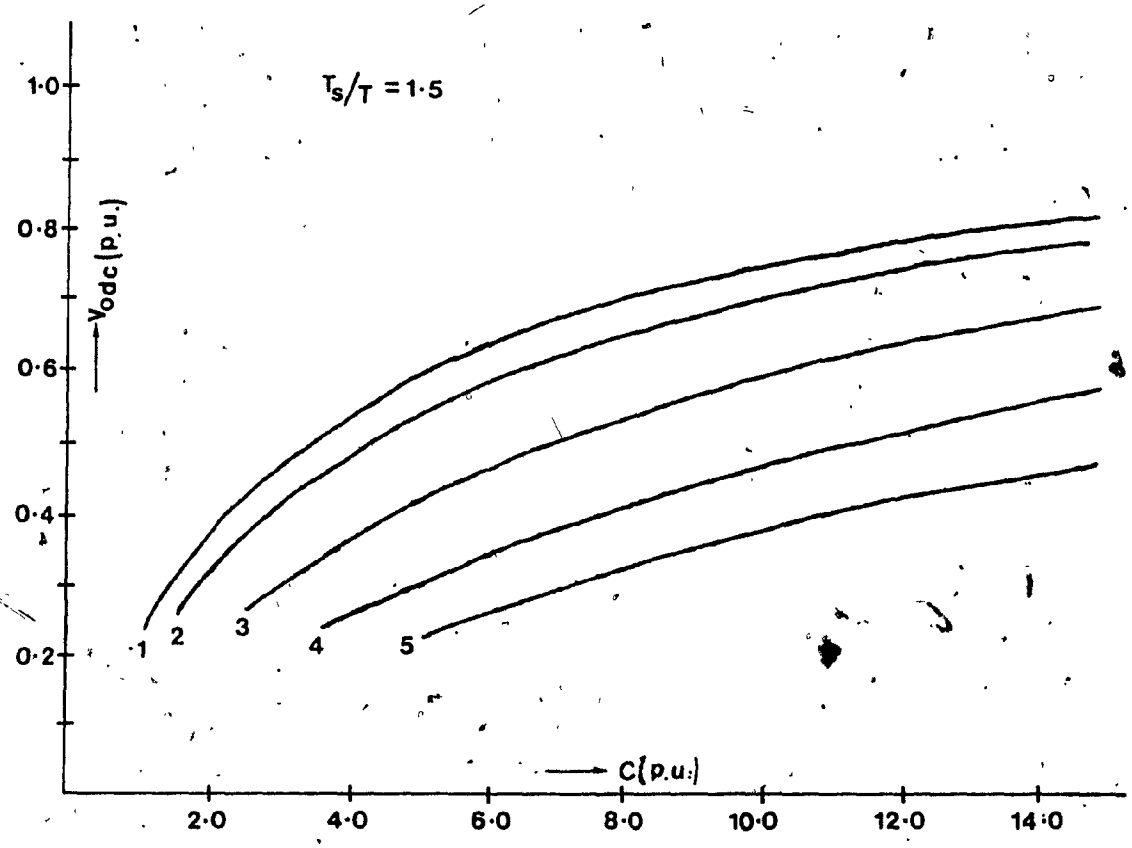

Fig. 4.5a

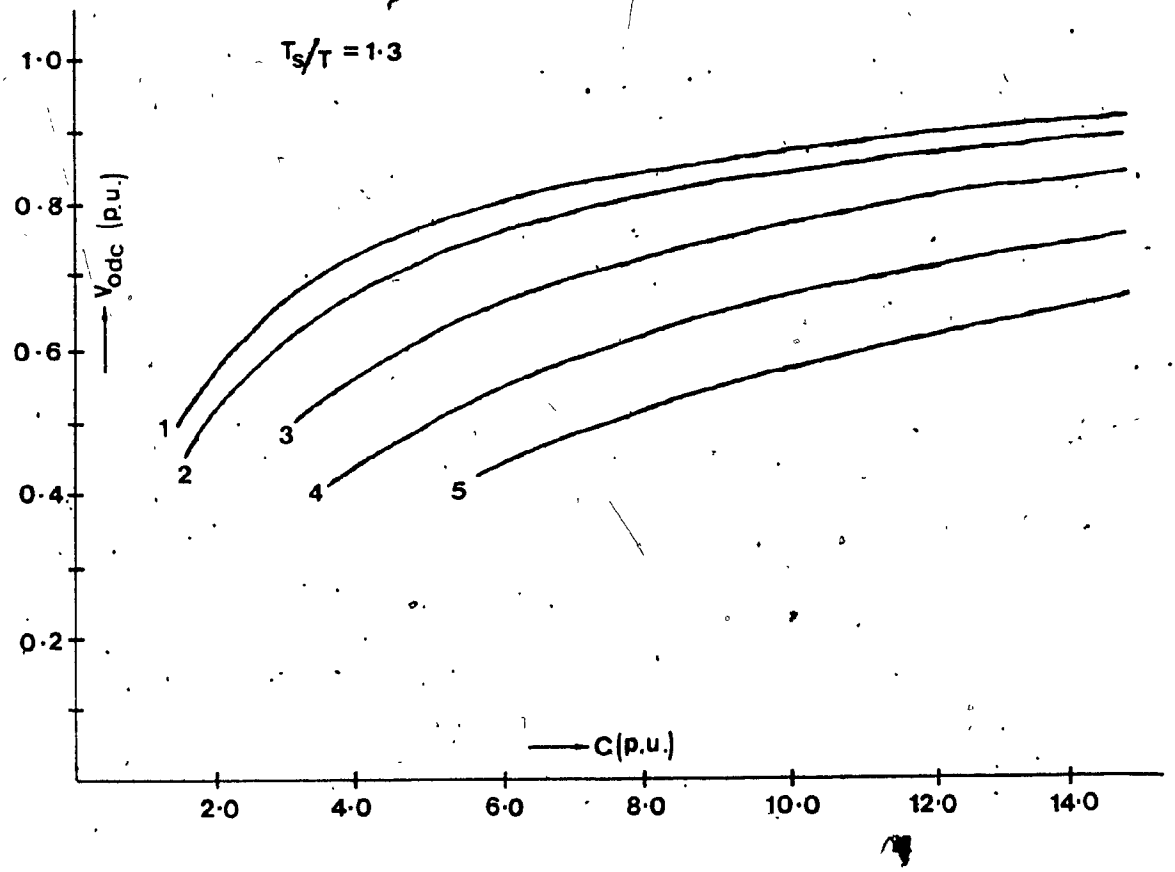
$T_s/T = 1{\cdot}3$
1·0
0·8
0·6
0·4
0·2
V_{odc} (p.u.)
1
2
3
4
5
C(p.u.)
2·0
4·0
6·0
8·0
10·0
12·0
14·0

Fig. 4.5b

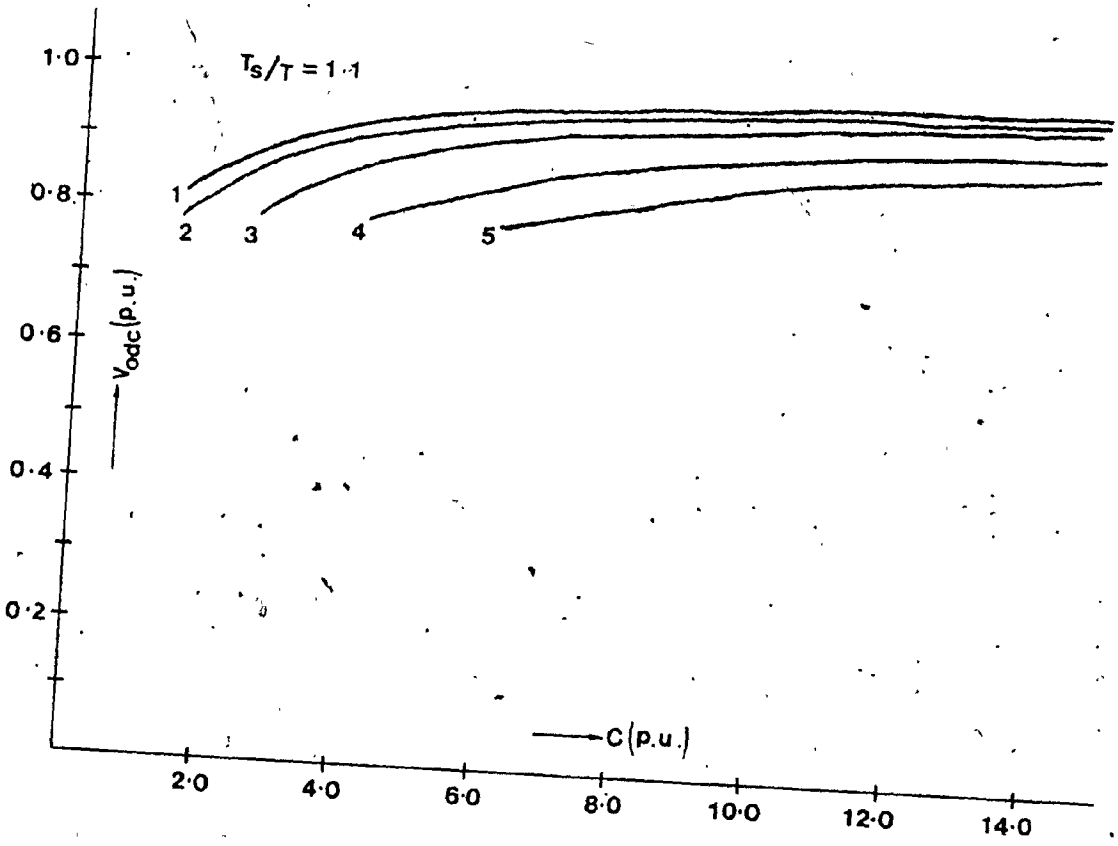

Fig. 4.5c

Fig. 4.5 Variation of output dc voltage with capacitor value.
1-R_L = 1.0 p.u., 2-R_L = 0.8 p.u.; 3-R_L = 0.5 p.u.;
4-R_L = 0.3 p.u.; 5-R_L = 0.2 p.u.

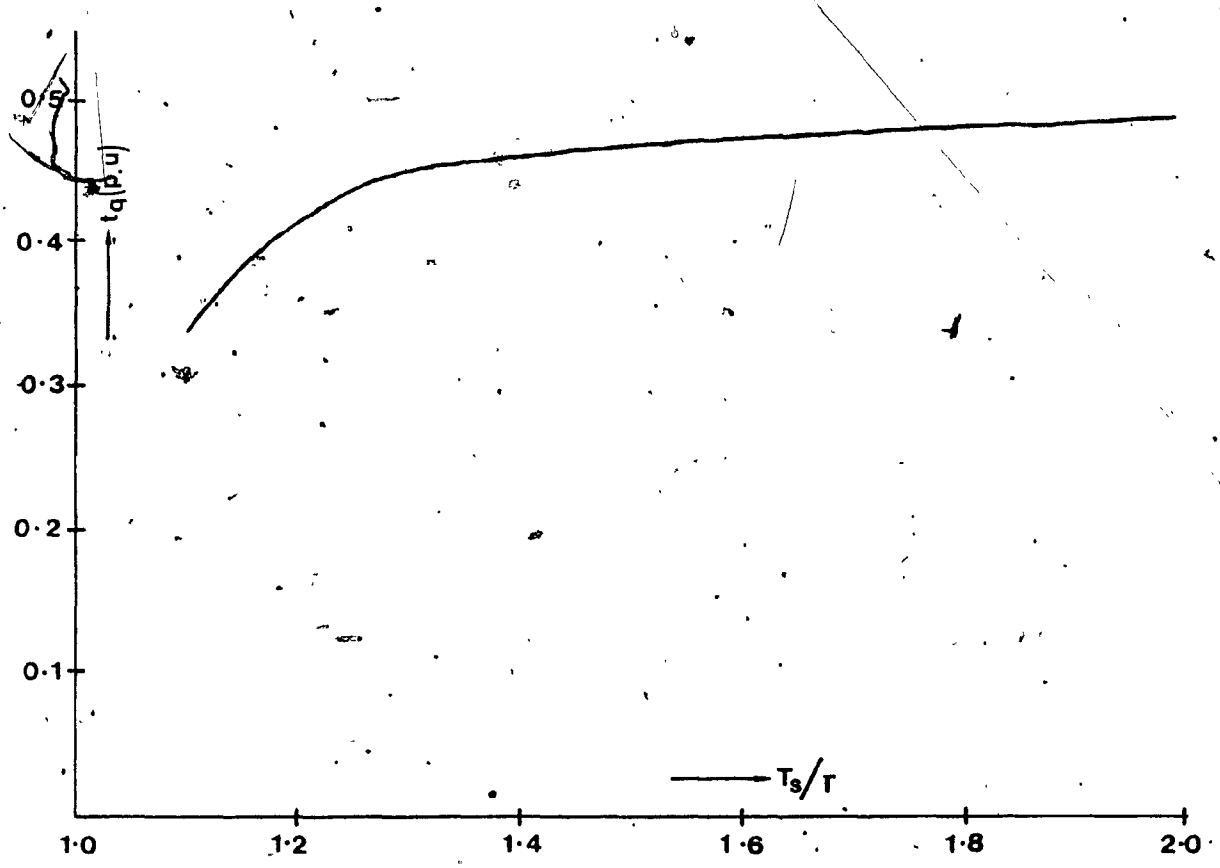

Fig. 4.6 Variation of recovery time with switching period.

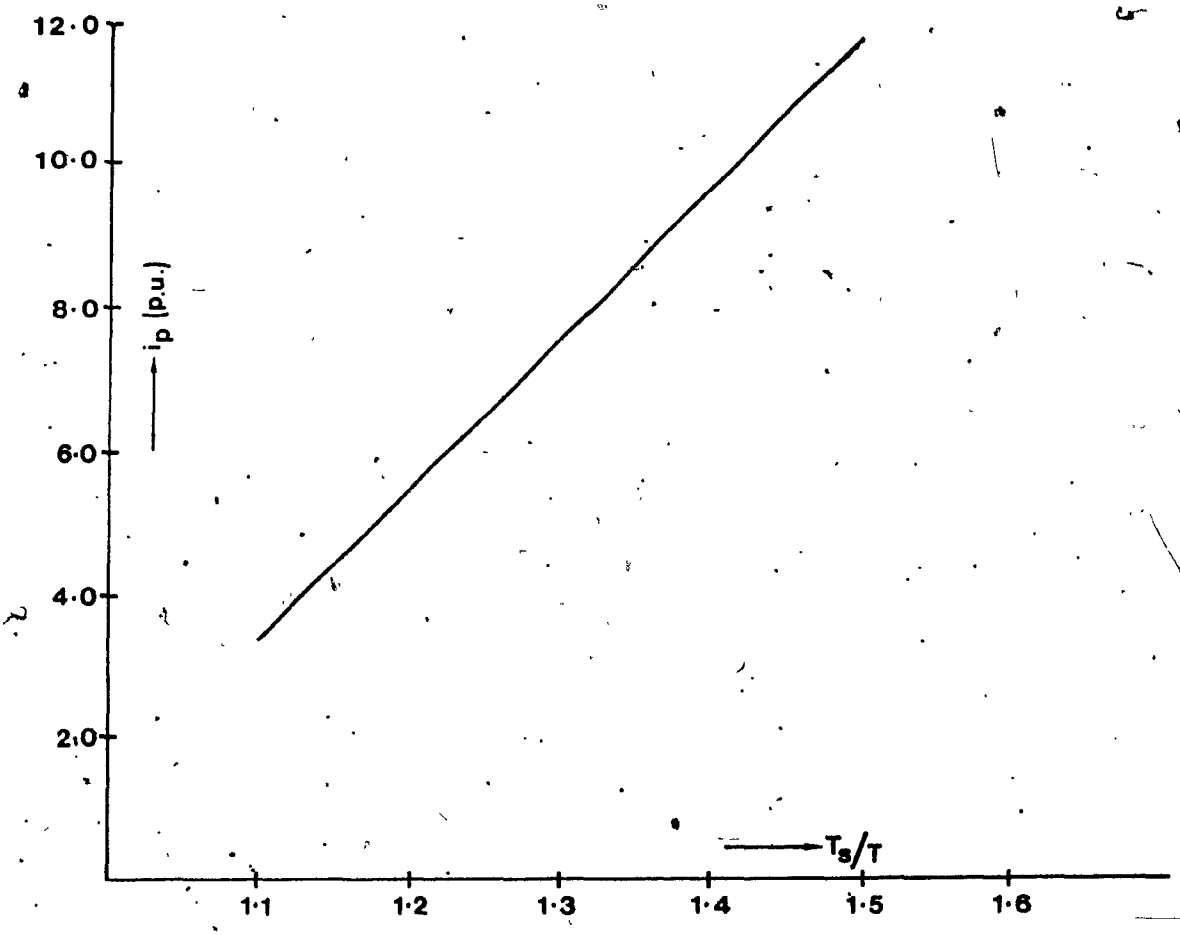

Fig. 4.7 Variation of peak resonant current with switching period.

Fig. 4.6. Again, under rated load conditions, the maximum value of the oscillating current i.e. i_m is decided by the ratio T_s/T and the variation is shown in Fig. 4.7. It can be seen that in order to minimise i_m and consequently the losses in the circuit, it is desirable to operate at a value of T_s/T which is as close to unity as possible without losing the minimum commutation margin required by the thyristors.

So for it has been assumed that the converter is operating under rated load conditions and is consequently functioning as a chopper. When the load current is made to follow a reference, the controller is active and thyristors are fired when the slope of the load current is to be reversed. From the point of view of analysing the circuit behaviour, it is important to note that in this case the initial conditions for the first oscillation are $i(0) = 1$ and $v(0) = -E$. The solutions to (4.1) which describe the first oscillation have to take the initial current in the reactor into account and can be written as follows:

$$i(t) = [\frac{2E}{z} - \frac{2I}{2Q}]\ e^{-\alpha t}\sin\omega_d t + I \qquad (4.6)$$

$$v(t) = E-[2E-RI]e^{-\alpha t}\cos w_d t - \frac{2E}{2Q}\ e^{-\alpha t}\sin w_d t - RI \qquad (4.7)$$

For subsequent oscillations the initial current is zero and the solutions are given by (4.2) and (4.3), v_0 being determined by circuit conditions.

4.3 Design Procedure

It is assumed that the dc supply voltage E, the maximum load P_0, the maximum load current I and the resonant frequency $f=1/2\pi\sqrt{LC}$ of the oscillating circuit have been specified. Using the information in Figs. 4.5 to 4.7, it is possible to select a suitable switching frequency to give sufficient commutation margin and consequently to select component values to meet load requirements. The procedure may be illustrated by an example.

Given,

DC supply voltage

P_0 = 125 V.

Maximum load power

P_0 = 1 kW.

Rated load current

I = 10 A.

Resonant frequency

f = 30 kHz.

Recovery time of thyristors

t_q = 15μsec.

Selecting V_{base}=125V, I_{base}=10A, E=1.0 p.u., I = 1.0 p.u.

Output power

$$P_0 = \frac{P_0}{V_{base} \times I_{base}} = \frac{1000}{125 \times 10} = 0.8 \text{ p.u.}$$

Average load voltage

$$V_{odc} = \frac{P_0 \text{ p.u.}}{I_{p.u.}} = 0.8 \text{ p.u.}$$

Equivalent load resistance

$$R_L = \frac{P_0 \text{ p.u.}}{(I \text{ p.u.})^2} = 0.8$$

Period of oscillation

$$T = \frac{1}{30 \times 10^3} = 33.3 \text{ μsec}$$

Select T_{base}=T = 33.3 μsec

Then the commutation time t_q in per-unit is

$$t_q = 15\mu\text{sec}/33.3\mu\text{sec} = 0.45 \text{ p.u.}$$

From Fig. 4.7, the T_s/T ratio which provides a commutation time of 0.45 p.u. is found to be 1.3. Therefore the switching frequency f_s is given by

$$f_s = \frac{30\text{kHz}}{1.3} \simeq 23 \text{ kHz}$$

From Fig. 4.5b, which corresponds to $T_s/T = 1.3$, the minimum capacitance which will result in a V_{odc} of 0.8 p.u. for $R_L = 0.8$ p.u. is found to be 7.7 p.u.; consequently $L = (1/7.7)$ p.u.

$$w_{base} = 2\pi f = 2\pi \times 30 \times 10^3 \text{ rad/sec}$$

$$C_{base} = \frac{I_{base}}{V_{base} \times W_{base}} = \frac{10}{125 \times 2\pi \times 30 \times 10^3} = 0.42 \ \mu F$$

$$L_{Base} = \frac{V_{base}}{I_{base} \times W_{base}} = \frac{125}{10 \times 2\pi \times 30 \times 10^3} = 66 \ \mu H$$

Therefore,

$C = 7.7 \times 0.42 = 3.23 \ \mu F$

$L = 66/7.7 = 8.57 \ \mu H$

From Fig. 4.7, the peak oscillating current i_m is found to be 7.5 p.u., corresponding to $T_s/T = 1.3$. Therefore,

Peak thyristor current = $7.5 \times 10 = 75A$

4.4 Experimental Results:

An experimental version of the converter was constructed in the laboratory, employing asymmetrical SCRs with low recovery times. The inductor and capacitor that constituted

the resonant circuit had the values 5μH and 5μF respectively. The oscillograms shown in figs. 4.8 to 4.11 illustrate the performance of the converter when feeding a resistive-inductive load, with a load inductance of 2mH.

Fig. 4.8 shows the resonant current i and the capacitor voltage v for different loading conditions. The corresponding waveforms for the capacitor current i_C are shown in Fig. 4.9. It can be seen that the natural frequency of the HF link is approximately 33kHz while the switching frequency ($f_s = 1/T_s$) is approximately 23 kHz. The ability of the converter to respond to a varying external current command signal I_R is depicted in Figs. 4.10 and 4.11. The reference signal I_R and the load current I_L have been recorded as mirror images of each other. Fig. 4.10 shows converter response to dc I_R signal, while Fig. 4.11 shows the response to ac I_R signals. It can be seen that the converter exhibits very fast response, while operating either as a chopper or as an inverter.

4.5 Conclusion

The resonant inverter, in conjunction with the principle of current regulation, thus yields a converter which combines the performance characteristics of a high frequency inverter and a cycloconverter in one stage of power conversion. The converter has a frequency range of

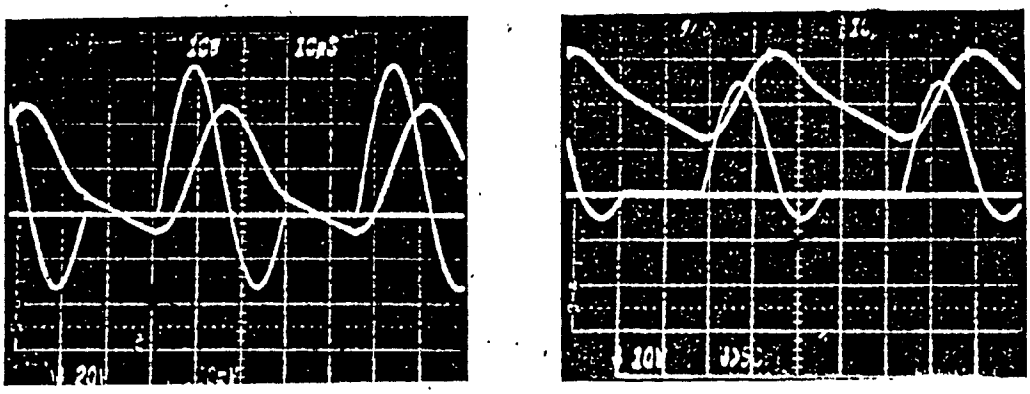

a) b)

Fig. 4.8 Waveforms of resonant current and capacitor voltage.

a) With negative initial capacitor voltage.

b) With positive initial capacitor voltage.

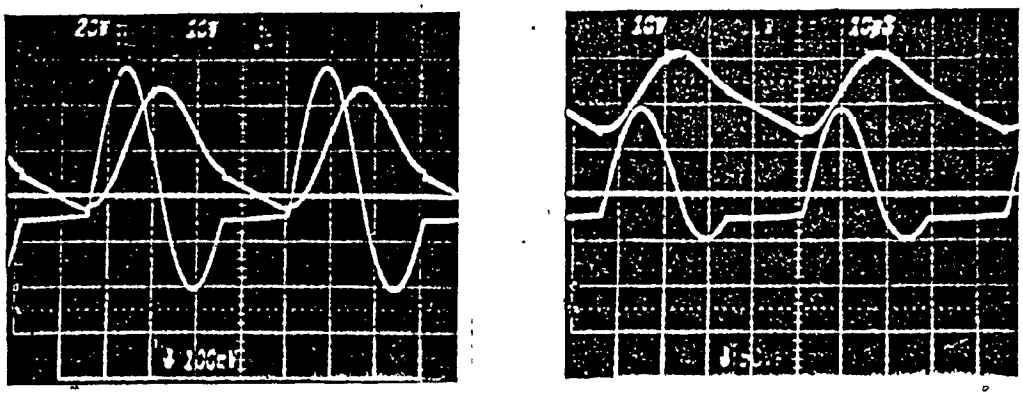

a) b)

Fif. 4.9 Waveforms of capacitor current and capacitor voltage.

a) With negative initial capacitor voltage.

b) With positive initial capacitor voltage.

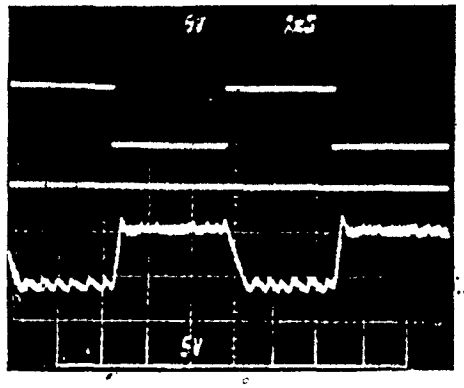

a)

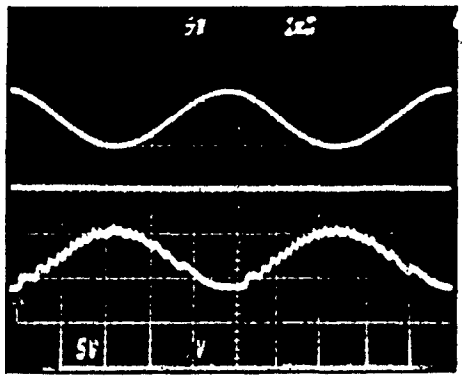

b)

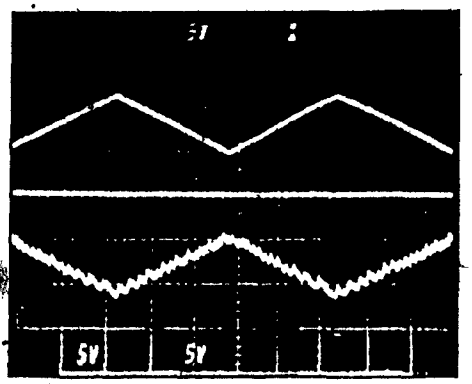

c)

Fig. 4.10 Waveforms of reference signal I_R and load current I_L, (DC I_R signals-chopper operation); a) step load current command, b) Sinusoidal load current command, c) Ramp load current command.

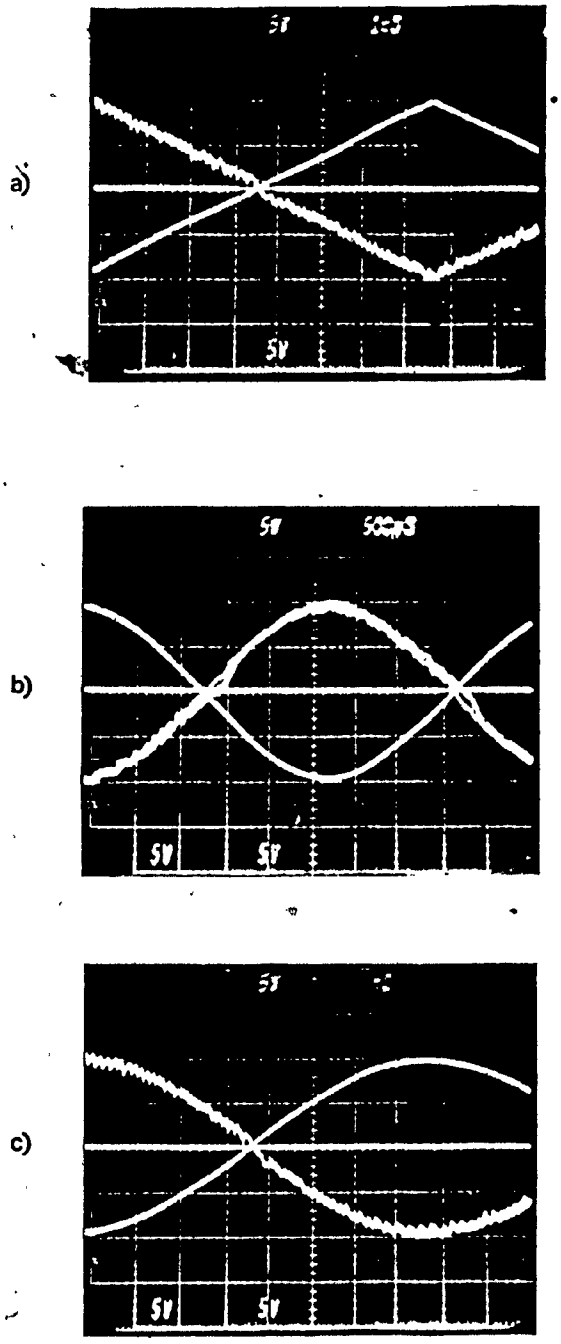

Fig. 4.11 Waveforms of reference signal I_R and load current I_L (AC I_R signals-inverter operation); a) Triangular ac reference at 70 Hz, b) Sinusoidal ac reference at 70 Hz; c) Sinusoidal ac reference at 180 Hz.

operation and quick response to external commands. It can modulate the load current I_L according to any reference signal I_R with controlled ripple in the load current.

CHAPTER 5

DC-AC POWER CONVERSION USING TWIN HIGH FREQUENCY LINKS

5.1 Introduction:

In dc-ac power conversion systems employing a high frequency link, the low frequency (50/60 Hz) output is usually realised by typical cycloconversion methods [13], [15],[16]. An alternative method to achieve dc-ac power conversion is possible by utilising two high frequency links, each being realised by means of a high frequency inverter, with their operating frequencies differing by twice the required low output frequency. The technique of combining the outputs of inverters operating at the same frequency but with a phase shift between their outputs, in order to achieve cancellation of harmonics, is well-known [28]. It is also possible to achieve output voltage regulation by controlling the phase shift [29]. However, the possibilities offered by two inverters operating at different frequencies have not been investigated.

A dc-ac power conversion system which utilises twin high frequency links is investigated in this chapter. Fig.5.1 shows a block diagram of the dc-ac conversion process. The two high frequency inverters operate at

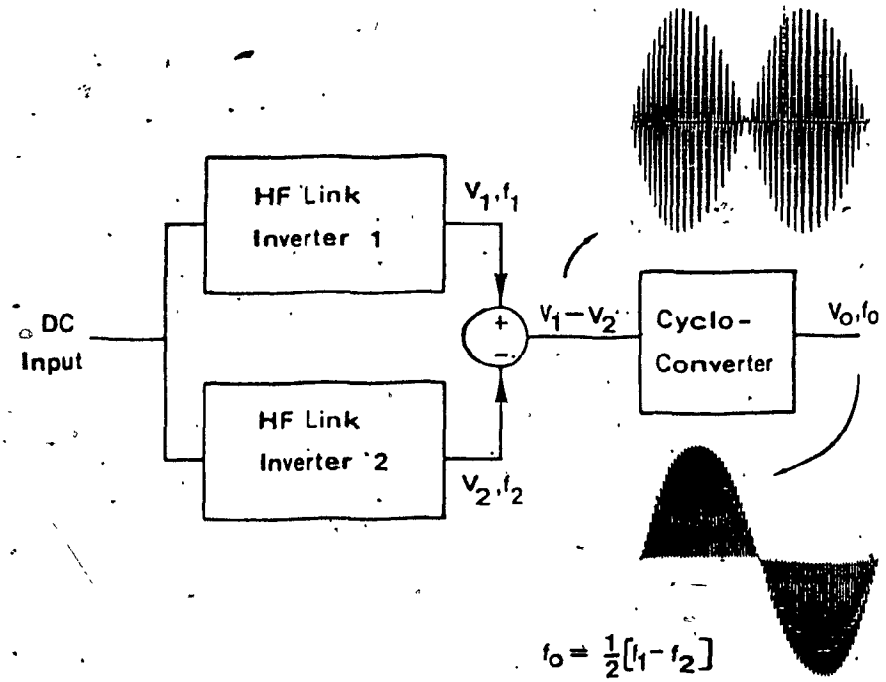

Fig. 5.1 Block diagram of dc-ac conversion process.

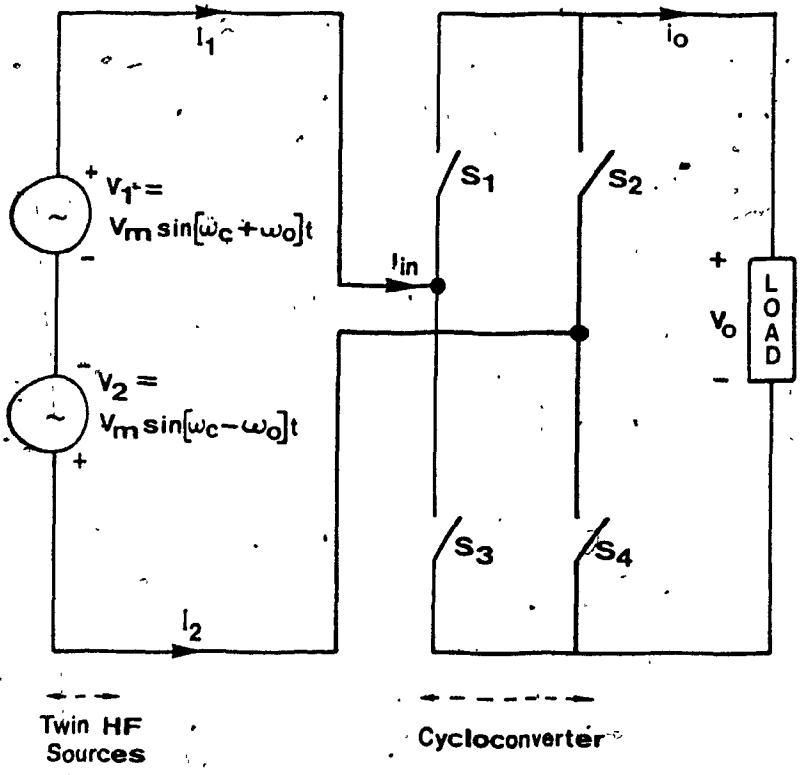

Fig. 5.2 Schematic diagram of dc-ac converter.

frequencies f_1 and f_2 respectively. The differences between f_1 and f_2 is $2f_0$, where f_0 is the required low output frequency. The difference between the two link voltages is a high frequency sinusoid, enveloped within another sinusoid at the output frequency f_0. This voltage can then be used as the input in a cycloconversion process. If the input to the cycloconverter is of constant amplitude as in normal cycloconversion, the firing angle of the cycloconverter has to be modulated about a quiescent value, using a sinusoidal reference signal, in order to obtain a sinusoidal output voltage. On the other hand, if the input voltage is modulated in amplitude as mentioned above, the firing angle does not have to be modulated. Sinusoidal output voltage can be constructed by simple rectification/inversion. The process can be viewed as a form of cycloconversion in which the modulation is incorporated in the input voltage instead of the switching. Ohmic isolation can still be provided at high frequency. The frequency of the output voltage can be varied by varying the difference between the frequencies of the two HF links.

5.2 Basic Principle:

Consider two sinusoidal high frequency voltage sources operating at the frequencies f_c+f_0 and f_c-f_0, where f_c is very much greater than the output frequency f_0. The two voltages can then be represented by

$$V_1 = V_m \sin(w_c+w_o)t \qquad (5.1)$$

$$V_2 = V_m \sin(w_c-w_o)t$$

where $w_c=2\pi f_c$ and $w_o=2\pi f_o$. The difference of V_1 and V_2 is therefore given by

$$V_3 = V_1-V_2 = V_m \sin(w_c+w_o)t - V_m \sin(w_c-w_o)t \qquad (5.2)$$

$$\text{i.e. } V_3 = 2V_m \cos w_c t \sin w_o t \qquad (5.3)$$

Equation (5.3) represents an alternating voltage at the high frequency f_c whose amplitude follows the low frequency envelope described by $2V_m \sin w_o t$. The nature of this waveform is shown in Fig.5.3a. The required output voltage V_o at the low frequency f_o can be obtained by suitably inverting alternate half-cycles of the voltage in Fig 5.3a, resulting in the voltage waveform shown in Fig.5.3b.

The frequency components in the output voltage waveform V_o can be obtained in the following manner. The process of obtaining the output voltage is equivalent to multiplying the expression in (5.3) by a square wave V_{sw} of unit amplitude, in phase with $\cos w_c t$. Since such a square wave has a Fourier series expansion of the form:

$$V_{sw} = \sum_{\substack{n=1 \\ n \text{ odd}}}^{\infty} (-1)^{\frac{n-1}{2}} \frac{4}{\pi n} \cos n w_c t \qquad (5.4)$$

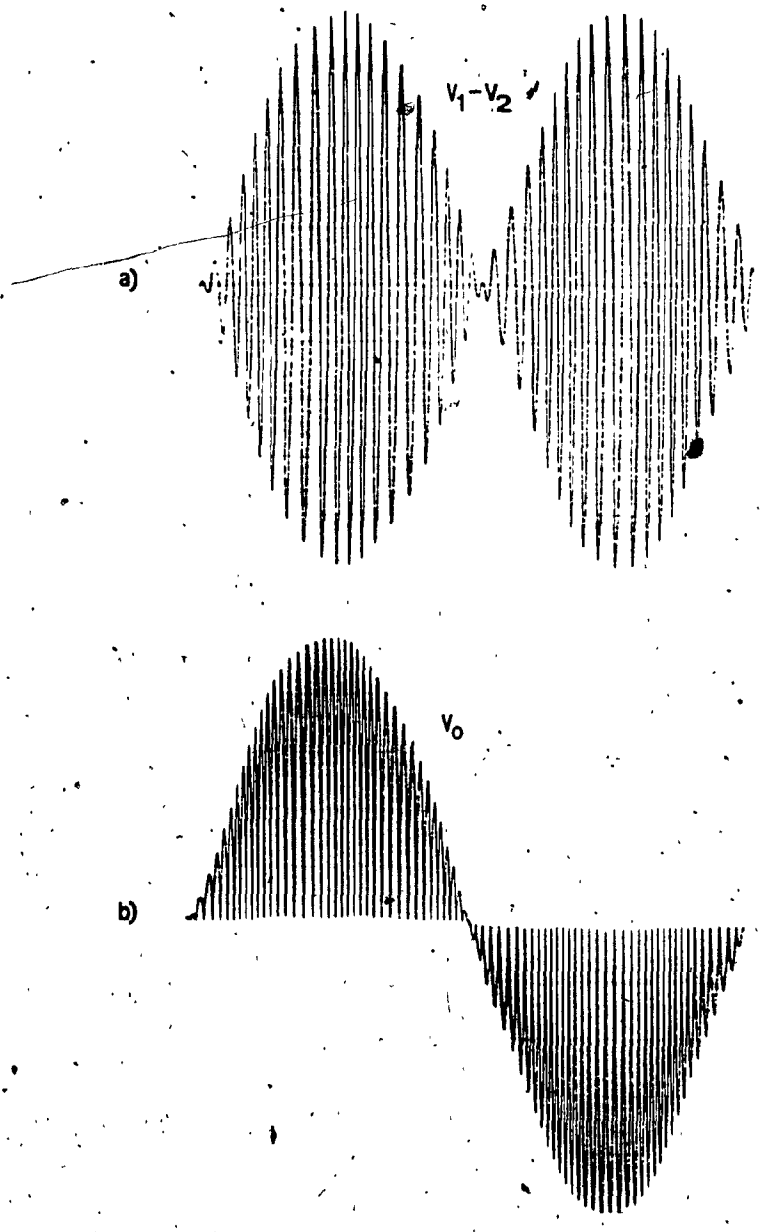

Fig. 5.3 Input and output voltage waveforms of the cycloconverter.

the output voltage V_o can be expressed as

$$V_o = V_3 x V_{sw}$$

i.e. $$V_o = \{V_m \sin(w_c + w_o)t - V_m \sin(w_c - w_o)t\}$$

$$x\{\sum_{\substack{n=1 \\ n \text{ odd}}}^{\infty} (-1)^{\frac{n-1}{2}} \frac{4}{\pi n} \cos n w_c t\}$$

$$V_o = \frac{4V_m}{\pi} \sin w_o t$$

$$+ \frac{2V_m}{\pi} \left(\frac{1}{1} - \frac{1}{3}\right)\{\sin(2w_c + w_o)t - \sin(2w_c - w_o)t\} \qquad (5.5a)$$

$$- \frac{2V_m}{\pi} \left(\frac{1}{3} - \frac{1}{5}\right)\{\sin(4w_c + w_o)t - \sin(4w_c - w_o)t\}$$

$$+ \ldots\ldots\ldots\ldots$$

i.e. $$V_o = \frac{4V_m}{\pi} \sin w_o t \qquad (5.5b)$$

$$- \sum_{k=1}^{\infty} \frac{2V_m}{\pi} \left(\frac{1}{2k-1} - \frac{1}{2k+1}\right)(-1)^k \{\sin(2kw_c + w_o)t - \sin(2kw_c - w_o)t\}$$

Equation (5.5b) shows that the voltage V_o has a component at the frequency f_o of amplitude $(4V_m/\pi)$, this being the required output voltage. The spectrum of the output voltage is shown in Fig.5.4. It can be seen that the first pair of unwanted frequency components in the output occurs at the frequencies $2f_c+f_o$ and $2f_c-f_o$. Since f_o is of the order of 60Hz, while f_c is of the order of kHz, the unwanted components can be easily filtered.

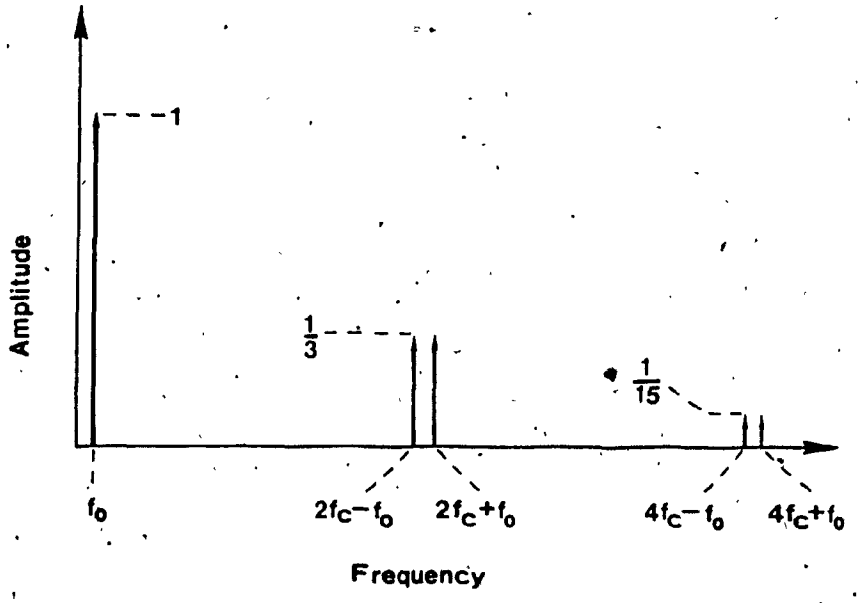

Fig. 5.4 Frequency spectrum of voltage V_o.

While the amplitude of each of the voltage sources V_1 and V_2 is V_m, the amplitude of the wanted frequency component in the voltage V_o constructed from the difference of V_1 and V_2 is $4V_m/\pi$ instead of $2V_m$, as may be expected ideally. This may be regarded as a derating in voltage, computed as:

$$\text{Voltage derating} = (4V_m/\pi)/2V_m = (2/\pi)=.637 \quad (5.6)$$

Let θ be the phase angle of the load at the output frequency f_o. The load current i_o (Fig.5.2) can be expressed in the form

$$i_o = i_m \sin(w_o t-\theta) \quad (5.7)$$

assuming that there is sufficient inductance in the load to smooth out ripple currents. The input current i_{in} of the cycloconverter in Fig.5.2 can then be obtained by the same method that was employed to obtained the expression for the output voltage V_o i.e. by multiplying the output current i_o by a square wave of unit amplitude in phase with $\cos w_c t$. The resulting expression is:

$$\begin{aligned} i_{in} &= (2i_m/\pi)\{\sin((w_c+w_o)t-\theta)-\sin((w_c-w_o)t+\theta)\} \\ &-(2i_m/\pi)\{\sin((3w_c+w_o)t-\theta)-\sin((3w_c-w_o)t+\theta)\} \quad (5.8) \\ &+(2i_m/\pi)\{\sin((5w_c+w_o)t-\theta)-\sin((5w_c-w_o)t+\theta)\} \\ &-\ldots\ldots\ldots\ldots\ldots \end{aligned}$$

From this expression, the active powers supplied by the two sources are seen to be the same. From (5.1) and (5.8)

Active power supplied by each source

$$= \frac{V_m i_m}{\pi} \cos\theta \qquad (5.9)$$

From the expression (5.7) for the output current i_o and the expression (5.5b) for the output voltage V_o,

Active power absorbed by the load

$$= \frac{1}{2} \frac{4V_m}{\pi} i_m \cos\theta$$

$$= \frac{2V_m i_m}{\pi} \cos\theta \qquad (5.10)$$

Thus each source supplies half the total active power demanded by the load. The apparent power handled by each source can be obtained as follows:

RMS voltage of each source = $V_m/\sqrt{2}$ (5.11)

RMS current in each source = $i_m/\sqrt{2}$ (5.12)

Hence the apparent power handled by each source

$$= \frac{V_m i_m}{2} \qquad (5.13)$$

From (5.9) and (5.13),

Power factor at which each source operates

$$= \frac{V_m i_m \cos\theta}{\pi} \div \frac{V_m i_m}{2}$$

$$= \frac{2}{\pi} \cos\theta \qquad (5.14)$$

From (5.14) it can be seen that the best power factor at which each source can operate is $(2/\pi)=.637$.

5.3 Circuit Implementation:

The power circuits that have to be realised in order to use the above dc-ac power conversion technique are the two high frequency inverters to obtain the two link voltages and the output cycloconverter to construct the low frequency output voltage from the two link voltages.

a) DC-High Frequency AC Inverters:

These may be regarded as the 'master' stage in the power conversion process. The amplitude and frequency of the output voltage are decided by the amplitudes and frequencies of the two link inverters. The output cycloconverter merely performs appropriate rectification/inversion to construct the output voltage from the difference of the two link voltages, as shown in Fig.5.2. It is not possible to incorporate the functions of voltage regulation or frequency variation in the output converter,

which may be regarded as a 'slave' stage. Therefore the high frequency inverters employed to realise the two links must have the capability to perform these functions, in addition to producing sinusoidal output, which, of course, is a primary requirement.

The resonant inverter of Fig.1.3b satisfies the above requirements. The output voltage of this inverter can be regulated by varying the frequency, as was shown in Chapter 3. The expression for the output voltage V_o of the dc-ac converter, given in (5.5b) shows that the amplitube of the wanted frequency component in the output depends on the amplitude of the individual link voltages, while its frequency is decided by the difference between the frequencies of the two high frequency sources. Since only the frequency difference decides the output frequency, the individual link frequencies can be varied to perform output voltage regulation, while keeping the difference in frequencies constant.

The half-bridge configuration is used for the inverter. If full-bridge circuits are employed, it becomes necessary to use a transformer to obtain the difference of the two link voltages. The centre-tapped dc supply in the half-bridge configuration makes it possible to obtain the difference voltage without a transformer, as can be seen

from the complete converter circuit shown in Fig.5.5.

b) Output Cycloconverter:

Although the output converter is structurally a cycloconverter, the gating signals do not have to be modulated. The input voltage to the cycloconverter is the voltage V_1-V_2 shown in Fig.5.3a. The amplitude of the input voltage is very small as the envelope crosses zero and therefore, if thyristors are used to realise the cycloconverter, commutation will be difficult at these points; especially with a reactive load. Consequently, switches capable of being force-commutated have to be employed. In Fig.5.5 MOSFET switches are indicated. While dual converters can be employed to carry output currents of opposite polarities, the use of bidirectional switches, as shown in Fig.5.5, eliminates the need for output current sensing and changeover logic and was therefore preferred in the prototype converter.

Although the two link circuits have a common point, as shown in Fig.5.5, this common point is electrically not always at the middle potential of the cycloconverter input lines. For this reason, it is not possible to use a mid-point configuration for the cycloconverter unless a transformer with a centre-tapped secondary is used.

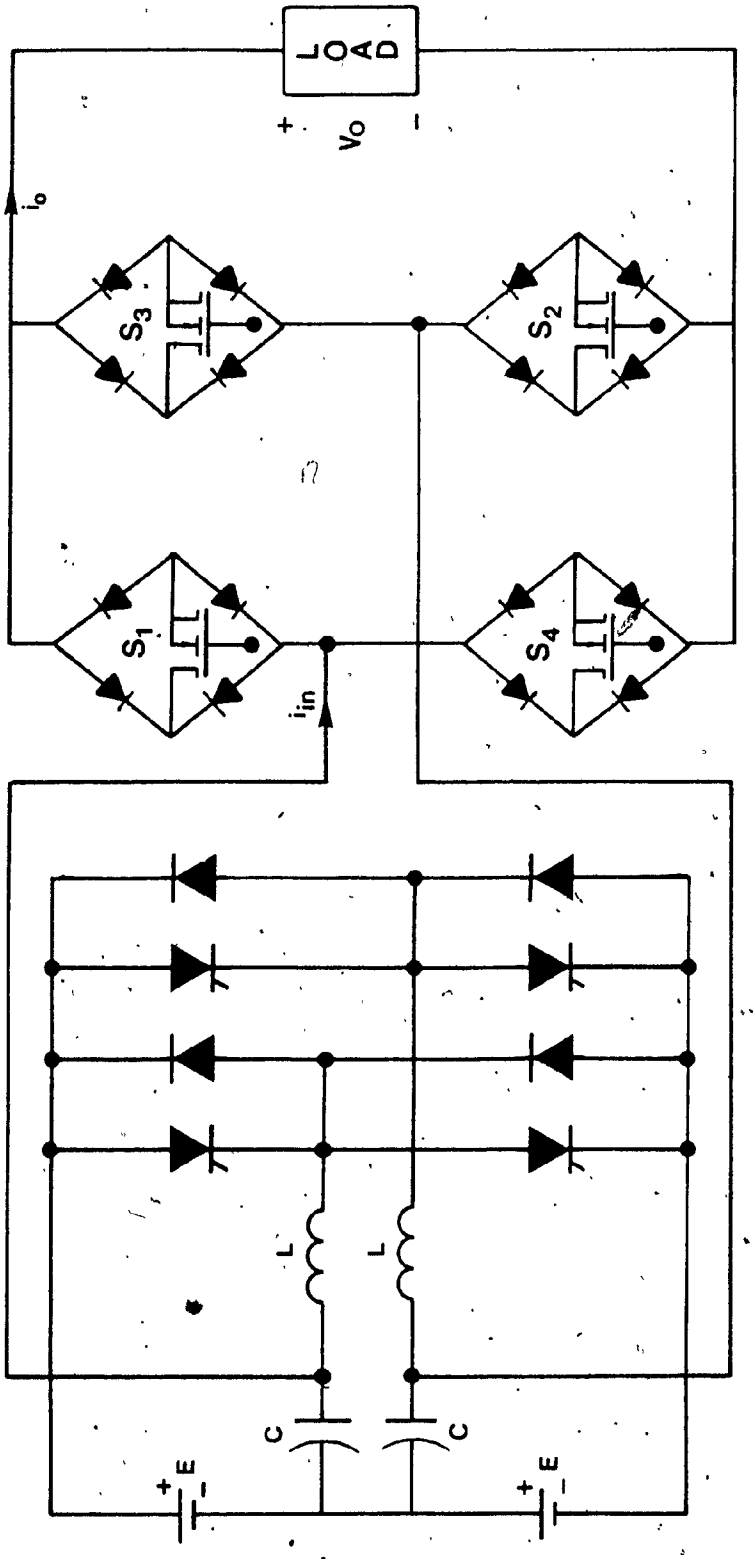

Fig. 5.5 Circuit diagram of dc-ac converter.

5.4 Operating Conditions for the Link Inverters:

Since the output current i_o (Fig. 5.5) is alternating at an angular frequency w_o which is very much less than w_c, the magnitude of i_o can be assumed to be constant over one cycle at the frequency of either link. Therefore the current reflected onto the link by the output converter can be represented by a square wave over one cycle at the link frequency, as illustrated by Fig. 5.6. The magnitude of this refelected load current follows the magnitude of the load current i_o and varies cyclically at a frequency $2f_o$ because the positive and negative half-cycles at the output of the cycloconverter give rise to the same current amplitude variations at the input.

Moreover, while the link voltages are alternating at the frequencies f_c+f_o, the load current seen by the links alternates at a slightly different frequency f_c. Consequently, the reflected load current 'slips' past the link voltages. The phase angle at which the links see the load current therefore varies from one cycle of the link frequency to the next. These variations repeat cyclically at the frequency $2f_o$. For a given load phase angle θ at the output, the range of phase angles over which the links see the load current can be established as follows.

Following the notation in Fig. 5.2, the link voltages V_1 and V_2 and the load currents I_1 and I_2 of the two links

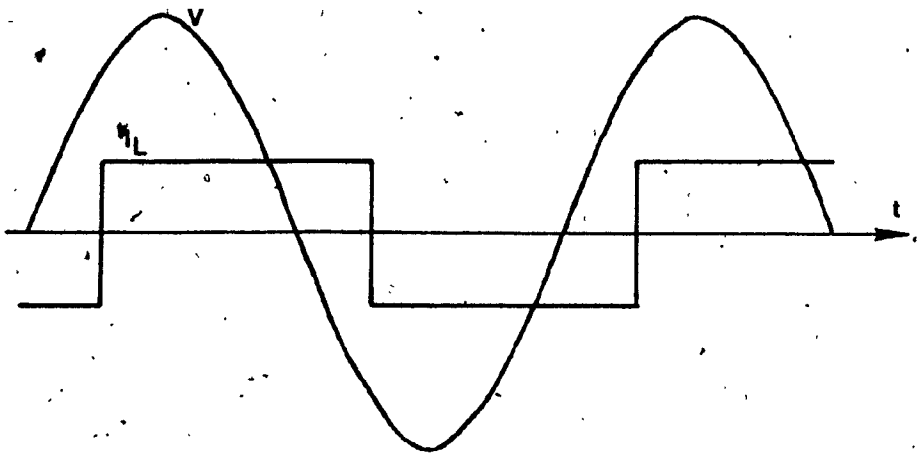

Fig. 5.6 Waveforms of link voltage and load current seen by the link.

obtained by reflecting the load current i_o can be represented by a phasor diagram, as shown in Fig.5.7. The frame of reference in Fig. 5.7 is assumed to rotate at the frequency f_c. Since I_1 and I_2 are alternating at the frequency f_c, their phasors are stationary. Furthermore the phase difference between I_1 and I_2 is always 180 because of the polarity conventions indicated in Fig.5.2. The two link voltages V_1 and V_2 are alternating at the frequencies f_c+f_o and f_c-f_o respectively. Therefore the phasor representing V_1 moves anticlockwise at a rate of w_o radians/sec, while the phasor representing V_2 moves clockwise at the same rate. θ_1 and θ_2 are the phase angles at which the two link voltages see the load current.

Consider the half-cycle of the output represented by the interval from one load current zero to the next. Waveforms of the output current and the wanted component of the output voltage are shown in Fig.5.8, where a lagging load has been assumed. Since the link frequencies are very much higher than the output frequency, the instantaneous power p_o at the output at any instant can be taken to equal the average power supplied over a cycle at the link frequency at that instant. The wanted component V_{ow} of the output voltage is obtained from (5.5b) as:

$$V_{ow} = \frac{4V_m}{\pi} \sin w_o t \qquad (5.15)$$

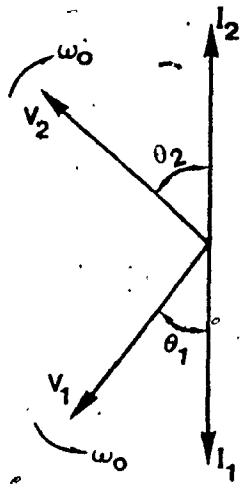

Fig. 5.7 Phasor diagram showing link voltages and load current seen by the links.

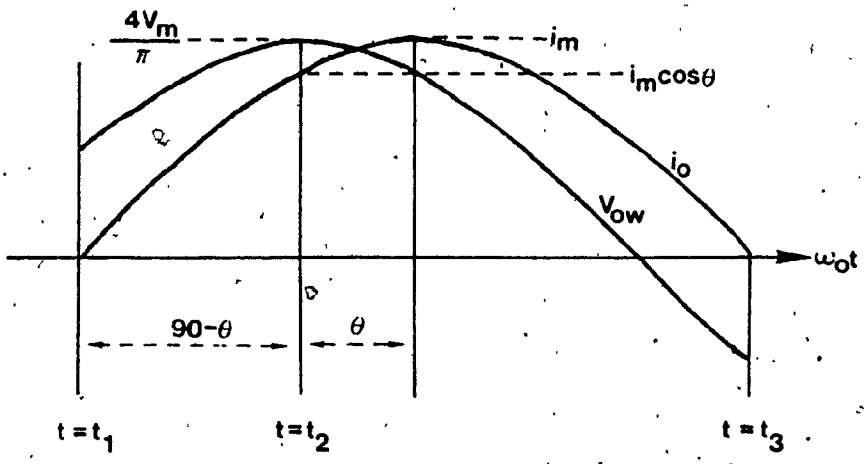

Fig. 5.8 Output current and wanted component of output voltage over one half-cycle.

Also, $i_o = i_m \sin(w_o t - \theta)$ (5.16)

$$P_o = \frac{1}{2} \frac{4V_m}{\pi} i_m (\cos\theta - \cos(2w_o t - \theta)) \quad (5.17)$$

The average powers P_1 and P_2 supplied over a cycle by the two links are given by:

$$P_1 = \frac{1}{2} V_m \frac{4i_o}{\pi} \cos\theta_1 \quad (5.18)$$

$$P_2 = \frac{1}{2} V_m \frac{4i_o}{\pi} \cos\theta_2 \quad (5.19)$$

The factor $(4/\pi)$ in (5.18) and (5.19) accounts for the fundamental component of the square current wave of amplitude i_o.

At any instant

$$P_o = P_1 + P_2 \quad (5.20)$$

Consider the instant t_2 in Fig.5.8, when the wanted component voltage V_{ow} has its peak value $4V_m/\pi$. At this instant the two phasors V_1 and V_2 are 180 degrees out of phase. Since the currents I_1 and I_2 are always 180 out of phase, the two phase angles θ_1 and θ_2 are equal at this instant. Consequently,

$$P_1 = P_2 = P_o \quad (5.21)$$

Now, at $t=t_2$, $w_o t = \pi/2$. From (5.17),

$$p_o = \frac{1}{2} \frac{4V_m}{\pi} i_m \, 2\cos\theta \qquad (5.22)$$

Also, $i_o = i_m \cos\theta$ and from (5.18) and (5.19),

$$P_1 = \frac{1}{2} V_m \frac{4}{\pi} i_m \cos\theta \cos\theta_1 \qquad (5.23)$$

$$P_2 = \frac{1}{2} V_m \frac{4}{\pi} i_m \cos\theta \cos\theta_2 \qquad (5.24)$$

From (5.22), (5.23) and (5.24), using the fact that $\theta_1 = \theta_2$ and $P_1 = P_2 = p_o$, it follows that

$$\theta_1 = \theta_2 = \theta \quad \text{at } t=t_2 \qquad (5.25)$$

Thus at the instant when V_{ow} attains its peak, the phase angles θ_1 and θ_2 seen by the two links are zero, irrespective of the load phase angle θ. Once this has been established, the phase relationships at other instants such as t_1 and t_3 can be deduced. Corresponding phasor diagrams are shown in Fig.5.9.

It can be seen that, for a lagging power factor angle θ at the output, the phase angle seen by the link voltage V_1 - operating at the frequency $(f_c + f_o)$ - varies from 90-θ leading to 90+θ lagging; the phase angle seen by the link voltage V_2 - operating at the frequency $(f_c - f_o)$ - varies from 90-θ lagging to 90+θ leading. At $t = t_3$, the output current i_o reverses polarity. Therefore the two currents I_1 and I_2 change in phase by 180 and the cycle repeats again.

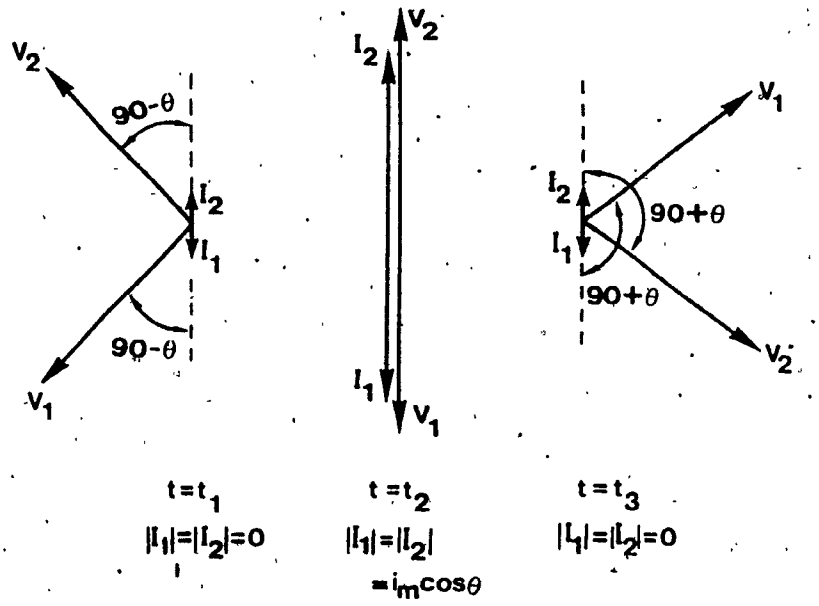

Fig. 5.9 Phasor diagrams at various instants.

From the analysis developed in Chapter 2, the behaviour of the inverter for various phase angles of the load current can be determined. Fig.5.10 shows the variation with frequency of the average rectified link voltage i.e. the volt-seconds under the link voltage waveform, at various load phase angles. It can be seen that irrespective of the load phase angle, an increase in the operating frequency results in an increase in the average rectified link voltage. However, for a given frequency, leading phase angles - corresponding to advance firing in the output converter in Fig.1.4 - give rise to an increase in the link voltage whereas lagging phase angles - corresponding to delayed firing in the output converter - give rise to a decrease. This is also borne out by the curves in Fig.5.11, which show the load regulation behaviour of the inverter at a particular operating frequency, for various load phase angles. Fig.5.12 shows the variation of some other circuit parameters with the load phase angle. The circuit recovery time t_q is lowest in the vicinity of 0 phase angle of the load. The rms link voltage and the rms reactor current in the inverter are higher for leading phase angles than for lagging phase angles.

5.5 Experimental Results:

A prototype dc-ac converter was constructed in the laboratory to demonstrate the power conversion principle.

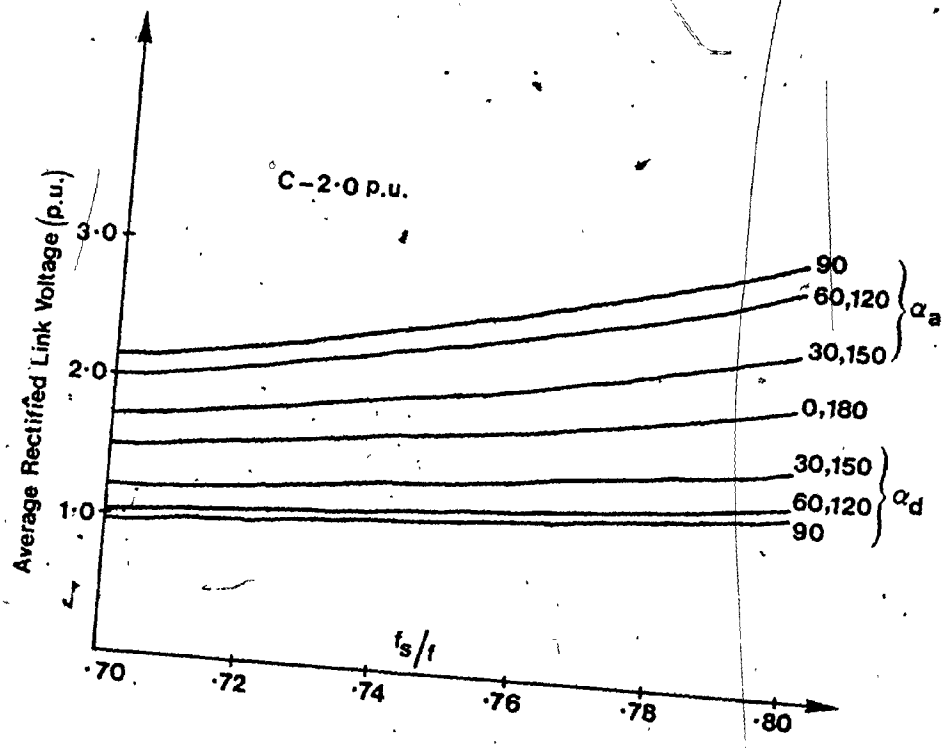

Fig. 5.10 Variation of average rectified link voltage with inverter frequency.

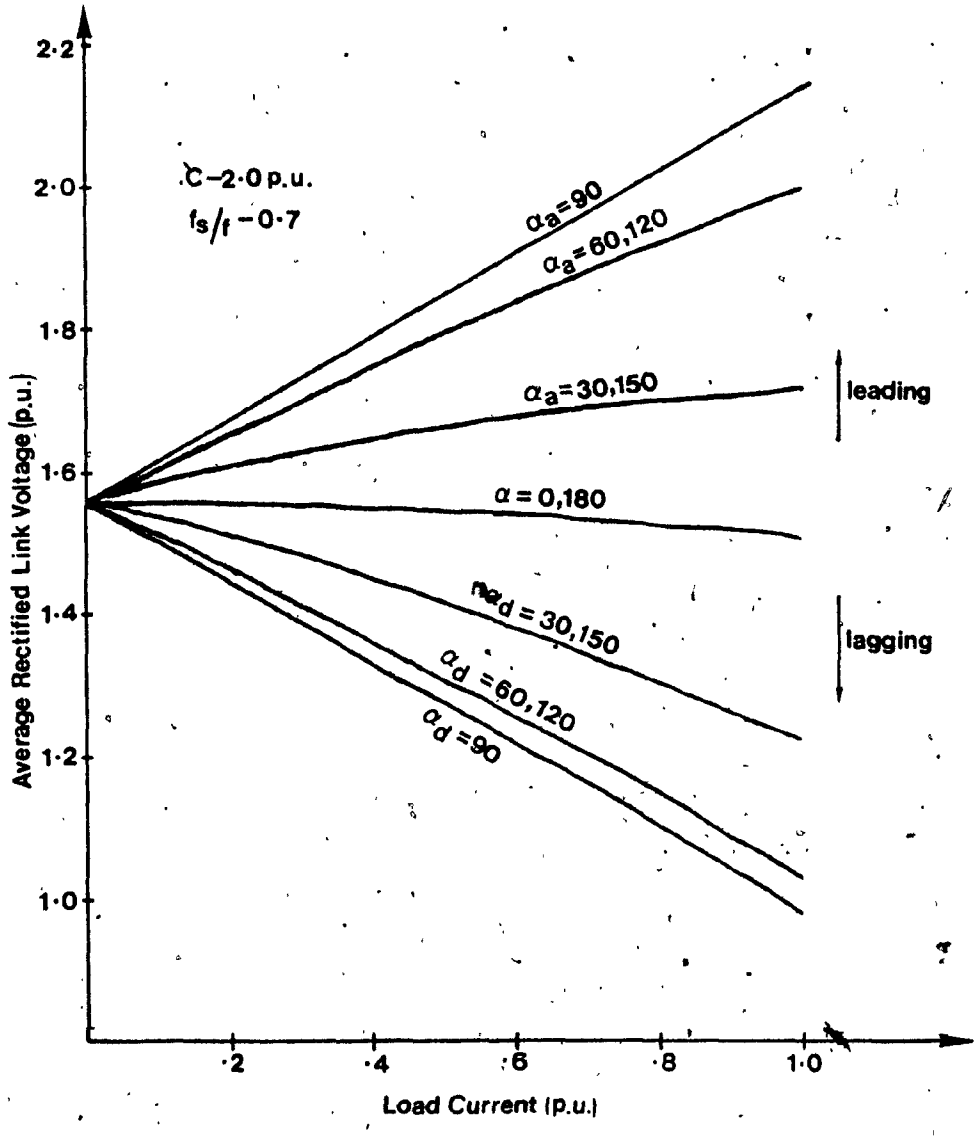

Fig. 5.11 Load regulation behaviour of the inverter for various load phase angles.

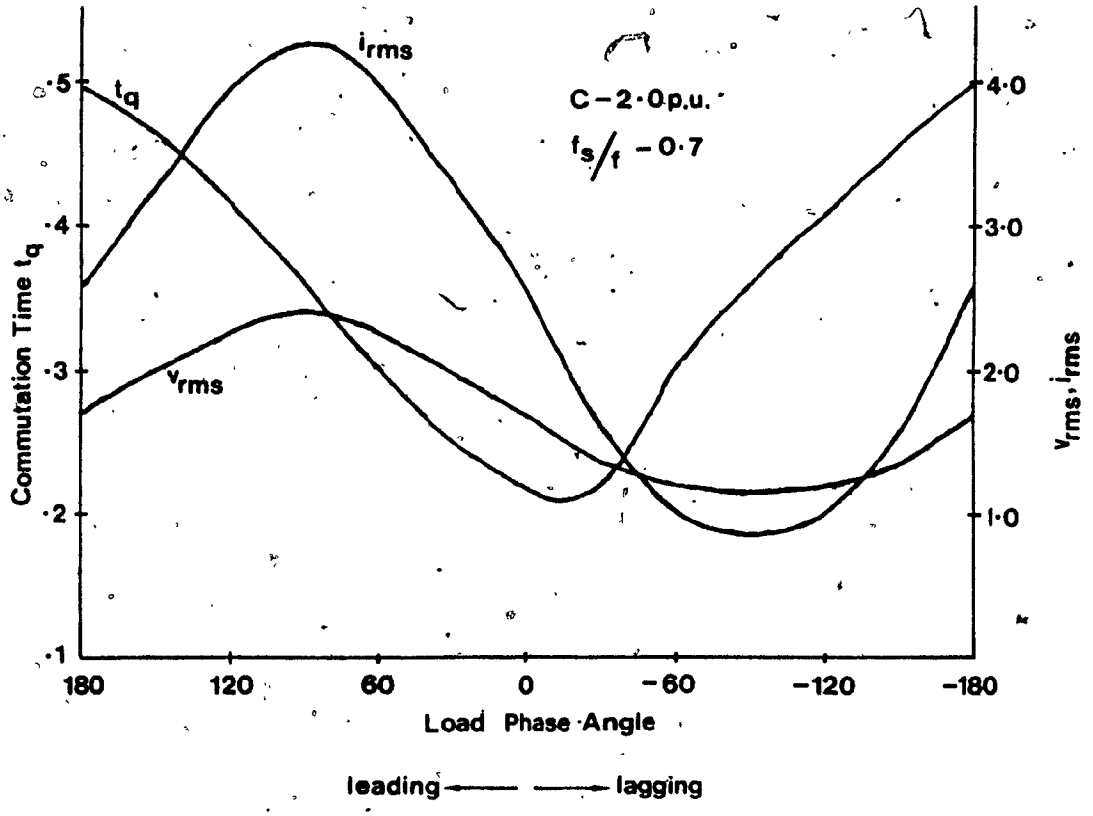

Fig. 5.12 Variation of recovery time, rms capacitor voltage and rms resonant current with load phase angle.

The converter utilised asymmetrical SCRs in the high frequency inverters. MOSFETs were used as the switches in the output converter. Fig.5.13 shows oscillograms from the experimental converter. The two link voltages v_1 and v_2, at frequencies of 6480 Hz and 6600 Hz respectively, are shown in Fig.5.13a. The difference voltage v_1-v_2 is shown in Fig.5.13b and consists of a high frequency ac enveloped within a sinusoid at 60 Hz. The output voltage waveform after cycloconversion and the output current with an RL load are shown in Fig.5.13c. The prototype converter provides a general verification of the conversion technique. Performance curves such as those in Figures 5.10 to 5.12 can be used to select circuit components to meet specific design objectives.

5.6 Extension Of The Technique For 3 Phase Output:

The twin resonant link power conversion technique can be extended for three phase output by using three of the basic converter circuits. A block diagram of a three phase arrangement is shown in Fig.5.14. The inverters in the three phases have to be appropriately phase shifted to obtain balanced three phase output voltages. This can be accomplished as follows.

The three pairs of sinusoidal voltages generated by the inverters of the three phases are represented as:

a)

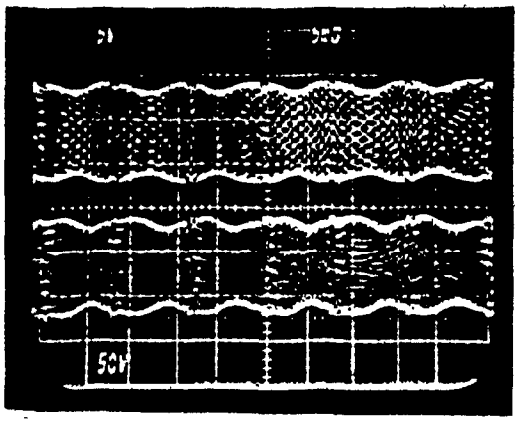

The two link voltage V_1, V_2.

b)

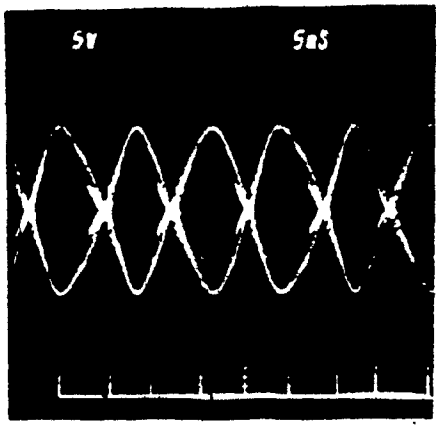

The difference voltage V_1-V_2.

c)

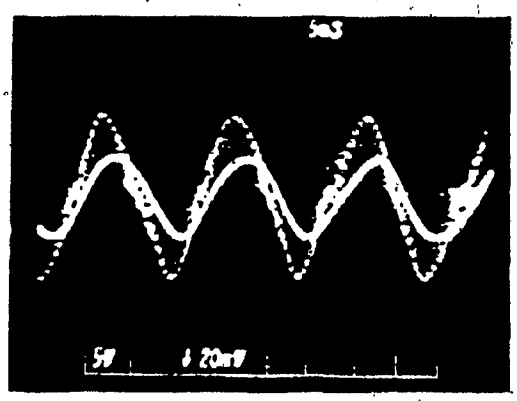

Output voltage V_o and current i_o.

Fig. 5.13 Waveforms from experimental converter; E = 20V; L = 60μH; C = 5μF; f_1 = 6480Hz; f_2 = 6600Hz. Scales: Time-5msec/div; voltage-50V/div Current-2A/div.

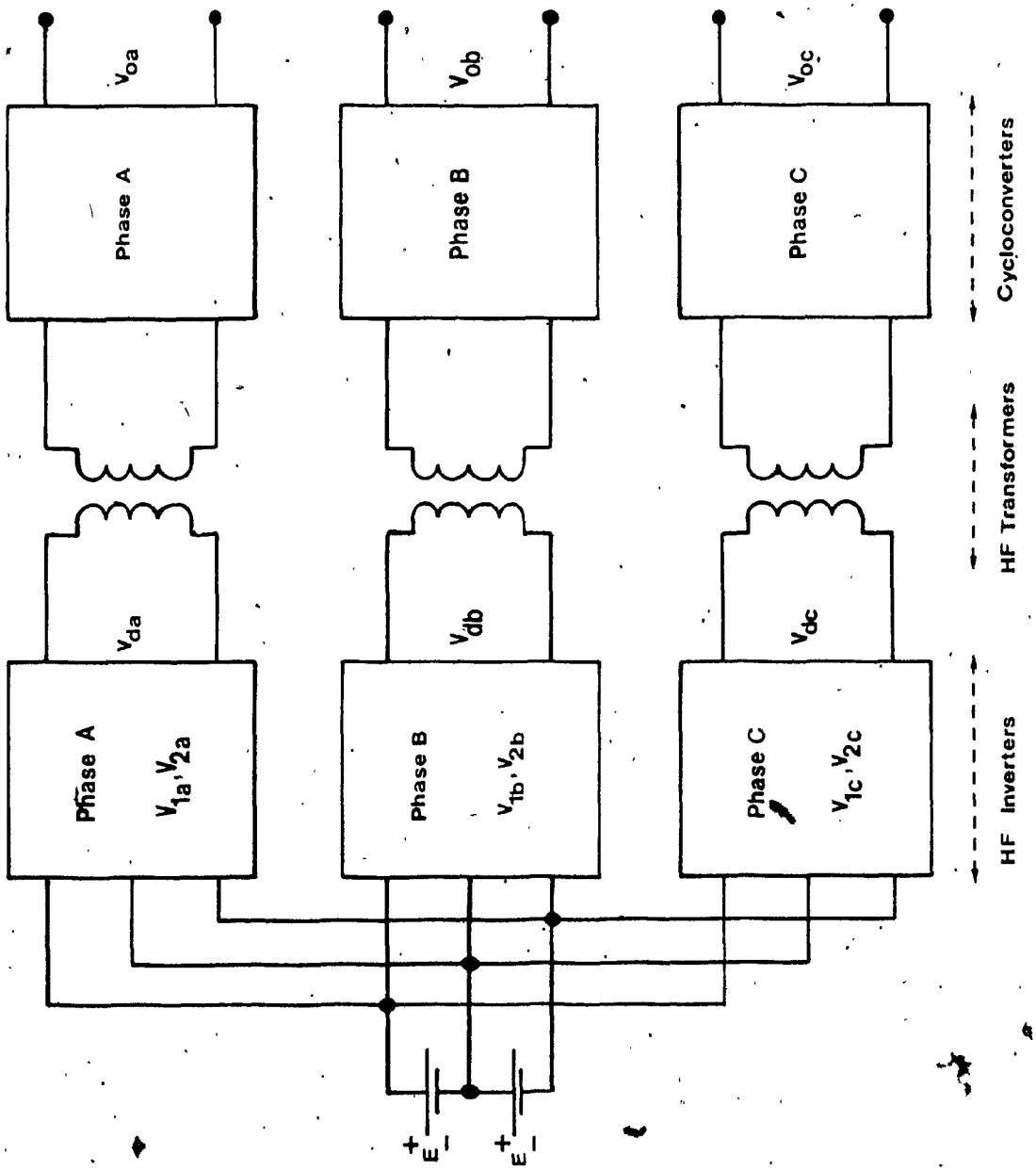

Fig. 5.14 Block diagram of three phase dc-ac conversion scheme.

$$V_{1a} = V_m \sin(w_c+w_o)t \qquad V_{2a} = V_m \sin(w_c-w_o)t$$

$$V_{1b} = V_m \sin\{(w_c+w_o)t-120\} \qquad V_{2b} = V_m \sin\{(w_c-w_o)t+120\} \quad (5.26)$$

$$V_{1c} = V_m \sin\{(w_c+w_o)t+120\} \qquad V_{2c} = V_m \sin\{(w_c-w_o)t-120\}$$

The three voltages at the frequency f_c+f_o form a balanced three phase set, as do the three voltages at the frequency f_c-f_o. The difference voltages for the three phases are then obtained as follows:

$$V_{da} = V_{1a}-V_{2a} = 2V_m \cos w_c t \sin w_o t$$

$$V_{db} = V_{1b}-V_{2b} = 2V_m \cos w_c t \sin(w_o t-120) \quad (5.27)$$

$$V_{dc} = V_{1c}-V_{2c} = 2V_M \cos w_c t \sin(w_o t+120)$$

The envelopes of the three difference voltages form a balanced three phase set, while the high frequency waves contained within the envelopes in the three phases are in phase. Cycloconversion now yields the required three phase output at the frequency f_o. The three outputs can be connected in either in wye or in delta because of the isolation provided by the transformers.

5.7 Conclusion:

A dc-ac power conversion technique can thus be realised

by using twin high frequency links. It was shown that if the two link inverters operate at frequencies f_c+f_o and f_c-f_o respectively, then the difference between their output voltages is an amplitude modulated sinusoid at the high frequency f_c, whose envelope is a low frequency wave at the frequency f_o. The output voltage waveform at the frequency f_o is constructed by a cycloconverter which merely performs appropriate rectification/inversion. The firing angle of the switches in the cycloconverter does not have to be modulated. Qutput voltage regulation is obtained by varying the frequency of operation of the two links, while keeping the difference between the two frequencies constant. As it is possible to provide isolation at high frequency, the technique can be utilised in lightweight dc-ac power conversion applications such as vehicle power supplies, portable power supplies for communication equipment etc.

CHAPTER 6

CONCLUSION

6.1 Conclusions

The performance of a series resonant inverter configuration with the load connected across the resonating capacitor, while acting as a high frequency link in dc-dc and dc-ac power conversion systems, has been investigated.

A technique has been developed for steady-state analysis of the inverter when it is acting as a high frequency link and feeding converter loads. The procedure assumes that the load current reflected onto the inverter is constant over a cycle of the inverter because of the high inverter frequency. Losses are ignored. A simple closed form solution results for the operating point of the inverter, for forward as well as regenerative power flow conditions.

A dc-dc conversion scheme using the inverter as a high frequency link has been investigated. The performance of the inverter is obtained using the above analysis. It is shown that the output voltage can be regulated by varying the operating frequency of the inverter. A design procedure is developed using the results of the analysis.

Moreover it has been shown that the resonant inverter can also be used to realise a four quadrant converter, in which the functions of dc to high frequency inversion and cycloconversion are performed in a single stage. Control of the output is achieved by controlling the on/off times of the inverter so as to force the load current to follow an external reference signal. The ability of the converter to respond quickly to external signals and operate over a wide range of frequencies was demonstrated.

A new dc-ac power conversion technique using two inverters as twin high frequency links has been developed. By operating the two inverters at frequencies differing by twice the required low output frequency, the difference between their output voltages is shown to be a high frequency wave whose amplitude follows an envelope at the low output frequency. The low output frequency is obtained by means of a cycloconverter, which merely performs appropriate rectification/inversion without modulation of the firing angles. The conditions of loading encountered by the two link inverters were established. It is shown that output voltage regulation can be performed by varying the frequencies of operation of the two inverters while keeping their difference constant.

6.2 Suggestions for Further Work

The performance of the twin link technique of dc-ac power conversion, when inverter configurations other than the one considered in this thesis are used as the links, is of interest. Also, with this technique, the synchronisation of the output voltage to other voltages such as the ac line is a subject that requires further investigation.

APPENDIX A

Steady-state analysis of the high frequency inverter with the load current reflected onto the link viz. I_L, leading the link voltage v:

Case A.1

Forward power flow; I_L leads v by α_a;

$0 \leq \alpha \leq \alpha_{ac}$.

This situation corresponds to Fig. 2.8a. Fig. A.1 shows the circuit waveforms in detail. The solution for the operating point is given as follows:

Solution: θ_{CD} is given by the solution of the equation

$$a\sin\theta_{CD}+b\cos\theta_{CD} = c \qquad (A.1.1)$$

where,

$$a = E\sin wT_s \qquad (A.1.2)$$

$$b = E(1+\cos wT_s) \qquad (A.1.3)$$

$$c = E(1+\cos wT_s)-zI\sin\theta_{adv}+zI\sin(wT_s-\theta_{adv}) \qquad (A.1.4)$$

$$\therefore \theta_{CD} = \{2\pi+\sin^{-1}(c/\sqrt{a^2+b^2})\}-\{\pi+\tan^{-1}(b/a)\} \qquad (A.1.5)$$

The initial conditions at the beginning of a half cycle are given by:

$$i_0 = I\,\frac{\cos(wT_s-\theta_{adv}-\theta_{CD}) + \cos(\theta_{adv}+\theta_{CD})}{1+\cos wT_s} - \frac{E\sin wT_s}{Z(1+\cos wT_s)} - I \qquad \text{(A.1.6)}$$

$$v_0 = ZI\,\frac{\sin(\theta_{adv}+\theta_{CD})-\sin(wT_s-\theta_{adv}-\theta_{CD})}{1+\cos wT_s} \qquad \text{(A.1.7)}$$

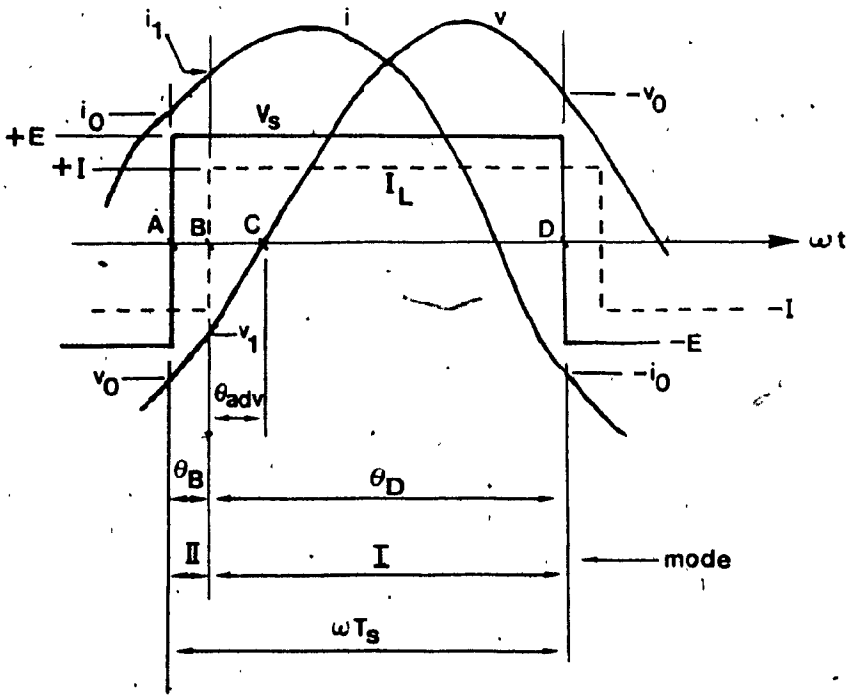

Fig. A.1 Circuit waveforms, forward power flow with I_L leading v; $0<\alpha_a<\alpha_{ac}$.

Case A.2

Forward power flow; I_L leads v by α_{ac} ($\alpha_{ac} < 90$)

This condition corresponds to Fig. 2.8b. Fig. A.2 shows circuit waveforms in detail.

Solution: The initial conditions are given by:

$$i_0 = - \frac{E \sin wT_s}{Z(1+\cos wT_s)} \qquad (A.2.1)$$

$$v_0 = ZI \quad \frac{\sin wT_s}{1+\cos wT_s} \qquad (A.2.2)$$

The critical advance angle θ_{advc} is given by the solution of:

$$a\sin\theta_{advc} + b\cos\theta_{advc} = c \qquad (A.2.3)$$

where,

$$a = E\sin wT_s + zI(1+\cos wT_s) \qquad (A.2.4)$$

$$b = E(1+\cos wT_s) - zI\sin wT_s \qquad (A.2.5)$$

$$c = E(1+\cos wT_s) \qquad (A.2.6)$$

$$\therefore \quad \theta_{advc} = \{\pi - \sin^{-1}(c/\sqrt{a^2+b^2})\} - \{\frac{1-S(a)}{2}\pi + \tan^{-1}(b/a)\} \qquad (A.2.7)$$

where $S(a) = 1$ if $a > 0$

$S(a) = -1$ if $a < 0$ (A.2.8)

$$\alpha_{ac} = \theta_{advc} x 180/wT_s \quad \text{(A.2.9)}$$

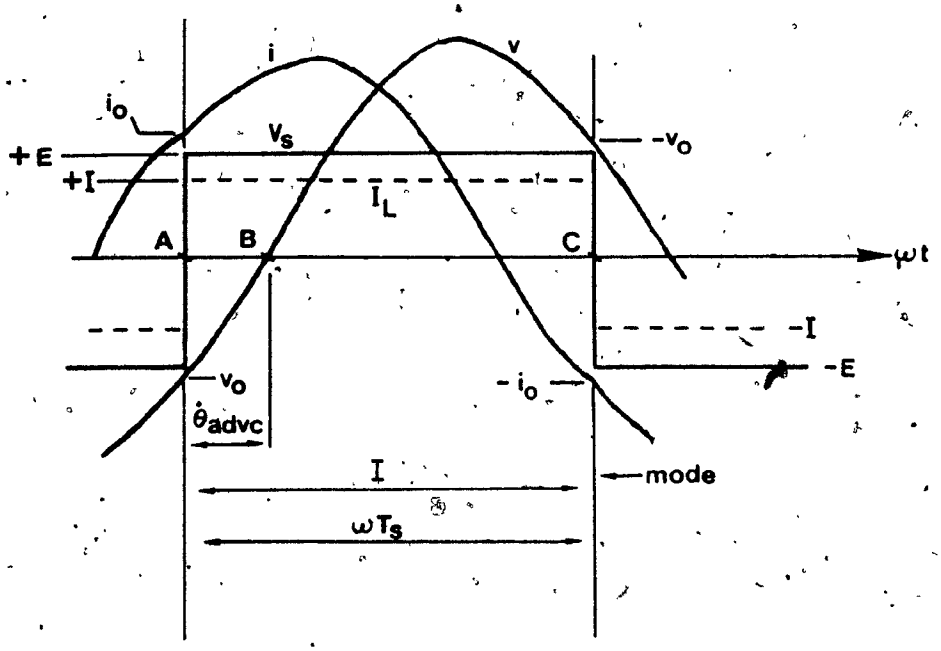

Fig. A.2 Circuit waveforms, forward power flow with I_L leading v; $\alpha_a = \alpha_{ac}$.

Case A.3

* Forward power flow; I_L leads v by α_a; $\alpha_{ac} < \alpha_a \leq 90^\circ$.

This situation corresponds to Fig. 2.8c. Detailed circuit waveforms are shown in Fig. A.3.

Solution: θ_B is given by the solution of

$$a\sin\theta_B + b\cos\theta_B = c \qquad (A.3.1)$$

where,

$$a = E\sin wT_s \qquad (A.3.2)$$

$$b = E(1+\cos wT_s) \qquad (A.3.3)$$

$$c = E(1+\cos wT_s) - zI\sin\theta_{adv} + zI\sin(wT_s - \theta_{adv}) \qquad (A.3.4)$$

$$\therefore \quad \theta_B = \{\pi - \sin^{-1}(c/\sqrt{a^2+b^2})\} - \{\pi + \tan^{-1}(b/a)\} \qquad (A.3.5)$$

The initial conditions are given by:

$$i_0 = I - \frac{E\sin wT_s}{Z(1+\cos wT_s)} - I\,\frac{\cos(\theta_{adv}-\theta_B)+\cos(wT_s-\theta_{adv}+\theta_B)}{1+\cos wT_s} \qquad (A.3.6)$$

$$v_0 = -zI\,\frac{\sin(\theta_{adv}-\theta_B)-\sin(wT_s-\theta_{adv}+\theta_B)}{1+\cos wT_s} \qquad (A.3.7)$$

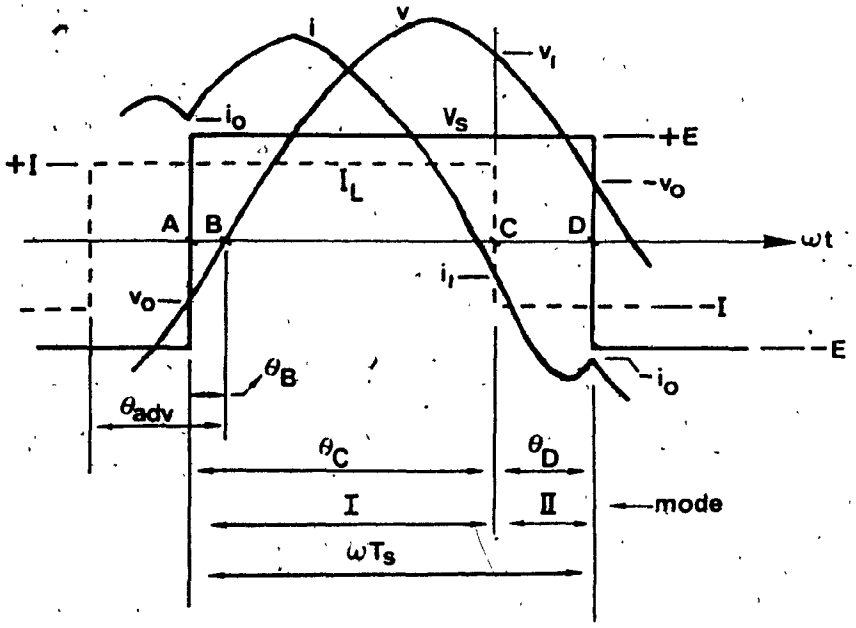

Fig. A.3 Circuit waveforms, forward power flow with I_L leading v; $\alpha_{ac} < \alpha_a < 90$.

Case A.4

Reverse power flow; I_L leads v by α_a; $90 < \alpha_a < 180-\alpha_{ac}$.

This condition corresponds to Fig. 2.8d. Detailed circuit waveforms are shown in Fig. A.4.

Solution: θ_{CD} is given by the solution of:

$$a\sin\theta_{CD}+b\cos\theta_{CD} = c \qquad (A.4.1)$$

where,

$$a = E\sin wT_s \qquad (A.4.2)$$

$$b = E(1+\cos wT_s) \qquad (A.4.3)$$

$$c = E(1+\cos wT_s)+zI\sin\theta_{adv}-zI\sin(wT_s-\theta_{adv}) \qquad (A.4.4)$$

$$\therefore \quad \theta_{CD} = \{\pi-\sin^{-1}(c/\sqrt{a^2+b^2})\}-\{\pi+\tan^{-1}(b/a)\} \qquad (A.4.5)$$

The initial conditions are given by:

$$i_0 = I - \frac{E\sin wT_s}{z(1+\cos wT_s)} - I\,\frac{\cos(\theta_{adv}+\theta_{CD})+\cos(wT_s-\theta_{adv}-\theta_{CD})}{1+\cos wT_s} \qquad (A.4.6)$$

$$v_0 = -zI\,\frac{\sin(\theta_{adv}+\theta_{CD})-\sin(wT_s-\theta_{adv}-\theta_{CD})}{1+\cos wT_s} \qquad (A.4.7)$$

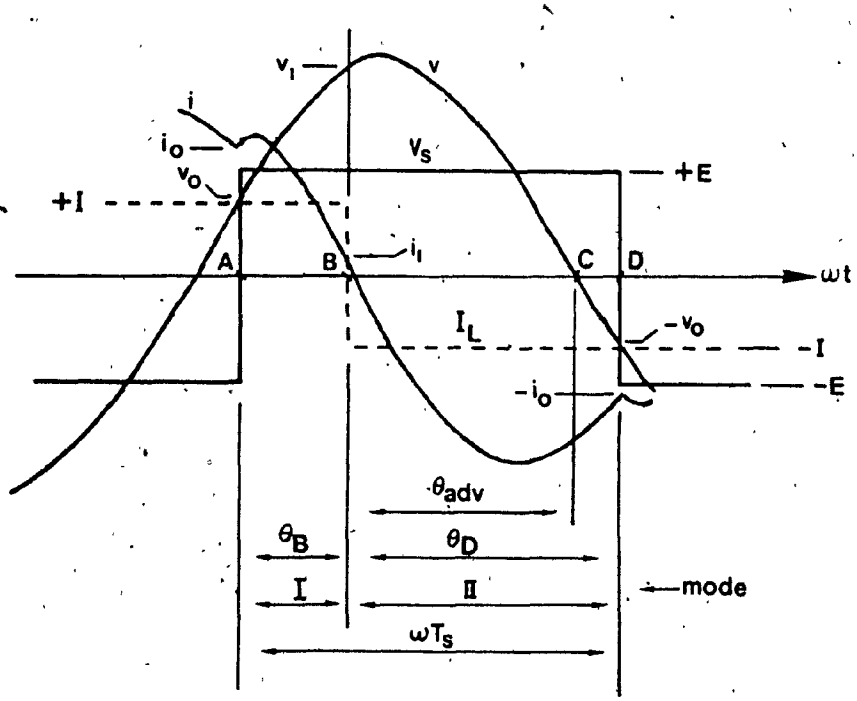

Fig. A.4 Circuit waveforms, reverse power flow with I_L leading v; $90<\alpha_a<180-\alpha_{ac}$.

Case A.5

Reverse power flow; I_L leads v by $180-\alpha_{ac}$.

This situation corresponds to Fig. 2.8e. Detailed circuit waveforms are shown in Fig. A.5.

Solution: The initial conditions are given by:

$$i_0 = - \frac{E \sin wT_s}{z(1+\cos wT_s)} \qquad (A.5.1)$$

$$v_0 = -zI \frac{\sin wT_s}{1+\cos wT_s} \qquad (A.5.2)$$

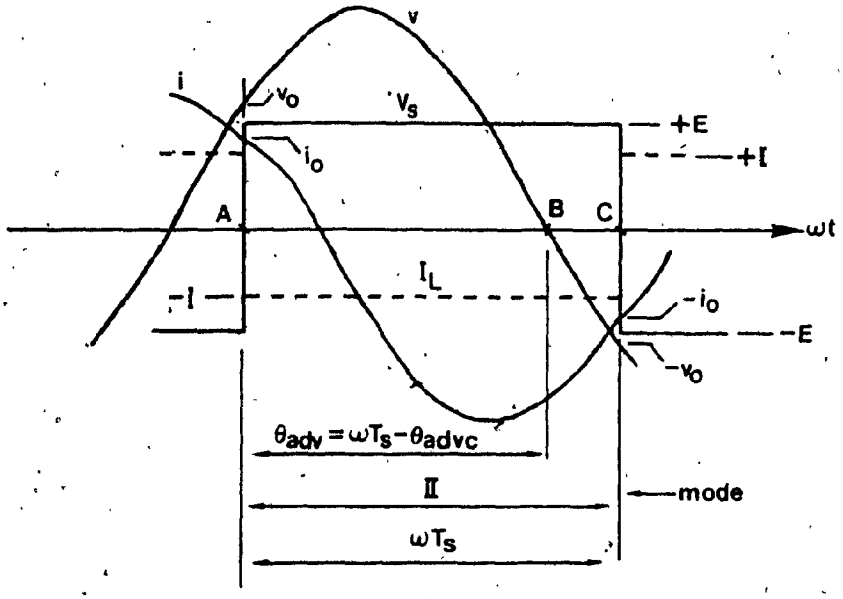

Fig. A.5 Circuit waveforms; reverse power flow with I_L leading v; $\alpha_a = 180 - \alpha_{ac}$.

Case A.6

Reverse power flow; I_L leads v by α_a; $180-\alpha_{ac}<\alpha_a<180$.

This situation corresponds to Fig. 2.8f. Detailed circuit waveforms are shown in Fig. A.6.

Solution: θ_B is given by the solution of:

$$a\sin\theta_B+b\cos\theta_B = c \qquad (A.6.1)$$

where

$$a = E\sin wT_s \qquad (A.6.2)$$

$$b = E(1+\cos wT_s) \qquad (A.6.3)$$

$$c = E(1+\cos wT_s)+zI\sin\theta_{adv}-zI\sin(wT_s-\theta_{adv}) \qquad (A.6.4)$$

$$\therefore\ \theta_B = \{2\pi+\sin^{-1}(c/\sqrt{a^2+b^2})\}-\{\pi+\tan^{-1}(b/a)\} \qquad (A.5.6)$$

The initial conditions are given by:

$$i_0 = I\,\frac{\cos(\theta_{adv}-\theta_B)+\cos(wT_s-\theta_{adv}+\theta_B)}{1+\cos wT_s} \angle \frac{E\sin wT_s}{z(1+\cos wT_s)} - I \qquad (A.6.6)$$

$$v_0 = zI\,\frac{\sin(\theta_{adv}-\theta_B)-\sin(wT_s-\theta_{adv}+\theta_B)}{1+\cos wT_s} \qquad (A.6.7)$$

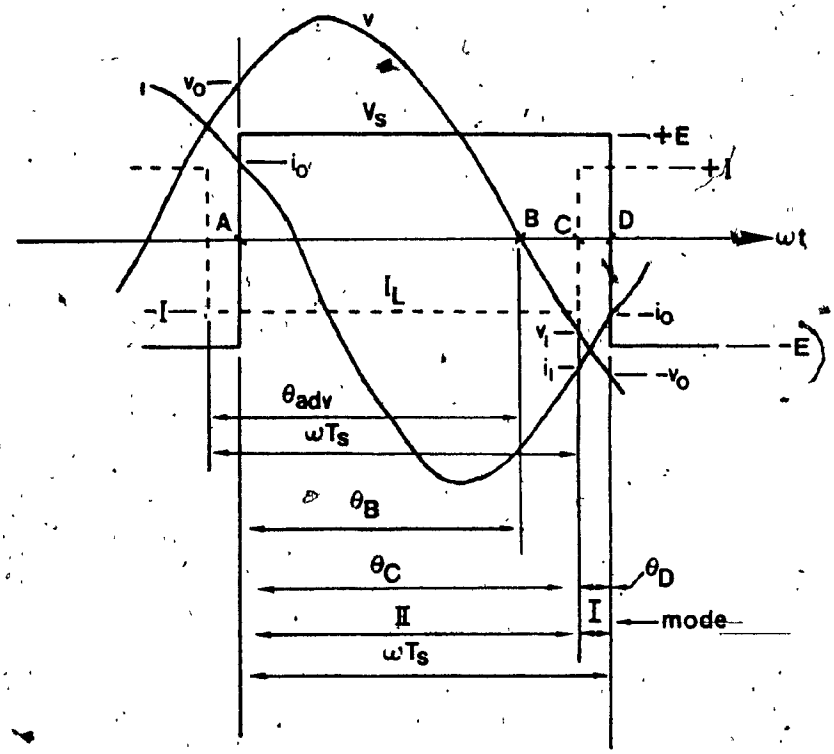

Fig. A.6 Circuit waveforms; reverse power flow with I_L leading v; $180-\alpha_{ac}<\alpha_a<180$.

APPENDIX B

Per-unit system of values followed in presenting inverter characteristics:

Base voltage V_{base} = Minimum dc supply voltage from centre-tap to either pole.

Base current I_{base} = Maximum value of load current reflected onto the inverter.

Base angular frequency w_{base} = $w = 1/\sqrt{LC}$, the resonant frequency of the LC circuit.

Base time $t_{base} = 2\pi/w_{base}$

Base inductance $L_{base} = V_{base}/(I_{base} \times w_{base})$

Base capacitance $C_{base} = I_{base}/(V_{base} \times w_{base})$

$V_{p.u.} = V/V_{base}$

$I_{p.u.} = I/I_{base}$

$w_{p.u.} = w/w_{base}$

$t_{p.u.} = t/t_{base}$

$L_{p.u.} = L_{base}$

$C_{p.u.} = C/C_{base}$

REFERENCES

[1] Dolaberidze,G.P. "Conversion of dc to controlled frequency ac for electric traction," Soviet Electrical Engineering, vol.36, no.5, pp.85-90, 1965.

[2] McMurray,W. "The Theory and Design of Cycloconverters," The MIT Press, Cambridge, Massachusettes, 1972 (Book).

[3] General Electric "SCR Manual," Sixth Edition, 1979 (Book).

[4] Lawson,L.J. "Fuel cell power conversion by the ac link type static inverter," 1966 Aerospace Systems Conf. Record; Suppl. IEEE Trans. Aerospace and Electronic Systems, vol.AES-2, no.5, pp.160-163, July 1966.

[5] Nishimura,M.,et. al. "A pulsewidth-controlled cycloinverter," Elec. Eng. (Japan),vol.89, no.10, pp.46-56, 1969.

[6] Bourbeau,F. "Synchronous motor railcar propulsion," IEEE Trans. Industry Applications, vol.IA-13, no.1, pp.8-17, Janurary/February 1977.

[7] Schwarz,F.C. "A method of resonant current pulse modulation for power converters," IEEE Trans. Industrial Electronics and Control Instrumentation, vol. IECI-17, no.3, pp.209-221, May 1970.

[8] Schwarz,F.C. "An improved method of resonant current pulse modulation for power converters," IEEE Trans. Industrial Electronics and Control Instrumentation, vol.IECI-23, no.2, pp.133-141, May 1976.

[9] Schwarz,F.C. and Ben Klaassens,J. "A controllable 45-KW current source for dc machines," IEEE Trans. Industry Applications, vol.IA-15, no.4, pp. 437-444, July/August 1979.

[10] Schwarz,F.C. and Ben klaassens,J. "A reversible smooth current source with momentary internal response for nondissipative control of multikilowatt dc machines," IEEE Trans. Power Apparatus and Systems, vol.PAS-100, no.6, pp.3008-3016, June 1981.

[11] Schwarz,F.C. "Certain system aspects of the double-sided cycloconverter," IEEE Trans. Aerospace and Electronic Systems, vol.AES-16, no.3, pp.363-372, May 1980.

[12] McMurray,W. "The thyristor electronic transformer: A power converter using a high frequency link," IEEE Trans. Industry and General Applications, vol.IGA-7, no.4, pp.451-457, July/August 1971.

[13] Bedford,B.D "Versatile cycloinverter power converter circuits," U.S. Patent 3742 336, June 26, 1973.

[14] McMurrary,W "A constant turn-off time control for variable frequency thyristor inverters," IEEE Trans. Industry Applications, vol.IA-13, no.5, pp.418-422, September/October 1977.

[15] Espelage,P.M and Bose,B.K. "High frequency link power conversion," IEEE Trans. Industry Applications, vol.IA-13, no.5, pp.387-394, September/October 1977.

[16] Gyugyi,L. and Cibulka,F. "The high frequency base converter - A new approach to static high-power conversion," IEEE Trans. Industry Applications, vol.IA-15, no.4, pp.420-429, July/August 1979.

[17] Gyugyi,L. and Pelly, B.R. "Static power frequency changers," Wiley- Interscience Publication, John Wiley and Sons, 1976 (Book).

[18] Steigerwald,R.L., Ferraro,A. and Turnbull,F.G. "Application of power transistors to residential and intermediate rating photovoltaic array power conditioners," Conf. Record, IEEE-IAS International Semiconductor Power Converter Conference, pp.84-96, 1982.

[19] Steigerwald,R.L. and Tompkins,R.E. "A comparison of high frequency link schemes for interfacing a dc source to a utility grid," Conf. Record, IEEE-IAS Annual Meeting, pp.759-766, 1982.

[20] Hoft,R.G. et. al. "30 kVA transistor inverter auxiliary power supply for people mover- Parts I and II," Conf. Record, IEEE-IAS Annual Meeting, pp.862-885, 1982.

[21] Mapham,N. "An SCR inverter with good regulation and sine-wave output," IEEE Trans. Industry and General Applications, vol. IGA-3, pp. 176-187, March/April 1967.

[22] Robertson,S.D.T. and Hebbar,K.M. "A variable low frequency inverter using thyristors," IEEE Trans. Ind. Gen. Appl., vol.IGA-4, pp. 501-507, Sept/Oct. 1968.

[23] Miyairi,S. and Fukao,T. "An SCR power amplifier," Elect. Engg. Japan, vol.87, no.3, pp.69-79, Mar. 1967.

[24] Palaniappan,R.G. and Vithayathil,J. "A control strategy for reference wave adaptive current regulation," IEEE Trans. Ind. Electron. Contr. Instrum., vol.IECI-27, no.2, pp.92-96, May 1980.

[25] Plunkett,A.B. "A current controlled PWM transistor inverter drive," in Conf. Rec. IEEE-IAS Ann. Meet. 1979, pp.785-792.

[26] Papaioannou,C. "A highly versatile current controller for static PWM inverters," Master's thesis, Concordia University, Montreal, Canada, July 1981.

[27] Kernick,A. et. al. "Static inverter with synchronous output waveform synthesised by time-optimal-response feedback," in Power Electronics Specialists Conference Record 1976, pp. 148-156.

[28] Bedford,B.D. and Hoft,R.g. "Principles of inverter circuits," John Wiley & Sons, 1964.

[29] Hatanaka, Y. et. al. "High frequency inverter by reverse-conducting thyristors for high power ultrasonic generator," INTELEC 81, pp. 120-126.